Studies Towards the *In Vivo* Inhibition of Oligosaccharyl Transferase

by

María de L. Ufret-Vincenty

B. S. Chemistry
University of Puerto Rico, Humacao, 1996

SUBMITTED TO THE DEPARTMENT OF CHEMISTRY IN PARTIAL FULFILLMENT OF THE REQUIREMENTS FOR THE DEGREE OF DOCTOR OF PHILOSOPHY FROM THE DEPARTMENT OF CHEMISTRY
AT THE
MASSACHUSETTS INSTITUTE OF TECHNOLOGY

September 2003

© 2003 Massachusetts Institute of Technology. All rights reserved.

Signature of Author:_____
Department of Chemistry
August 14, 2003

Certified by:_____
Barbara Imperiali
Ellen Swallow Richards Professor of Chemistry and Biology
Thesis Supervisor

Accepted by:_____
Robert W. Field
Chair, Departmental Committee on Graduate Students

MASSACHUSETTS INSTITUTE OF TECHNOLOGY
OCT 1 4 2003
LIBRARIES

ARCHIVES

This thesis has been examined by a committee of the Department of Chemistry as follows:

Professor Alexander Klibanov
Chair _____

Professor Barbara Imperiali
Thesis Supervisor _____

Professor Sarah O'Connor
_____

STUDIES TOWARDS THE *IN VIVO* INHIBITION OF OLIGOSACCHARYL TRANSFERASE

by

María de L. Ufret-Vincenty

Submitted to the Department of Chemistry
on August 14, 2003 in Partial Fulfillment of the Requirements for the
Degree of Doctor of Philosophy

ABSTRACT

Protein glycosylation is an important process because of the great diversity of glycoproteins that can be produced by the introduction of different oligosaccharide sequences. Our group has made significant progress in the study of asparagine-linked glycosylation. This process is catalyzed by *oligosaccharyl transferase* (OT), which is a membrane-associated enzyme found in the lumen of the endoplasmic reticulum (ER). A variety of inhibitors that bind tightly to OT *in vitro*, with K_is as low as 10 nM, have been synthesized. The development of peptides capable of inhibiting OT *in vivo* would be desirable, since there is no bio-available inhibitor that targets *N*-linked glycosylation directly. Both active and passive strategies for delivering inhibitors into cells were studied. Internalization sequences were attached to the inhibitors to be used as delivery vectors. An ER retrieval sequence was used to target inhibitors to the ER and fluorescent labels were used to trace the inhibitors in the interior of the cell. It was determined that inhibitors with the internalization sequences, both with and without the ER retrieval sequence, were internalized by cells in culture. Also, inhibitors with a BODIPY fluorophore were internalized by cells in culture. Those that contained the *C*-terminus ER retrieval sequence were concentrated in the ER, while the inhibitors without the ER retrieval sequence were found distributed throughout the cell. Nevertheless, inhibitors with an amide *C*-terminus were internalized with more ease that those with a free acid at the *C*-terminus, which were the ones that contained the ER retrieval sequence. Compounds were assayed for *in vivo* inhibition of OT with a system in which the activity of secreted alkaline phosphatase is related to the glycosylation state of this glycoprotein, since unglycosylated protein is not secreted from the cell. Some of the compounds containing internalization sequences were determined to be *in vivo* inhibitors of OT, as well as some of the compounds labeled with the BODIPY fluorophore.

Thesis Supervisor: Barbara Imperiali
Title: Ellen Swallow Richards Professor of Chemistry and Biology

Acknowledgements

I would like to take this opportunity to express my gratitude to all of those who, in one way or another, contributed to make the completion of this thesis possible. Many years have passed since I began this journey as a young undergraduate student at the University of Puerto Rico in Humacao. As a result of all the experiences lived throughout those years, both professional and personal, I am a different person today.

I would like to start by thanking my undergraduate research advisor, Prof. M. Ortiz-Marciales. Thanks for introducing me to research and organic synthesis techniques. Your constant advice led me to Caltech, where I started my graduate carrier in the laboratory of Prof. Barbara Imperiali, my current thesis advisor. I cannot express how grateful I am to Prof. Imperiali, but I am going to try with just a few words. Thanks for your constant inspiration and contagious enthusiasm in science; that is one of the things that keeps us all going. Thank you for giving me the opportunity, twice, to be part of your team. Thanks for your advice and understanding and for your efforts to make us all better professionals.

I would also like to thank my thesis committee, Prof. Sarah O'Connor and Prof. Alexander Klibanov. Sarah, thanks for your help during my graduate career and good luck in your new career as a professor. Prof. Klibanov, thanks a lot for your advice.

As a graduate student you realize how important the group you are in is. I would have to say that this is the best group ever! I thank previous members of the group for their help in lab and for their friendship. Dr. Christine Kellenberger, thanks for teaching me everything I know about peptide synthesis and for being my friend. Dr. Jens Pohlman, thanks a lot for your lasting friendship and organic chemistry advice. Prof. Sarah O'Connor, thanks so much for your help, discussions and advice. Dr. Vince Tai, you have no idea the impact you had on me! You form part of my fond memories in this lab. Thanks for all your help and thanks a lot for your "older brother" kind of advice and friendship. Dr. Kevin McDonnell (and Nani as well), thanks for your discussions, professional and personal; thanks a lot for your friendship. Dr. Jen Ottesen, thanks for your constant smile, it makes the world shine. Thanks to Dr. Michael Shrogen-Knaak and Dr. Adam Mezo for your unconditional help. Thanks to Dr. Paula Eason, a great lab mate who sang to my Spanish tunes (and then asked what it meant)! It was fun working with you. Dr. Dierdre Pierce, thanks for taking pictures of group activities and sharing them with all of us. Special thanks to Dr. Stephane Peluso, a good friend and a great lab mate and collaborator. I really liked working with you! Dr. Rob Dempski, good luck in Germany! Dr. Carlos Bosques, thanks a lot for your help and discussions in lab, and most importantly, thanks for your friendship. Share my gratitude with Dr. Karen Carrasquillo! Prof. Kathy Franz, good luck in Duke! I wish you the best in your academic career.

Thanks to current members of the group for being such great lab mates. Mary and Eranthie, thanks for your company, advice, discussions, and help in lab, and thanks for reading so much of this thesis for me. I will miss you guys a lot. Melissa, thanks for proofreading and thanks for sharing the MS responsibilities with me. Thanks a lot for your friendship and don't worry, I have not forgotten your "mofongo". Mayssam, Seungib, Debbie and Beth, good luck to all of you in graduate school. Becca and Ryu, good luck in your undergraduate work. Elvedin, thanks for your company in the cell culture room and good luck in graduate school. Dr. Jebrell Glover, thanks for your help with gels and thanks for general help in lab. Dr. Mark Nitz, good luck in your future academic career. Dr. Eugenio Vazquez, thanks for sharing your music and being a great bench-mate; thanks for your scientific advice. Dr. Christian Hackenberger, Dr.

Guofeng Zhang and Dr. Christina Carrigan, I hope you enjoy your post-doc in this lab, and good luck in your future careers. To all of you guys, thanks for making this lab such a great place to work!

I would like to thank my best friends Michelle Rojas-Soto and María Eugenia Hernández. You made my out-of-lab-life in Caltech a great experience. Mariu, you are the best roommate I ever had and I miss you every day; you form part of my family. Michelle, you are the best friend ever; I wish you were here with me to share this moment. I would also like to thank my friend Angel Custodio. Thanks for keeping me in touch with the rest of the world here in Boston. Carlos Burgos and Brenda, thanks for your friendship, your advice and for always been watching over my well-being. Felix, thanks a lot for your true friendship, I wish you the best in life! Jorge Villavicencio-Grossmann and Wendy Alas, thanks for your friendship and for sharing those long nights with us.

Finally, I would like to thank my family because without their constant support I would not be here today. Rafael L. Ufret and Carmen A. Vincenty, I cannot thank you enough. Dad, you are a great human being and a great father, I wish I could be like you someday. Mom, you are my model of "motherhood"; I wish I could be a mother like you someday. Thanks for all your love and thanks for everything you gave me. I would not be who I am and where I am today without you. I love you two more than words can express. My twin sister, María del Pilar, I do not believe in twin sister's connections, but somehow you always dropped an email or a phone call when I needed it the most. I guess it is just that you were always taking care of me. Thanks for being there for me! You know you are a very important part of me. Rafi and Carmencita, my older siblings, thanks for all your advice and support. Yadi, thanks a lot for your friendship. Fernando, thanks for all your advice. My younger brother, Carlos, I am sorry to tell you that you are still, and will always be, my dear little brother. Thanks for being the way you are. I wish I could hear you play the guitar more often... "Mama Ju", thanks for being so sweet and caring. Thanks a lot to my nieces Verónica, Gabi, Adriana, and baby Sofía, for always making me smile when I think of you. Thanks so much to Olga Hernández and Olga Carrasco for keeping in touch with me, reminding me how much you care and making me part of your family. Thanks to Mara Malpica for many long conversations.

Since I always like to leave the best for the end, I dedicate this thesis to Pedro R. Malpica Hernández. Thanks for your constant support, for always making me think about the next step whenever I came home frustrated because of a bad result. Thanks for always being there for me. Thanks for understanding the long lab hours! Thanks for your energy and contagious positivism, and for asking and listening with enthusiasm about my science, when you are a musician. Thanks for your beautiful music! Thanks for making my life so joyful. Thanks for the long philosophical discussions, and for your interest in science and general culture. Thanks for being who you are and thanks for being the love of my life! I could not have gone through these last years without you... I love you more than you can imagine.

Table of Contents

List of Figures

Chapter 1

Chapter 2

Chapter 3

Chapter 4

Chapter 5

List of Schemes

List of Tables

Abbreviations

Standard one and three letter codes are used for the naturally occurring amino acids.

Aβx:	β-hydroxylamine
Aβz:	β-hydrazide
Abu:	α-Aminobutanoic acid
Ac:	Acetyl
AcOH:	Acetic acid
Add:	(S)-α-Aminodecanedioic acid
Ahx:	6-aminohexanoic acid
Aib:	α-Aminoisobutyric acid
Alloc:	Allyloxycarbonyl
Asn(γS):	Thioasparagine
Boc:	*tert*-butoxycarbonyl
BODIPY:	4,4-difluoro-4-bora-3a,4a-diaza-s-indacene
Bz:	Benzoyl
Cbz:	Benzyloxycarbonyl
CDG:	Congenital disorders of glycosylation
$CHCl_3$:	Chloroform
Dab:	α,γ-diaminobutanoic acid
DCE:	Dichloroethane
DCM:	Methylene chloride
DCC:	Dicyclohexylcarbodiimide
CHO:	Chinese hamster ovary
DIPCDI:	Diisopropylcarbodiimide
DIPEA:	Diisopropylethylamine
DMAc:	Dimethylacetamide
DMAP:	4-Dimethylaminopyridine
DMEM:	Dulbecco's modified eagles media
DMF:	Dimethylformamide
DMSO:	Dimethylsulfoxide
Dol:	Dolichol
Dol-P-P:	Dolichol pyrophosphate
dpm:	Disintegrations per minute
EDT:	Ethane dithiol
ER:	Endoplasmic reticulum
ESMS:	Electrospray mass spectrometry
FBS:	Fetal bovine serum
FITC:	Fluorescein isothiocyanate
Fmoc:	9-fluorenylmethyloxycarbonyl
Glc:	Glucose
GlcNAc:	*N*-acetylglucosamine
GPI:	Glycosylphosphatidyl inositol
HATU:	O-1-hydroxy-7-azabenzotriazolyl tetramethyluronium hexafluorophosphate
HBTU:	Hydroxybenzotriazolyl tetramethyluronium hexafluorophosphate

HOAt:	1-hydroxy-7-azabenzotriazole
HOBt:	Hydroxybenzotriazole
HPLC:	High-performance liquid chromatography
Hz:	Hertz
Man:	Mannose
MeCN:	Acetonitrile
MeOH:	Methanol
MHC:	Major histocompatibility complex
MMTV:	Mouse mammary tumor virus
MUP:	4-methylumbelliferyl phosphate
Nle:	Norleucine
NLS:	Nuclear localization sequence
NMR:	Nuclear magnetic resonance
Nph:	*p*-Nitrophenylalanine
OPfp:	Pentafluorophenyl ester
OT:	Oligosaccharyl transferase
PAGE:	Polyacrylamide gel electrophoresis
PArg:	Polyarginine
PBS:	Phosphate buffer saline
PLAP:	Placental alkaline phosphatase
ψ-Pro:	pseudoproline
PyAOP:	7-Azabenzotriazol-1-yloxytris (pyrrolidino) phosphonium-hexafluorophosphate
PMA:	Phosphomolybdic acid
PTD:	Protein transduction domain
QAA:	Quantitative amino acid analysis
SDS:	Sodium dodecyl sulfate
SeAP:	Secreted alkaline phosphatase
TAP:	Transporter associated with antigen pocessing
TCEP:	Tris(2-carboxyethyl)phosphine
TFA:	Trifluoroacetic acid
THF:	Tetrahydrofuran
TIS:	Triisopropylsilane
TLC:	Thin layer chromatography
TMOF:	Trimethylorthoformate
Tn:	Tunicamycin
TNBS:	Trinitrobenzene sulfonic acid
t_R:	Retention time
UDP:	Uridine diphosphate
VTC:	Vesiculotubular clusters

Chapter 1

Introduction

Protein glycosylation can be described as one of the most complex types of protein modifications in eukaryotic cells.[1] In fact, it is a process essential for life. The existence of a wide variety of monosaccharide building blocks, and the possibility of different linkages between them yields a great diversity of glycoproteins.[1] The oligosaccharide attached to a protein can be as big as 15-40 saccharide units[2], resulting in a structure that can occupy or cover a large portion of the protein surface. As a result, in many cases, the function of a glycoprotein is significantly modulated by the oligosaccharide attached to it. Glycoproteins have been associated with different biological processes such as the immune response[3], proper intracellular targeting[4], intercellular recognition[5], and protein folding, stability and solubility.[6-10]

Carbohydrate modifications of proteins fall into three general categories: *N*-linked modification of asparagine (Asn), *O*-linked modification of serine (Ser) or threonine (Thr) and glycosylphosphatidyl inositol (GPI) derivatization.[11] *O*-linked glycosylation occurs post-translationally, and involves the transfer of a monosaccharide unit to a Ser or Thr within a folded protein. Several enzymes have been implicated with this process and the sequence specificity of the targeted protein is not fully understood.[12] GPI derivatization is a modification of the *C*-terminus carboxyl group and allows anchoring of the proteins to membrane bilayers.[13]

N-linked glycosylation is a co-translational process catalyzed by *oligosaccharyl transferase* (OT), which is a multimeric membrane-associated enzyme whose active site is located in the lumen of the rough endoplasmic reticulum (ER). In general, secretory pathway and membrane-associated proteins are synthesized by ribosomes attached to the membrane of the rough ER (see Figure 1.1). As the protein is being synthesized, it is translocated into the lumen of the ER by means of a signal peptide sequence at the amino terminus, which is recognized by the signal recognition particle (SRP), transferred to the translocon machinery, and then cleaved by a signal peptidase complex.[14] When OT recognizes a defined tri-peptide sequence, Asn-X_{aa}-Thr/Ser, it transfers a tribranched tetradecasaccharide containing three glucose, nine mannose and two *N*-acetylglucosamine residues ($GlcNAc_2Man_9Glc_3$), from a dolichol-linked pyrophosphate donor to the asparagine side chain in the nascent polypeptide.[2, 15] When

translation of the protein is completed, the protein folds with the assistance of several chaperones. The key chaperones exclusively involved in glycoprotein folding are calnexin and calreticulin. Calnexin is a membrane bound protein that binds partially deglucosylated, unfolded proteins and helps the protein fold properly. Calreticulin is a soluble protein that inhibits protein oligomerization and oligosaccharide degradation to allow the formation of fully folded proteins.[16] When the protein is properly folded, cleavage of the last three glucose residues and four mannoses signals the protein for transport to the Golgi apparatus, where the glycoprotein acquires its mature state with the action of different glycosidases and glycosyltransferases.[2] Proteins that could not fold properly are degraded either in the ER or the cytosol.[17]

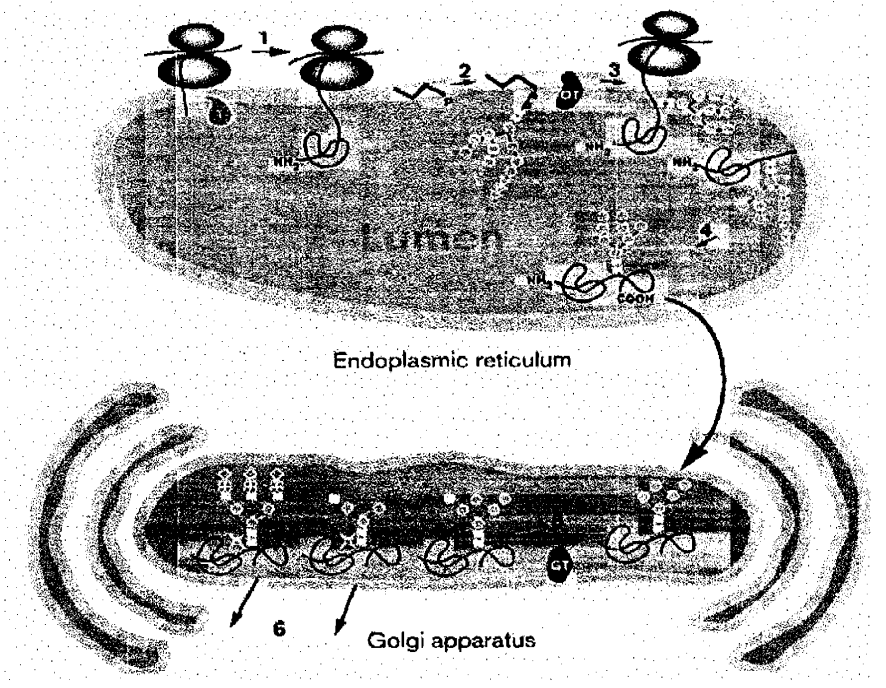

Figure 1.1. Schematic representation of the synthesis of *N*-linked glycoproteins. Proteins synthesized by ribosomes attached to the membrane of the ER are translocated into the lumen of the ER, where OT catalyses the transfer of the dolichol-linked tetradecasaccharide into the side chain of an Asn. Protein folding and trimming of the glucoses and some mannoses occurs in the ER; the protein is transported to the Golgi apparatus, where further maturation of the oligosaccharide occurs. Figure taken from *Chem. Biol.*, **1996**, *3*, 803-812.[17]

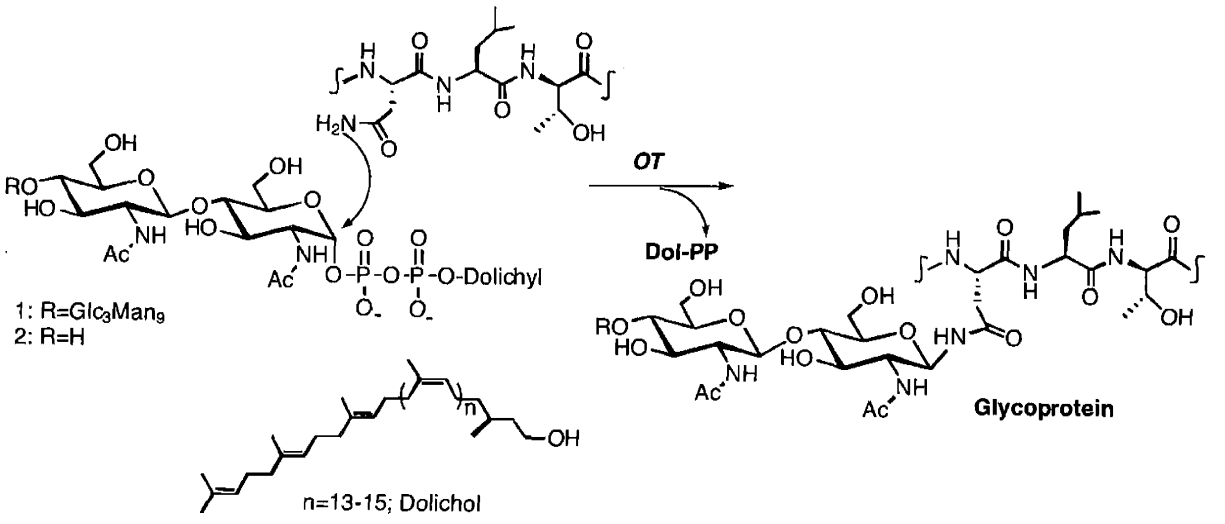

Figure 1.2. The reaction catalyzed by Oligosaccharyl Transferase.

N-linked glycosylation affects protein stability, folding and function

Oligosaccharides play an important role in the proper folding, stability and function of many *N*-linked glycoproteins. For example, one of the proteins whose folding and function is affected by *N*-linked glycosylation is the human formyl peptide receptor (FPR). This receptor is found in the plasma membrane of phagocytes and has three glycosylation sites. Upon binding to formyl peptides produced by bacteria, the receptor undergoes a conformational change to an active state, which results in the release of reactive oxygen species and lysosomal enzymes to destroy the bacteria. Researchers have shown that two of the glycosylation sites at the *N*-terminus of the receptor are essential for proper folding and function of the protein.[10]

Another interesting example of the relevance of *N*-linked glycosylation is the HIV envelope glycoprotein gp120, which contains over 20 glycosylation sites. This protein binds to the extracellular portion of the T-cell marker CD4, which has two glycosylation sites necessary for proper folding and secretion.[18] Researchers have shown that completely unglycosylated gp120 will not bind to CD4[19], while mutation of three glycosylation sites leads to reduced CD4 binding efficiency[20]. It is important to note that if the protein is deglycosylated after secretion it binds to CD4; this suggests that glycosylation is necessary for proper folding of the protein. Inhibiting glycosylation would impede folding and therefore, binding to CD4, avoiding viral

infectivity. Additional interesting examples of the effect of asparagine-linked glycosylation on protein structure and function can be found in a review article by O'Connor et al.[17]

Importance of *N*-linked glycosylation for cell viability

As mentioned earlier, protein glycosylation is not only an extremely complex modification, it is also essential for viability of eukaryotic cells. Deletion of the essential subunits of the OT multimeric protein complex of *S. cerevisiae* results in a lethal phenotype.[21] For example, deletion of the gene of UDP-GlcNAc:dolichol phosphate *N*-acetyl-glucosamine-1-phosphate transferase, the enzyme that catalyzes the transfer of P-GlcNAc to dolichol-P, the first step in the biosynthesis of the dolichol-linked tetradecasaccharide, results in a lethal phenotype.[22] On the other hand, viability is still possible with mutations of other enzymes involved in the biosynthesis or processing of *N*-linked oligosaccharides, but commonly results in diseases called congenital disorders of glycosylation (CDG). These diseases include physicomotor retardation, nervous system deficiencies, coagulation disorders and dysmorphic features.[23, 24]

CDGs are divided into two classes: CDG1 defects include those associated with mutations that affect the assembly of the dolichol-linked tetradecasaccharide. CDG2 diseases are associated with mutations in the enzymes involved in processing of the oligosaccharide after it has been transferred into the polypeptide.[23, 25, 26]

Currently, six CDG1 diseases are known. Three of these are associated with enzymes involved in the assembly of the tetradecasaccharide, and the other three are associated with enzymes involved in the synthesis of the monosaccharide building blocks.

Substrate specificity

Oligosaccharyl transferase recognizes a tripeptide sequence (Asn-Xaa-Thr/Ser) where the Asn is located one residue away from a hydroxy amino acid, Ser or Thr (see Figure 1.2). A statistical study on glycoproteins has shown that Thr containing sequences are approximately three times more likely to be glycosylated than Ser containing analogs.[27] *In vitro*, sequences containing Thr are glycosylated 40-fold more efficiently than sequences containing Ser.[28] The central residue can be any of 20 natural amino acids except proline,[29-31] due to conformational

requirements. In fact, the exclusion of Pro may account for the fact that 10-30% of the NXT/S sequences remain unglycosylated.[27, 32] When the reaction occurs, the targeted glycosylation site is in relative proximity to the ER membrane, 12-14 residues away, and the polypeptide is still attached to the membrane-bound ribosome. Because of the relative proximity to the membrane the nascent polypeptide can only be partially folded at the time of glycosylation.[33] *In vitro*, a tripeptide is sufficient for recognition by OT, as long as both the amino and carboxy termini are capped to mimic an internal protein sequence.[34] It is also important to note that *in vitro*, the enzyme recognizes a truncated version of the oligosaccharide, dolichol-PP-$GlcNAc_2$, as the sugar substrate.[2, 35]

A wide variety of substrate analogs have been prepared to study the mechanism of OT, conformational and sequence requirements for *N*-linked glycosylation. Some of these tripeptides include asparagine surrogates, and others include modifications in the Thr of the NXT/S sequence. A summary of the results obtained for asparagine modifications is presented in Figure 1.3. Most of the compounds fail to bind OT (NB), demonstrating the enzyme specificity for asparagine.

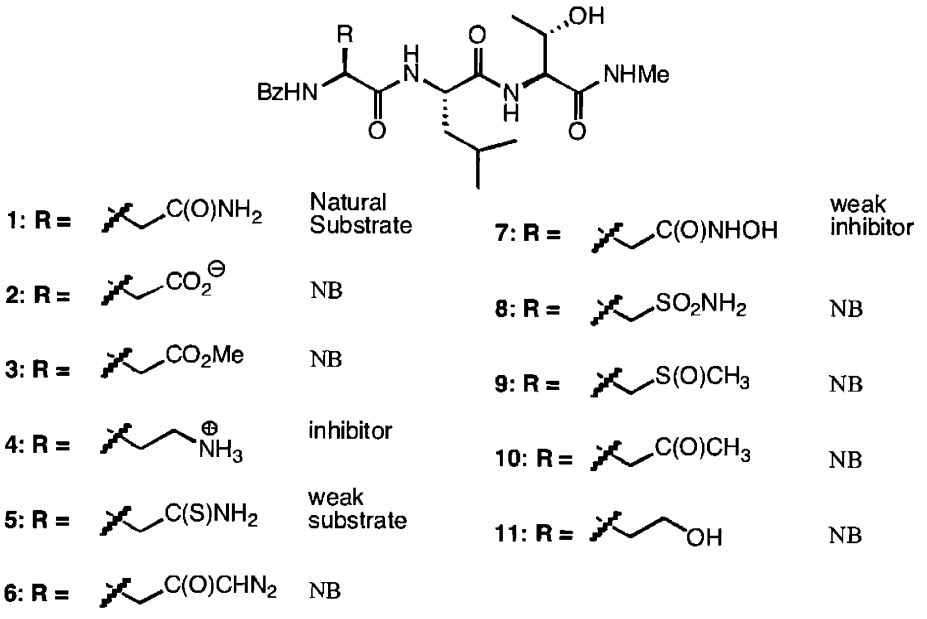

Figure 1.3. Summary of tripeptides with modifications at the asparagine position of the consensus sequence.[36-38]

Oligosaccharyl transferase is also highly specific for the hydroxy amino acid one residue away from the asparagine. Tripeptides of the sequence Bz-Asn-Gly-Yaa-NHMe, where a wide variety of natural and non-natural amino acids were introduced at the Yaa position, show that changing this essential hydroxy amino acid greatly affects enzyme recognition and catalysis.[37, 39] The introduction of Cys and L-β-hydroxynorleucine result in approximately 375-fold and 750-fold reduction in rate, respectively, while other residues where the hydroxy group has been substituted for other functional groups are not accepted by OT. The stereochemistry of the hydroxy amino acid is also an important recognition factor. Changing the stereochemistry of the α- or β-carbon is detrimental for binding, suggesting the presence of a defined hydrophobic binding pocket for this residue in OT.

Conformational relevance for *N*-linked glycosylation

The conformation of the polypeptide at the consensus sequence must play an important role in catalysis. The reactivity of the Asn amide is relatively low compared to other amino acids; therefore, the Asn must be activated for glycosylation to occur. As mentioned above, OT recognizes a tripeptide sequence for catalysis, NXT/S, and the hydroxyl amino acid one residue away from the Asn is essential for *N*-linked glycosylation. The two most likely conformations adopted by the tripeptide are the Asx-turn and the β-turn, shown in Figure 1.4. A β-turn is a compact structure formed by a hydrogen bond between the carbonyl preceding the Asn and the amide of the Thr. The Asx-turn is a more extended structure characterized by a hydrogen bond between the carbonyl on the side chain of the Asn and the Thr amide.[2]

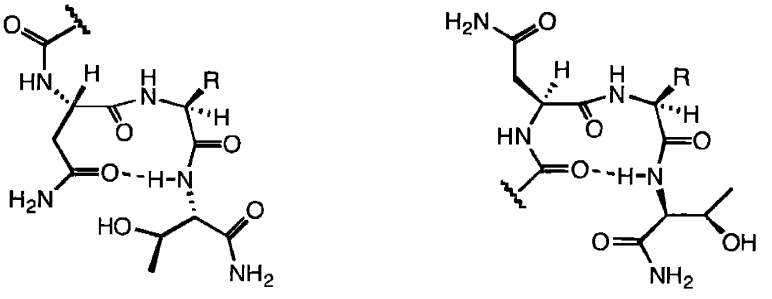

Figure 1.4. Hydrogen bonding pattern of the Asx-turn and the β-turn.

A statistical survey of globular proteins has shown that 55% of all hydrogen bonds to the side chain carbonyl of the Asn are provided by the backbone amide of the (i + 2) residue.[40] Also, another study shows that ~18% of all Asn and Asp residues in proteins appear to be involved in Asx-turns.[41] Moreover, it has been shown, through NMR studies, that an unglycosylated peptide (based on the A282-288 sequence of hemagglutinin), has an Asx-turn conformation in the site of glycosylation (Figure1.5A), while the glycosylated analog undergoes a complete chain reversal to a more compact type I β-turn conformation (Figure 1.5B).[42]

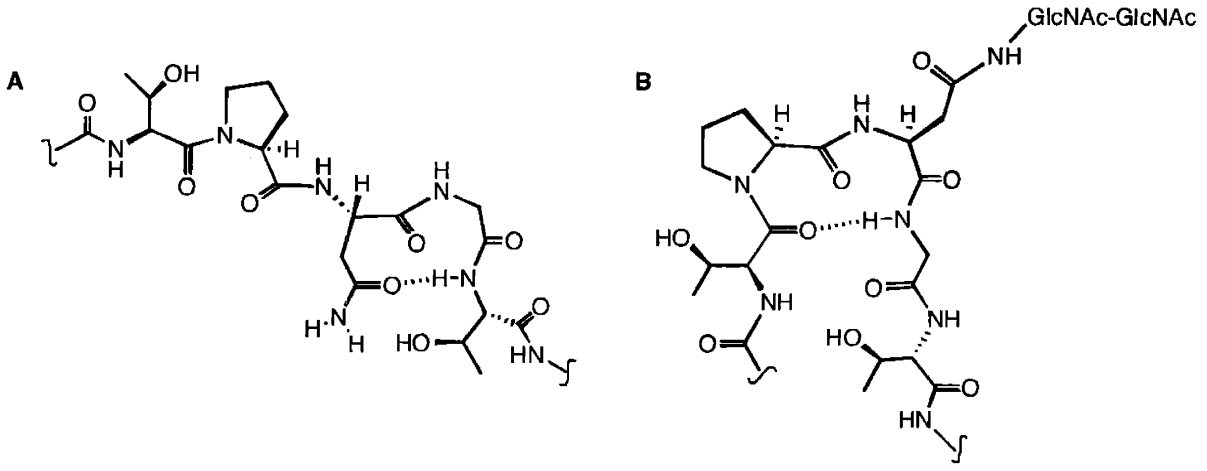

Figure 1.5. Glycosylation effects on the secondary sructure of a hemagglutinin peptide. **A.** The unglycosylated polypeptide acquires a more extended, Asx-turn conformation. **B.** The glycosylated polypeptide changes its conformation to a more compact β-turn conformation.[42]

Furthermore, kinetic analysis of two compounds with covalently constrained β-turn conformations showed no substrate behavior.[43] These data suggest that the Asx-turn is the preferred conformation of unglycosylated peptides. To provide more evidence, the Imperiali group synthesized a peptide with a constrained Asx-turn conformation (see Figure 1.6B). This peptide was a better substrate than the linear analog (Figure 1.6A) by a factor of ten, which indicated that the pre-organized Asx-turn enhanced the enzyme/substrate affinity.[44]

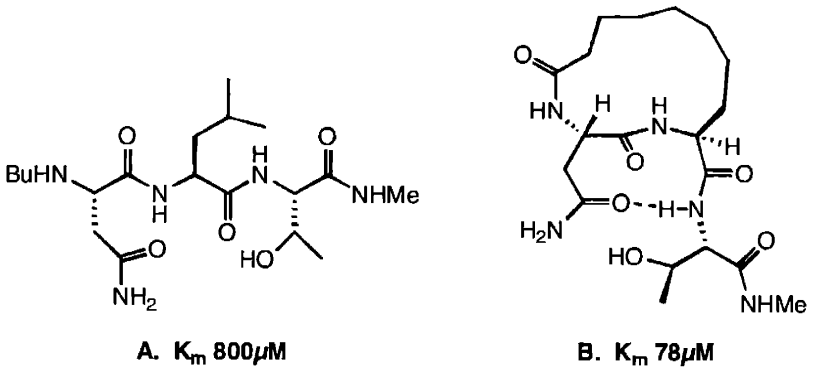

Figure 1.6. Effect of cyclization on substrate/enzyme affinity. **A.** Linear substrate has a K_m of 800μM. **B.** The cyclized substrate, with a constrained Asx-turn conformation has a higher affinity for the enzyme.

Proposed mechanisms for asparagine-linked protein glycosylation

Oligosaccharyl transferase is a complex multimeric membrane bound protein that catalyzes a reaction essential for life, the synthesis of glycoproteins. Understanding how such an important process occurs is of great interest to the scientific community. The development of different substrate analogs or inhibitors of OT provided enough information from which to propose a mechanism for *N*-linked glycosylation.

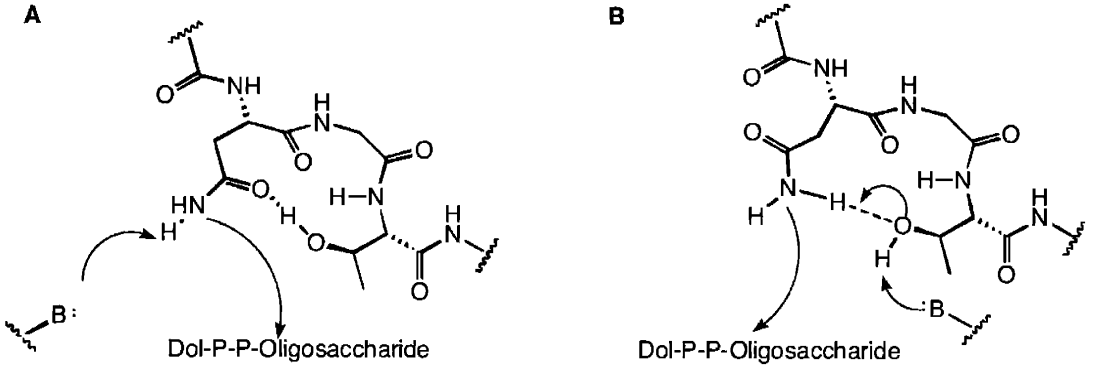

Figure 1.7. Proposed mechanisms of *N*-linked glycosylation according to: **A.** Marshall[29] and **B.** Bause[28]

Initially, Marshall[29] and Bause[28] proposed mechanisms in which an intermediate with a negative charge at the nitrogen of the Asn side chain is generated (see Figure 1.7). Tripeptides in which the Asn side chain was substituted with groups having different ionization properties were synthesized (see Table 1.1). Compounds with an Asp (peptide **2** and Tyr-Asp-Leu-Thr-Ser-Val) instead of an Asn in the consensus sequence should mimic the negative charge distribution

proposed by Marshall and Bause et al., and act as competitive inhibitors of OT. When assayed against porcine liver OT, the peptides did not show any inhibitory activity at high concentrations, suggesting that a negatively charged intermediate is not formed during the course of the *N*-linked glycosylation reaction.

Peptide **4** (Table 1.1), containing a α,γ-diaminobutanoic acid (Dab) in place of the Asn, showed a K_i similar to the K_M of the minimal tripeptide substrate. This compound is not capable of adopting an Asx-turn conformation because it does not have a carbonyl functionality, but it has a much lower pK_a and this increase in acidity seems to compensate for the lack of a stabilized Asx-turn structure. Peptide **5**, containing a thioasparagine in place of the Asn, is a substrate for porcine OT, although the relative maximal velocity is 8.4% when compared to peptide **1** (natural substrate). The sulfur substitution allows the peptide to obtain an Asx-turn conformation, although it might induce steric perturbations due to its larger bond size (C=S > C=O) and atomic radius when compared to the corresponding carboxamide. Also, the basicity of the sulfur is lower than that of the oxygen; this affects the hydrogen bonding capabilities of the thioasparagine and may account for its lower rate of turnover.[36]

Table 1.1. Kinetic analysis of substrate analogs with porcine OT[36]

Peptide	Apparent K_M (mM)	Relative V (%)[a]	K_i (mM)
Bz-Asn-Leu-Thr-NHMe (**1**)	0.24	100	
Bz-Asp-Leu-Thr-NHMe (**2**)			>10[b]
Bz-Asp(Oγ Me)-Leu-Thr-NHMe (**3**)			>10[b]
Bz-Dab-Leu-Thr-NHMe (**4**)			1.0
Bz-Asn(γS)-Leu-Thr-NHMe (**5**)	0.26	8.4	

a) Peptide 1 as standard; b) no inhibition below 5 mM.

As mentioned earlier, OT has a higher affinity for peptides constrained into an Asx-turn conformation. The Imperiali group has proposed a mechanism in which this type of turn assists in activating the Asn carboxamide.[36] As shown in Figure 1.8, protonation of the side chain carbonyl group is facilitated by the hydrogen bonding array provided by the Asx-turn. Simultaneously, the amide is deprotonated by an enzyme active site base, which leads to tautomerization of the carboxamide to an imidol species. This neutral nucleophilic intermediate can now attack the lipid-linked oligosaccharide to form the glycopeptide. This mechanism takes

into consideration the primary sequence and conformational requirements for glycosylation. Furthermore, it suggests that the probability of an NXT/S to be glycosylated depends on the ability of the substrate to adopt an Asx-turn conformation. Additional insight into the mechanism of OT, provided by product inhibitors of the enzyme, will be provided in Chapter 3.

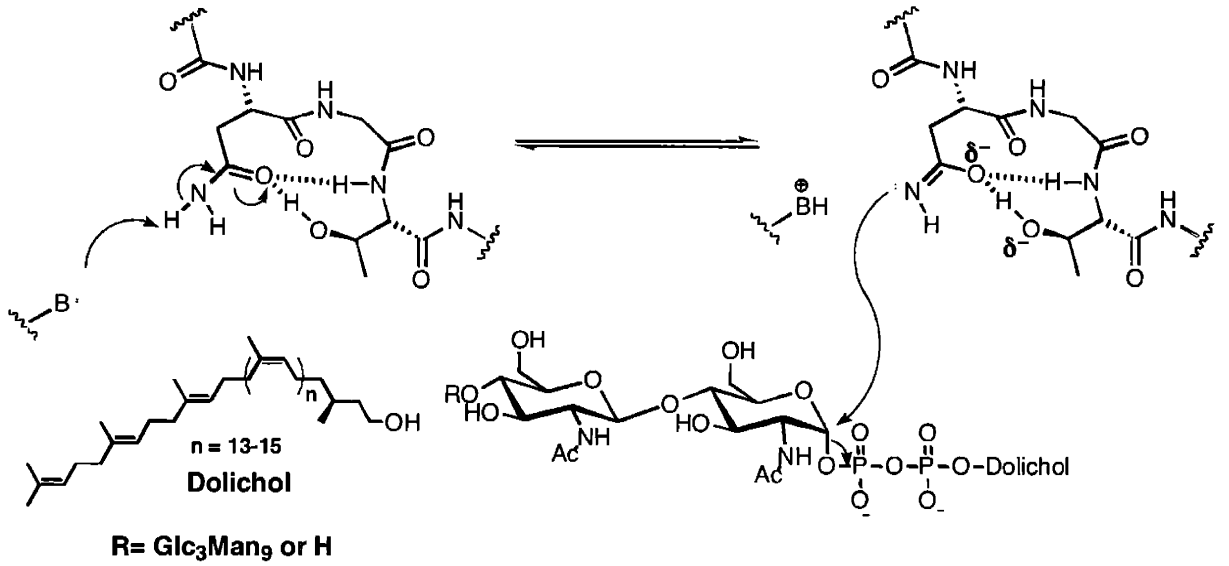

Figure 1.8. Mechanism proposed by Imperiali et al.[36] The Asx-turn assists in activating the side chain of the Asn.

Extended binding determinants of OT

It has been demonstrated that the pre-organization provided by the Asx-turn enhances enzyme-substrate affinity by placing the asparagine side chain in proximity to the required hydroxy amino acid.[44, 45] Also, statistical studies on *N*-linked glycoproteins suggest that glycosylation is modulated by amino acids beyond the consensus sequence.[27] These observations gave rise to studies to determine the extended binding determinants that would favor the interaction of the peptide substrate with the enzyme.

In an improved solid phase synthesis approach, the Imperiali group introduced a constrained Asx-turn conformation into inhibitors by the incorporation of a protected cysteine [Fmoc-Cys(S-S-*tert*-butyl)] as the central residue of the consensus sequence. After selective deprotection on the resin, cyclization was effected via alkylation of an *N*-terminal 6-bromohexanoyl moiety. Incorporation of the unnatural amino acid α,γ-diaminobutanoic acid at

the Asn position in the NXT sequence produced an inhibitor for OT. Introduction of the two most probable residues (Val-Thr) at the positions following the consensus sequence and a *p*-nitrophenylalanine, used for quantification purposes, yielded a potent, slow, tight binding inhibitor for oligosaccharyl transferase, with a K_i of 37 nM (see Figure 1.9).[45]

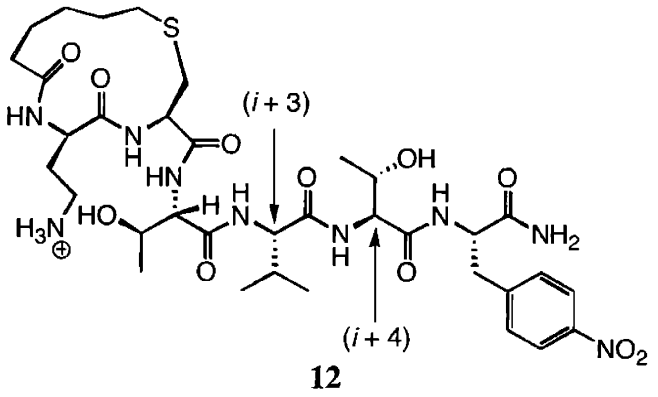

12

Figure 1.9. Structure of the most potent inhibitor of *N*-linked glycosylation (peptide **12**). The Val (*i* + 3) and Thr (*i* + 4) positions where substituted with hydrophobic, hydrophilic, basic and acidic residues to study the extended binding determinants of OT.[45, 46]

A small library of peptides was synthesized, in which the residues in the positions corresponding to the Val-Thr, (*i* + 3) and (*i* + 4) respectively, were substituted with acidic (Glu), basic (Lys), hydrophobic (Val) or hydrophilic and neutral (Thr) residues. The peptides were tested with both *S. cerevisiae* and porcine liver OT in competitive assays against the tripeptide substrate Bz-Asn-Leu-Thr-NHMe. From the kinetic data we can conclude that the amino acids at positions (*i* + 3) and (*i* + 4) which provide an inhibitor with a higher affinity for OT are Val and Thr, respectively. Also, the enzyme does not tolerate basic and acidic amino acids at these positions. Finally, in general, the inhibitors are more potent against yeast OT than against porcine OT.[46]

Chapter 2 will discuss further studies directed toward determining extended binding determinants for OT.

In vivo inhibitors of *N*-linked glycosylation

The development of specific and potent enzyme inhibitors has been an extremely powerful tool that has provided insight into the mechanisms of key biological transformations, as well as invaluable information about the implications of specific biological processes.[47] *N*-linked glycosylation is one of the most complex protein modifications in eukaryotic systems[1], but currently the only bioavailable inhibitor of this process is tunicamycin, a microbial product[48-51]. However, tunicamycin is neither a specific nor an immediate inhibitor of *N*-linked glycosylation; it inhibits the first step in the biosynthesis of the oligosaccharide (see Figure 1.10).[52-58] This step involves the transfer of *N*-acetylglucosamine-1-phosphate from UDP-*N*-acetylglucosamine to dolichyl-phosphate, to produce dolichyl pyrophosphate-*N*-acetylglucosamine, a reaction catalyzed by UDP-*N*-acetylglucosamine: dolichyl-phosphate *N*-acetylglucosamine-1-phosphate transferase.[49] As seen in Figure 1.10, the following 13 sugars in the oligosaccharide are added one by one in a sequential manner, so that the process inhibited by tunicamycin occurs fourteen metabolic steps before the actual *N*-linked glycosylation reaction occurs.[59]

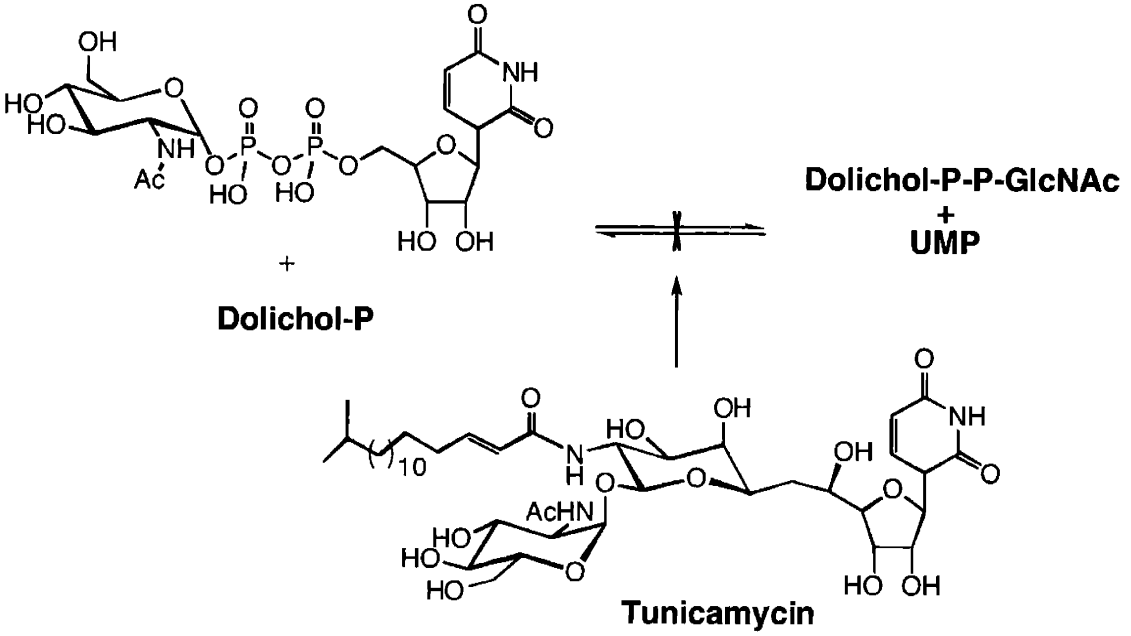

A

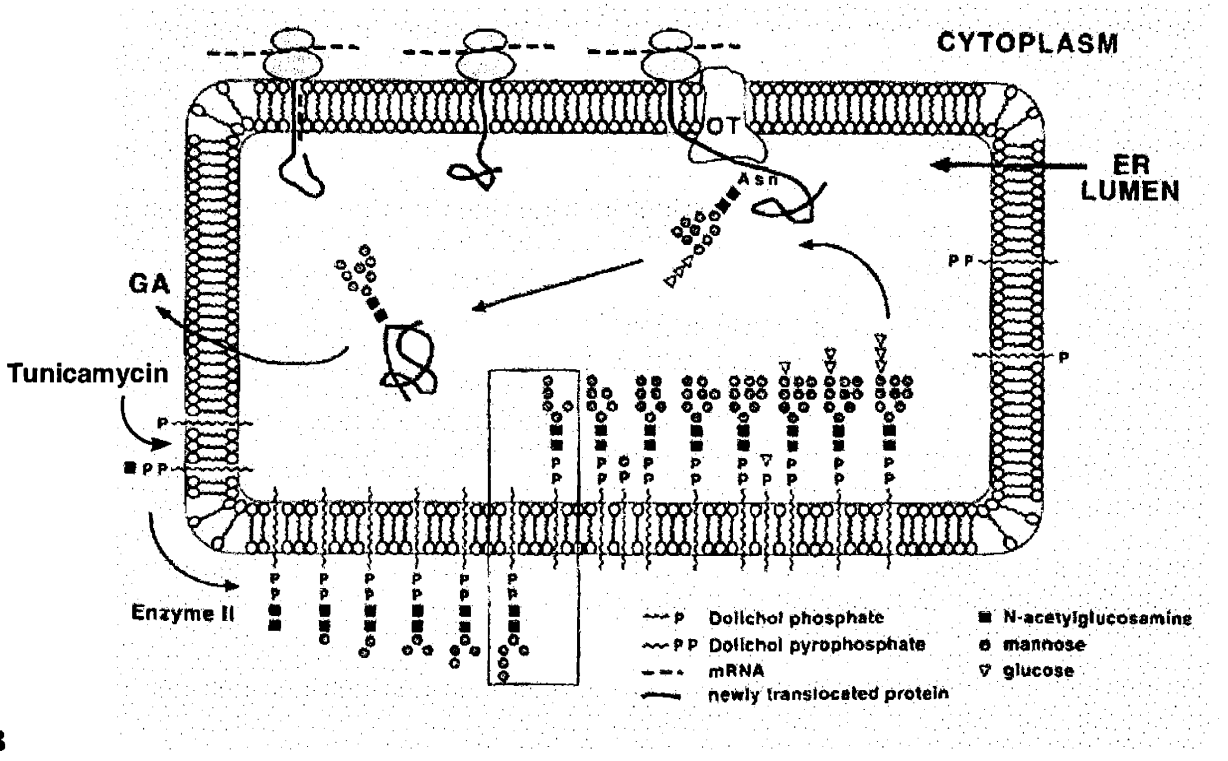

B

Figure 1.10.A. The reaction inhibited by tunicamycin. **B.** Schematic representation of the dolichol pathway (biosynthesis of the dolichol-linked tetradecasaccharide), followed by *N*-linked glycosylation

Since tunicamycin targets such an early event, it takes several cell cycles to completely deplete the cell of its sugar donor supply, and therefore, affect *N*-linked glycosylation.[51] In summary, the microbial product tunicamycin does not directly target OT and its effect on glycosylation is not immediate.

Other available glycosylation inhibitors include castanospermine, deoxymannojirimycin and deoxynojirimycin, but these inhibitors target enzymes involved in the maturation of the glycoprotein, after the core tetradecasaccharide has been transferred (Figure 1.11). Deoxynojirimycin is a competitive inhibitor of glucosidases I and II.[60, 61] Deoxymannojirimycin is a competitive inhibitor of mammalian Golgi α-mannosidase I.[62-64] Castanospermine inhibits glycoprotein processing by inhibiting α- and β-glucosidases, glucosidase I, β-mannosidase and β-xylosidase.[65, 66]

.

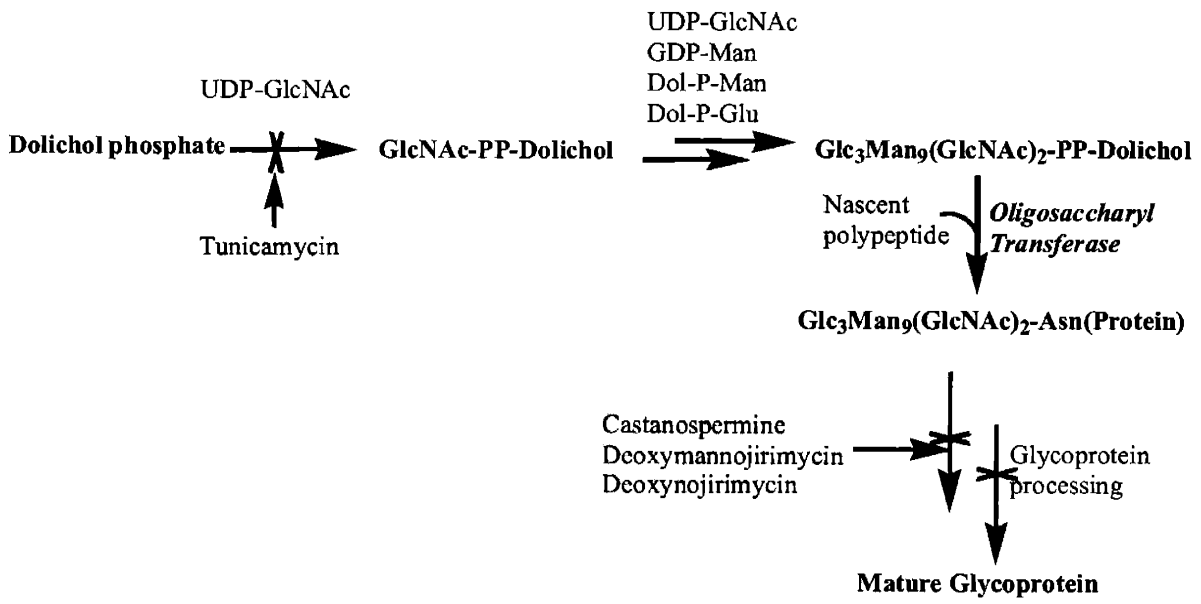

Figure 1.11. Different glycosylation inhibitors. The only bioavailable inhibitor of N-linked glycosylation is tunicamycin. Other inhibitors target steps in the maturation of the glycoprotein.

The Imperiali group has synthesized a potent peptide that inhibits oligosaccharyl transferase purified from the yeast *S. cerevisiae* and from porcine liver.[45, 46] In the attempt to make peptide **12** a bioavailable inhibitor, the cyclic hexapeptide was attached to a transporter associated with antigen processing (TAP) sequence, and to a cell permeable tag.[67] The TAP sequence targets a specific channel in the membrane of the ER, the TAP receptor. The targeted channel translocates peptides, which are destined to bind and stabilize the major histocompatibility complex (MHC) class I proteins, from the cytosol into the lumen of the ER.[68] This ATP dependent process requires the recognition sequence to be at the *C*-terminus of the peptides; sequences of 8-16 amino acids are optimal for translocation.[69] Asparagine-linked glycosylation of TAP peptides has been shown to serve as an ER retention device and allows measurement of the translocated peptides.[70]

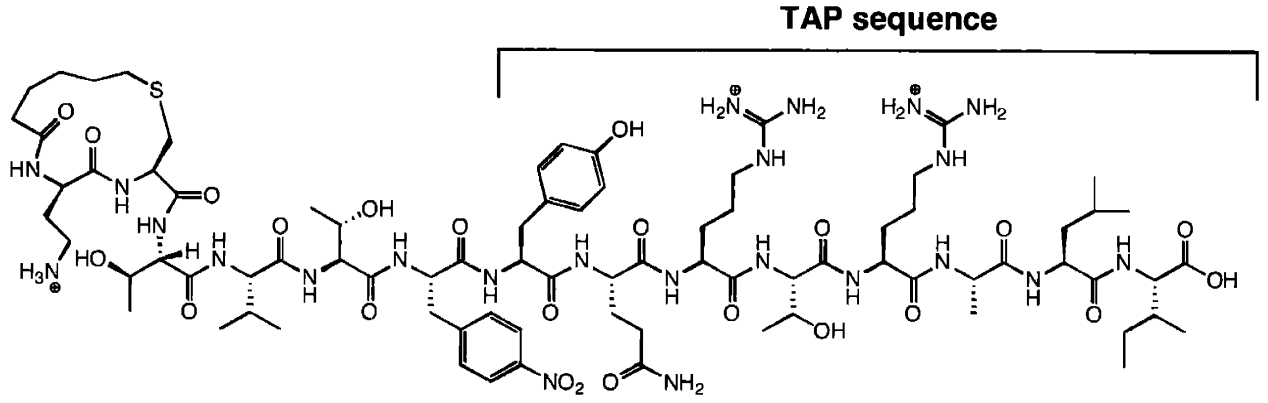

13

The cyclic inhibitor **12** was synthesized at the *N*-terminus of an eight amino acid sequence that was shown to be optimal for mouse TAP translocators, to produce peptide **13**. This peptide retained its potency against solubilized yeast microsomes (K_i = 97 nM). When assayed against intact ER membranes obtained from mouse liver, spleen and thymus, the inhibitor-TAP peptide failed to show inhibition. The analogous substrate with the same sequence as peptide **13**, where the Dab was substituted with an Asn, was successfully translocated and glycosylated in the same system. Peptide **13** was assayed against solubilized mouse microsomes and inhibition was observed, obtaining a K_i of 3.8 μM when using Bz-NLT-NHMe as a substrate. Therefore, the lack of inhibition was attributed to a failure in translocation, which was thought to be due to the extra charge in the side chain of the Dab.[67]

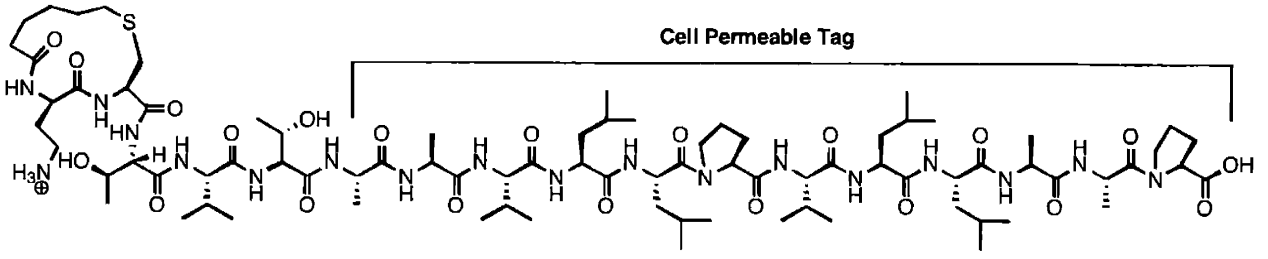

14

The cell permeable tag used in peptide **14** is based on a modified hydrophobic region of the signal sequence of the Kaposi fibroblast growth factor.[71] This sequence has been used as a carrier of many cell permeable peptides, where the size of the cargo molecule does not seem to

be relevant.[72] The twelve residue sequence forms an α-helix that is thought to interact strongly with the membrane bilayer, which results in a passive transport of the sequence and its cargo across the cellular membrane.[73]

Peptide **14** retained its potency when assayed *in vitro* against *S. cerevisiae* OT (K_i = 41 nM), even though a twelve residue sequence was added at the *C*-terminus of the inhibitor. This inhibitor was assayed using intact ER organelles and showed concentration-dependent inhibition of OT. The K_i and IC_{50} were determined using either Bz-NLT-NHMe or a TAP sequence (Tyr-**Asn-Arg-Thr**-Arg-Ala-Leu-Ile) as the substrate, yielding an IC_{50} and K_i of 3.2 μM and 2.6 μM for the TAP substrate, and 0.5 μM and 0.05 μM for the NLT substrate. However, no inhibition was observed when the peptide was assayed with intact cells using concentrations of up to 100 μM, suggesting that the peptide could not cross the cellular membrane efficiently.[67]

Designing bioavailable inhibitors

The potential for intracellular therapeutic use of peptides, proteins, and oligonucleotides has been limited by the impermeable nature of the cell membrane to these compounds.[74] A wide variety of methods have been proposed for the delivery of proteins and other macromolecules into living cells for either experimental or therapeutic uses. These active transport methods include microinjection, scrape loading, electroporation, liposomes,[75-81] bacterial toxins,[82-84] and receptor-mediated endocytosis.[85-90]

A major effort in many laboratories has been devoted to the development of peptide mimetics to produce molecules that can diffuse through the cellular membrane passively. Potent enzyme inhibitors and receptor antagonists have been obtained from these efforts. Many of these compounds resemble the peptides they were derived from, with one or two residues replaced by an organic compound whose function is to span one or more peptide units of a given sequence.[91] Others replace the peptide backbone by a nonpeptidic framework.[92, 93] The removal of peptide bonds in compounds containing dipeptide mimetics may significantly enhance their bioavalability and metabolic stability. Compounds have been categorized into three main types: dipeptide isosteres, lactam-constrained mimetics, and torsionally constrained mimetics (see

Figure 1.12).[94] Dipeptide isosteres are defined by the isosteric replacement of the peptide backbone. They include mimetics such as ketomethylene derivatives,[95] (E)-olefin isosteres,[96] aminomethylene,[97] hydroxylethyl,[98] and thiomethylene[99] derivatives.

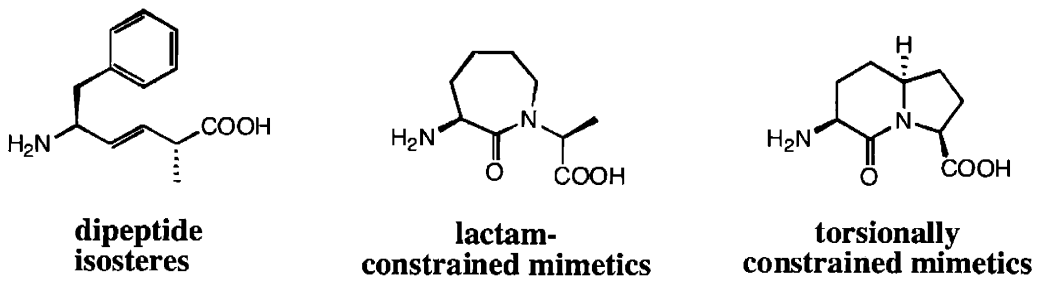

dipeptide isosteres **lactam-constrained mimetics** **torsionally constrained mimetics**

Figure 1.12. Examples of the three main types of dipeptide mimetics.

Another method for passive transport is the use of protein translocation domains (PTDs). PTDs are small portions of proteins, 9-30 amino acids in length, that have been identified as capable of crossing biological membranes efficiently.[100, 101] These domains seem to target the lipid bilayer directly; they have not been associated to any receptor or transporter and the mechanism they use to translocate through the membrane is not fully understood (see Figure 1.13). A wide variety of hydrophilic proteins, DNA, or other compounds, could be delivered inside the cell by linking them covalently to PTDs.[100, 102-110]

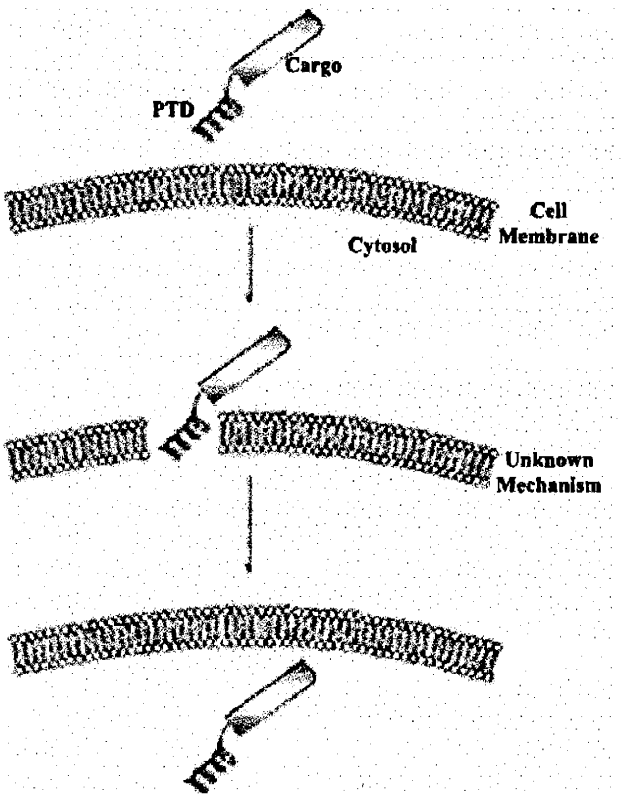

Figure 1.13. Transport of different cargo molecules into the cell through the use of PTDs. The PTD interacts with the cell membrane and translocates its cargo to the interior of the cell.

Some of the PTDs are comprised only of hydrophobic amino acids.[111, 112] Others, such as the Tat fragment,[113] the Penetratin,[114] the Transportan,[115] VP-22, [116] the Loligomer,[117] and the arginine peptide,[118, 119] are composed of highly positively charged sequences. Attachment of our inhibitors to a protein transduction domain could transport the peptides into the cells. We know from previous studies[67] that the hydrophobic sequences were not efficient in transporting the inhibitors into the cells and into the lumen of the ER. In fact, other studies suggest that the Penetratin sequence is more efficient in transporting peptides into the cell.[120]

The purpose of the work described herein is to develop peptides capable of inhibiting OT *in vivo*. The targeted inhibitors would have to be able to cross the cellular membrane through passive transport. For this purpose, peptides that include hydrophobic groups have been synthesized. Also, the synthesis of peptidomimetics will be presented. These peptidomimetics should be more hydrophobic than the parent peptides, since they have a reduced amide content. The reduced amide content should also make these compounds more stable to degradation due to

cytosolic proteases in the cellular environment, allowing them to reach the ER, cross its membrane bilayer and access the active site of OT.

We will also present the synthesis of inhibitors attached to PTDs. Active targeting of inhibitors to the ER will be pursued through the use of an ER retrieval sequence attached to the *C*-terminus of the peptides. The results of *in vitro* experiments to determine the binding constant of inhibitors against yeast and/or porcine OT will be presented. *In vivo* assays to determine the membrane permeability of the inhibitors, and their activity against OT from mammalian cells will be presented. Fluorescein and BODIPY fluorophores were used to determine the membrane permeability of some of the inhibitors.

References

1. Varki, A., "Biological Roles of Oligosaccharides: All of the Theories Are Correct". *Glycobiology*, **1993**. *3*, 97-130.

2. Imperiali, B. and Hendrickson, T.L., "Asparagine-Linked Glycosylation: Specificity and Function of Oligosaccharyl Transferase". *Bioorg. Med. Chem.*, **1995**. *3*(12), 1565-1578.

3. Opdenakker, G., Rudd, P.R., Ponting, C.P., and Dwek, R.A., "Concepts and Principles of Glycobiology". *FASEB*, **1993**. *7*, 1330-1337.

4. Gleeson, P.A., Teasdale, R.D., and Burke, J., "Targeting of Proteins to the Golgi-Apparatus". *Glycoconjugate J.*, **1994**. *11*(5), 381-394.

5. Wagner, G. and Wyss, D.F., "Cell-Surface Adhesion Receptors". *Curr. Opin. Struct. Biol.*, **1994**. *4*(6), 841-851.

6. Imperiali, B. and Rickert, K.W., "Conformational Implications of Asparagine-Linked Glycosylation". *Proc. Natl. Acad. Sci. USA*, **1995**. *92*, 97-101.

7. Riederer, M.A. and Hinnen, A., "Removal of *N*-Glycosylation Sites of the Yeast Acid-Phosphatase Severely Affects Protein Folding". *J. Bacteriol.*, **1991**. *173*(11), 3539-3546.

8. Duranti, M., Gius, C., Sessa, F., and Vecchio, G., "The Saccharide Chain of Lupin Seed Conglutin Gamma Is Not Responsible for the Protection of the Native Protein from

Degradation by Trypsin, but Facilitates the Refolding of the Acid-Treated Protein to the Resistant Conformation". *Eur. J. Biochem.*, **1995**. *230*, 886-891.

9. Allen, S., Naim, H.Y., and Bulleid, N.J., "Intracellular Folding of Tissue-Type Plasminogen Activator". *J. Biol. Chem.*, **1995**. *270*, 4797.

10. Wenzel-Seifert, K. and Seifert, R., "Critical Role of *N*-Terminal *N*-Glycosylation for Proper Folding of the Human Formyl Peptide Receptor". *Biochem. Biophys. Res. Commun.*, **2003**. *301*, 693-698.

11. Rudd, P.M. and Dwek, R.A., "Glycobiology - a Coming of Age". *Chem. Ind.*, **1991**. *18*, 660-663.

12. Wilson, I.B.H., Gavel, Y., and von Heijne, G., "Amino Acid Distribution around *O*-Linked Glycosylation Sites". *Biochem. J.*, **1991**. *275*, 529-534.

13. Englund, P.T., "The Structure and Biosynthesis of Glycosyl Phosphatidylinositol Protein Anchors". *Ann. Rev. Biochem.*, **1993**. *62*, 121-138.

14. Young, B., Craven, R., Reid, P., Willer, M., and Stirling, C., "Sec63p and Far2p Are Required for Translocation of Srp-Dependent Precursors into the Yeast Endoplasmic Reticulum *In Vivo*". *EMBO J.*, **2001**. *20*, 262-271.

15. Silberstein, S. and Gilmore, R., "Biochemistry, Molecular Biology, and Genetics of the Oligosaccharyltransferase". *FASEB J.*, **1996**. *10*, 849-858.

16. Ellgard, L. and Helenius, A., "ER Quality Control: Towards an Understanding at the Molecular Level". *Curr. Opin. Cell Biol.*, **2001**. *13*, 431-437.

17. O'Connor, S.E. and Imperiali, B., "Modulation of Protein Structure and Function by Asparagine-Linked Glycosylation". *Chem. Biol.*, **1996**. *3*, 803-812.

18. Tifft, C.J., Proia, R.L., and Camerini-Otero, R.D., "The Folding and Cell Surface Expression of CD4 Requires Glycosylation". *J. Biol. Chem*, **1993**. *267*, 3268-3273.

19. Li, Y., Luo, L., Rasool, N., and Yong Kang, C., "Glycosylation Is Necessary for the Correct Folding of Human Immunodeficiency Virus Gp120 and CD4 Binding". *J. Virol.*, **1993**. *67*, 584-588.

20. Dirckx, L., Lindemann, D., Ette, R., Manzoni, C., Moritz, D., and Mous, J., "Mutation of Conserved *N*-Glycosylation Sites around the CD4 Binding Site of Human

Immunodeficiency Virus Type 1 Gp120 Affects Viral Infectivity". *Virus Res.*, **1990**. *18*, 9-20.

21. Dempski, R.E. and Imperiali, B., "Oligosaccharyl Transferase: Gatekeeper to the Secretory Pathway". *Curr. Opin. Chem. Biol.*, **2002**. *6*, 844-850.

22. Marek, K., Vijay, I.K., and Marth, J., "A Recessive Deletion in the GlcNAc-1-Phosphotransferase Gene Results in Periimplantation Embryonic Lethality". *Glycobiology*, **1999**. *9*, 1263-1271.

23. Matthijs, G. and Jaeken, J., "Congenital Disorders of Glycosylation". *Ann. Rev. of Genom. and Hum. Genet.*, **2001**. *2*, 129-151.

24. Barone, R., Pavone, V., Pennisi, P., Fiumara, A., and Fiore, C.E., "Assessment of Skeletal Status in Patients with Congenital Disorder of Glycosylation Type Ia". *International J. of Tissue Reactions- Experimental and Clinical Aspects*, **2002**. *24*(1), 23-28.

25. Carchon, H., Van Schaftingen, E., Matthijs, G., and Jaeken, J., "Carbohydrate-Deficient Glycoprotein Syndrome Type Ia (Phosphomannomutase-Deficiency)". *Biochim. Biophys. Acta*, **1999**. *1455*, 155-165.

26. Freeze, H.H. and Aebi, M., "Molecular Basis of Carbohydrate-Deficient Glycoprotein Syndromes Type I with Normal Phosphomannomutase Activity". *Biochim. Biophys. Acta*, **1999**. *1455*, 167-178.

27. Gavel, Y. and von Heijne, G., "Sequence Differences between Glycosylated and Non-Glycosylated Asn-X-Thr/Ser Acceptor Sites: Implications for Protein Engineering". *Protein Eng.*, **1990**. *3*(5), 433-442.

28. Bause, E., "Model Studies on *N*-Glycosylation of Proteins". *Biochem. Soc. Trans.*, **1984**. *12*, 514-517.

29. Marshall, R.D., "The Nature and Metabolism of the Carbohydrate-Peptide Linkages of Glycoproteins". *Biochem. Soc. Symp.*, **1974**. *40*, 17-26.

30. Bause, E., "Structural Requirements of *N*-Glycosylation of Proteins. Studies with Proline Peptides as Conformational Probes". *Biochem. J.*, **1983**. *209*, 331-336.

31. Roitsch, T. and Lehle, L., "Structural Requirements for Protein *N*-Glycosylation. Influence of Acceptor Peptides on Cotranslational Glycosylation of Yeast Invertase and Site-Directed Mutagenesis around a Sequon Sequence". *Eur. J. Biochem.*, **1989**. *181*, 525-529.

32. Mononen, I. and Karjalainen, E., "Structural Comparison of Protein Sequences around Potential *N*-Glycosylation Sites". *Biochim. Biophys. Acta*, **1984**. *788*, 364-367.

33. Nilsson, I. and von Heijne, G., "Determination of the Distance between the Oligosaccharyl Transferase Active Site and the Endoplasmic Reticulum Membrane". *J. Biol. Chem.*, **1993**. *268*, 5798-5801.

34. Welply, J.K., Shenbagamurthi, P., Lennarz, W.J., and Naider, F., "Substrate Recognition by Oligosaccharyltransferase: Studies on Glycosylation of Modified Asn-X-Thr/Ser Tripeptides". *J. Biol. Chem.*, **1983**. *258*, 11856-11863.

35. Sharma, C.B., Lehle, L., and Tanner, W., "*N*-Glycosylation of Yeast Proteins: Characterization of the Solubilized Oligosaccharyl Transferase". *Eur. J. Biochem.*, **1981**. *116*, 101-108.

36. Imperiali, B., Shannon, K.L., Unno, M., and Rickert, K.W., "A Mechanistic Proposal for Asparagine-Linked Glycosylation". *J. Am. Chem. Soc.*, **1992**. *114*, 7944-7945.

37. Bause, E., Breuer, W., and Peters, S., "Investigation of the Active Site of Oligosaccharyltransferase from Pig Liver Using Synthetic Tripeptides as Tools". *Biochem. J.*, **1995**. *312*, 979-985.

38. Xu, T., Werner, R.M., Lee, K.-C., Fettinger, J.C., Davis, J.T., and Coward, J.K., "Synthesis and Evaluation of Tripeptides Containing Asparagine Analogues as Potential Substrates or Inhibitors of Oligosaccharyltransferase". *J. Org. Chem.*, **1998**. *63*, 4767-4778.

39. Breuer, W., Klein, R.A., Hardt, B., Bartoschek, A., and Bause, E., "Oligosaccharyltransferase Is Highly Specific for the Hydroxy Amino Acid in Asn-Xaa-Thr/Ser". *FEBS Lett.*, **2001**. *501*, 106-110.

40. Baker, E.N. and Hubbard, R.E., "Hydrogen Bonding of Globular Proteins". *Prog. Biophys. Mol. Biol.*, **1984**. *44*, 97-179.

41. Abbadi, A., Mcharfi, M., Aubry, A., Premilat, S., Boussard, G., and Marraud, M., "Involvement of Side Functions in Peptide Structures: The Asx Turn. Occurrence and Conformational Aspects". *J. Am. Chem. Soc.*, **1991**. *113*(7), 2729-2735.

42. O'Connor, S.E. and Imperiali, B., "Conformational Switching by Asparagine-Linked Glycosylation". *J. Am. Chem. Soc.*, **1997**. *119*, 2295-2296.

43. Imperiali, B., Shannon, K.L., and Rickert, K.W., "Role of Peptide Conformation in Asparagine-Linked Glycosylation". *J. Am. Chem. Soc.*, **1992**. *114*, 7942-7944.

44. Imperiali, B., Spencer, J.R., and Struthers, M.D., "Structural and Functional Characterization of a Constrained Asx-Turn Motif". *J. Am. Chem. Soc.*, **1994**. *116*, 8424-8425.

45. Hendrickson, T.L., Spencer, J.R., Kato, M., and Imperiali, B., "Design and Evaluation of Potent Inhibitors of Asparagine-Linked Glycosylation". *J. Am. Chem. Soc.*, **1996**. *118*, 7636-7637.

46. Kellenberger, C., Hendrickson, T.L., and Imperiali, B., "Structural and Functional Analysis of Peptidyl Oligosaccharyl Transferase Inhibitors". *Biochemistry*, **1997**. *36*, 12554-12559.

47. Silverman, R.B., *Enzyme Inhibition and Inactivation*, in *The Organic Chemistry of Drug Design and Drug Action*. 1992, Academic Press, Inc.: San Diego. p. 146-219.

48. Elbein, A.D., "The Tunicamycins: Useful Tools for Studies on Glycoproteins". *Trends Biochem. Sci.*, **1981**. *6*, 291-293.

49. Heifetz, A., Keenan, R.W., and Elbein, A.D., "Mechanism of Action of Tunicamycin on the UDP-GlcNAc:Dolichyl-Phosphate GlcNAc-1-Phosphate Transferase". *Biochemistry*, **1979**. *18*(11), 2186-2192.

50. Keller, R.K., Boon, D.Y., and Crum, F.C., "*N*-Acetylglucosamine-1-Phosphate Transferase from Hen Oviduct: Solubilization, Characterization, and Inhibition by Tunicamycin". *Biochemistry*, **1979**. *18*, 3946-3952.

51. Tamura, G., *Tunicamycin*. 1982, Tokyo: Japan Scientific Society Press.

52. Heifetz, A. and Elbein, A.D., "Solubilization and Properties of Mannose and *N*-Acetylglucosamine Transferases Involved in Formation of Polyprenyl-Sugar Intermediates". *J. Biol. Chem.*, **1977**. *252*, 3057-3063.

53. Struck, D.L. and Lennarz, W.J., "Evidence for the Participation of Saccharide-Lipids in the Synthesis of the Oligosaccharide Chain of Ovalbumin". *J. Biol. Chem.*, **1977**. *252*, 1007-1013.

54. Lehle, L. and Tanner, W., "The Specific Site of Tunicamycin Inhibition in the Formation of Dolichol-Bound *N*-Acetylglucosamine Derivatives". *FEBS Lett.*, **1976**. *71*, 167-170.

55. Tkacz, J.S. and Lampen, J.O., "Tunicamycin Inhibition of Polyisoprenyl *N*-Acetylglucosaminyl Pyrophosphate Formation in Calf-Liver Microsomes". *Biochem. Biophys. Res. Commun.*, **1975**. *65*(1), 248-257.

56. Kuo, S.C. and Lampen, J.O., "Tunicamycin: Inhibitor of Yeast Glycoprotein Synthesis". *Biochem. Biophys. Res. Commun.*, **1974**. *58*, 287-295.

57. Waechter, C.J. and Hartford, J.B., "Evidence for Enzymatic Transfer of *N*-Acetylglucosamine from UDP-*N*-Acetylglucosamine into Dolichol Derivatives and Glycoproteins by Calf Brain Membranes". *Arch. Biochem. Biophys.*, **1977**. *181*(1), 185-198.

58. Heifetz, A. and Elbein, A.D., "Biosynthesis of Man-Beta-GlcNAc-GlcNAc-Pyrophosphoryl-Polyprenol by a Solubilized Enzyme from Aorta". *Biochem. Biophys. Res. Commun.*, **1977**. *75*(1), 20-28.

59. Burda, P. and Aebi, M., "The Dolichol Pathway of *N*-Linked Glycosylation". *Biochim. Biophys. Acta*, **1999**. *1426*, 239-257.

60. Neverova, I., Scaman, C.H., Srivastava, O.P., Szweda, R., Vijay, I.K., and Palcic, M.M., "A Spectrophotometric Assay for Glucosidase I". *Anal. Biochem.*, **1994**. *222*(1), 190-195.

61. Yamashita, Y., Shimokata, K., Saga, S., Mizuno, S., Tsurumi, T., and Nishiyama, Y., "Rapid Degradation of the Heavy-Chain of Class-I Major Histocompatibility Complex Antigens in the Endoplasmic Reticulum of Human Cytomegalovirus-Infected Cells". *J. Virol.*, **1994**. *68*(12), 7933-7943.

62. Winchester, B., Barker, C., Baines, S., Jacob, G.S., Namgoong, S.K., and Fleet, G., "Inhibition of Alpha-L-Fucosidase by Derivatives of Deoxyfuconojirimycin and Deoxymannojirimycin". *Biochem. J.*, **1990**. *265*(1), 277-282.

63. Elbein, A.D., "Inhibitors of the Biosynthesis and Processing of *N*-Linked Oligosaccharide Chains". *Ann. Rev. Biochem.*, **1987**. *56*, 497-534.

64. Suzuki, S.S. and Piette, L.H., "Effect of Retinyl Acetate on the Assembly of the Fibronectin Extracellular-Matrix and the Processing of the Fibronecting Receptor Beta-Subunit of Confluent C3H/10TL/2 Mouse Embryo Fibroblasts". *J. Cell. Biochem.*, **1993**. *51*(2), 181-189.

65. Ahmed, S.P., Nash, R.J., Bridges, C.G., Taylor, D.L., Kang, M.S., Porter, E.A., and Tyms, A.S., "Antiviral Activity and Metabolism of the Castanospermine Derivative MDL-28,574 in Cells Infected with Herpes-Simplex Virus Type-2". *Biochem. Biophys. Res. Commun.*, **1995**. *208*(1), 267-273.

66. Bartlett, M.R.E., Warren, H.S., Cowden, W.B., and Parish, C.R., "Effects of the Antiinflammatory Compounds Castanospermine, Mannose-6-Phosphate and Fucoidan on Allograft-Rejection and Elicited Peritoneal Exudates". *Immunol. Cell Biol.*, **1994**. *72*(5), 367-374.

67. Eason, P.D. and Imperiali, B., "A Potent Oligosaccharyl Transferase Inhibitor that Crosses the Intracellular Endoplasmic Reticulum Membrane". *Biochemistry*, **1999**. *38*, 5430-5437.

68. Heemels, M.T. and Ploegh, H., "Generation, Translocation, and Presentation of MHC Class I-Restricted Peptides". *Ann. Rev. Biochem.*, **1995**. *64*, 463-491.

69. Momburg, F., Roelse, J., Hammerling, G.J., and Neefjes, J.J., "Peptide Size Selection by the Major Histocompatibility Complex-Encoded Peptide Transporter". *J. Exp. Med.*, **1994**. *179*(5), 1613-1623.

70. Heemels, M.T., Schumacher, T.N.M., Wonigeit, K., and Ploegh, H., "Peptide Translocation by Variants of the Transporter Associated with Antigen-Processing". *Science*, **1993**. *262*, 2059-2063.

71. Bovi, P.D., Curatola, A.M., Kern, F.G., Greco, A., Ittmann, M., and Basilico, C., "An Oncogene Isolated by Transfection of Kaposis-Sarcoma DNA Encodes a Growth Factor That Is a Member of the FGF Family". *Cell*, **1987**. *50*, 729-737.

72. Rojas, M., Donahue, J.P., Tan, Z., and Lin, Y.Z., "Genetic Engineering of Proteins with Cell Membrane Permeability". *Nat. Biotechnol.*, **1998**. *16*(4), 370-375.

73. Du, C., Yao, S., Rojas, M., and Lin, Y.Z., "Conformational and Topological Requirements of Cell-Permeable Peptide Function". *J. Pept. Res.*, **1998**. *51*(3), 235-243.

74. Fawell, S., Seery, J., Daikh, Y., Moore, C., Chen, L.L., Pepinsky, B., and Barsoum, J., "Tat-Mediated Delivery of Heterologous Proteins into Cells". *Proc. Natl. Acad. Sci., USA*, **1994**. *91*, 664-668.

75. Foldvari, M., Mezei, C., and Mezei, M., "Intracellular Delivery of Drugs by Liposomes Containing Po Glycoprotein from Peripheral Nerve Myelin into Human M21 Melanoma Cells". *J. Pharm. Sci.*, **1991**. *80*, 1020-1028.

76. Chakrabarti, R., Wylie, D.E., and Schuster, S.M., "Transfer of Monoclonal Antibodies into Mammalian Cell by Electroporation". *J. Biol. Chem.*, **1989**. *264*, 15494-15500.

77. Connor, J. and Huang, L., "Efficient Cytoplasmic Delivery of a Fluorescent Dye by pH-Sensitive Immunoliposomes". *J. Cell Biol.*, **1985**. *101*, 582-589.

78. Ortiz, D., Baldwin, M.M., and Lucas, J.J., "Transient Correction of Genetic Defects in Cultured Animal Cells by Introduction of Functional Proteins". *Mol. Cell. Biol.*, **1987**. *7*, 3012-3017.

79. McNeil, P.L., Murphy, R.F., Lanni, F., and Taylor, D., "A Method for Incorporating Macromolecules into Adherent Cells". *J. Cell Biol.*, **1984**. *98*, 1556-1564.

80. Renneisen, K., Leserman, L., Matthes, E., Schroder, H.C., and Muller, W.E., "Inhibition of Expression of Human Immunodeficiency Virus-I *In Vitro* by Antibody-Targeted Liposomes Containing Antisense RNA to the Eno Region". *J. Biol. Chem.*, **1990**. *265*, 16337-16342.

81. Wu, G.Y. and Wu, C.H., "Delivery Systems for Gene Therapy". *Biotherapy*, **1991**. *3*, 87-95.

82. Prior, T.I., Fitzgerald, D.J., and Pastan, I., "Barnase Toxin: A New Chimeric Toxin Composed of Pseudonomas Exotoxin A and Barnase". *Cell*, **1991**. *64*, 1017-1023.

83. Prior, T.I., Fitzgerald, D.J., and Pastan, I., "Translocation Mediated by Domain II of Pseudonomas Exotoxin A: A Transport of Barnase into the Cytosol". *Biochemistry*, **1992**. *31*, 3555-3559.

84. Stenmark, H., Moskaug, J.O., Madshus, I.H., Sandvig, K., and Olsnes, S., "Peptides Fused to the Amino-Terminal End of Diphtheria Toxin Are Translocated to the Cytosol". *J. Cell Biol.*, **1991**. *113*, 1025-1032.

85. Ishihara, H., Hara, T., Aramaki, Y., Tsuchiya, S., and Hosoi, K., "Preparation of Asialofetuin-Labeled Liposomes with Encapsulated Human Interferon-Gamma and Their Uptake by Isolated Rat Hepatocytes". *Pharm. Res.*, **1990**. *7*, 542-546.

86. Basu, S.K., "Receptor-Mediated Endocytosis of Macromolecular Conjugates in Selective Drug Delivery". *Biochem. Pharm.*, **1990**. *40*, 1941-1946.

87. Wu, G.Y. and Wu, C.H., "Evidence for Targeted Gene Delivery to HepG2 Hepatoma Cells *In Vitro*". *Biochemistry*, **1988**. *27*, 887-892.

88. Wilson, J.M., Grossman, M., Wu, C.H., Chowdhury, N.R., Wu, G.Y., and Chowdhury, J.R., "Hepatocyte-Directed Gene Transfer *In Vivo* Leads to Transient Improvement of Hypercholesterolemia in Low Density Lipoprotein Receptor-Defficient Rabbits". *J. Biol. Chem.*, **1992**. *267*, 963-967.

89. Leamon, C.P. and Low, P.S., "Delivery of Macromolecules into Living Cells: A Method That Exploits Folate Receptor Endocytosis". *Proc. Natl. Acad. Sci., USA*, **1991**. *88*, 5572-5576.

90. Leamon, C.P. and Low, P.S., "Cytotoxicity of Momordin-Folate Conjugates in Cultured Human Cells". *J. Biol. Chem.*, **1992**. *267*, 24966-24971.

91. Sharma, T.A., Carr, A.J., Davis, R.S., Reynolds, I.J., and Hamilton, A.D., "Aromatic Analogs of Arcaine Inhibit MK-801 Binding to the NMDA Receptor". *Bioorg. Med. Chem. Lett.*, **1998**. *8*(24), 3459-3464.

92. Olson, G.L., Bolin, D.R., Bonner, M.P., Bos, M., Cook, C.M., Fry, D.C., Graves, B.J., Hatada, M., Hill, D.E., Kahn, M., Madison, V.S., Rusiecki, V.K., Sarabu, R., Sepinwall, J., Vincent, G.P., and Voss, M.E., "Concepts and Progress in the Development of Peptide Mimetics". *J. Med. Chem.*, **1993**. *36*, 3039-3049.

93. Hirschmann, R., Nicolaou, K.C., Pietranico, S., Salvino, J., Leahy, E.M., Sprengeler, P.A., Furst, G., Smith, A.B., Strader, C.D., Cascieri, M.A., Candelore, M.R., Donaldson, C., Vale, W., and Maechler, L., "Nonpeptidal Peptidomimetics with a Beta-D-Glucose Scaffolding - A Partial Somatostatin Agonist Bearing a Close Structural Relationship to a Potent Selective Substance-P Antagonist". *J. Am. Chem. Soc.*, **1992**. *114*(23), 9217-9218.

94. Gillespie, P., Cicariello, J., and Olson, G.L., "Conformational Analysis of Dipeptide Mimetics". *Peptide Science*, **1997**. *43*, 191-218.

95. Almquist, R.G., Chao, W.R., Ellis, M.E., and Johnson, H.L., "Synthesis and Biological Activity of a Ketomethylene Analogue of a Tripeptide Inhibitor of Angiotensin Converting Enzyme". *J. Med. Chem.*, **1980**. *23*, 1392-1398.

96. Hann, M.M., Sammes, P.G., Kennewell, P.D., and Taylor, J.B., "On the Double-Bond Isostere of the Peptide-Bond - Preparation of an Enkephalin Analog". *J. Chem. Soc., Perkin Trans. 1*, **1982**. *1*, 307-314.

97. Szelke, M., Leckie, B., Hallett, A., Jones, D.M., Sueiras, J., Atrash, B., and Lever, A.F., "Potent New Inhibitors of Renin". *Nature*, **1982**. *299*, 555-557.

98. Evans, B.E., Rittle, K.E., Homnick, C.F., Springer, J.P., Hirshfield, J., and Veber, D.F., "A Stereocontrolled Synthesis of Hydroxyethylene Dipeptide Isosteres Using Novel, Chiral Aminoalkyl Epoxides and Gamma-(Aminoalkyl) Gamma-Lactones". *J. Org. Chem.*, **1985**. *50*(23), 4615-4625.

99. Spatola, A.F., Agarwal, N.S., Bettag, A.L., Yankeelov, J.A., Bowers, C.Y., and Vale, W.W., "Synthesis and Biological Activities of Pseudopeptide Analogues of LH-RH: Agonists and Antagonists". *Biochem. Biophys. Res. Commun.*, **1980**. *97*, 1014-1023.

100. Schwarze, S.R. and Dowdy, S.F., "*In Vivo* Protein Transduction: Intracellular Delivery of Biologically Active Proteins, Compounds and DNA". *Trends Pharm. Sci.*, **2000**. *21*, 45-48.

101. Tung, C.-H. and Weissleder, R., "Arginine Containing Peptides as Delivery Vectors". *Adv. Drug Delivery Rev.*, **2003**. *55*, 281-294.

102. Schwartz, J.J. and Zhang, S., "Peptide-Mediated Cellular Delivery". *Curr. Opin. Mol. Ther.*, **2000**. *2*, 162-167.

103. Kueltzo, L.A. and Middaugh, C.R., "Potential Use of Non-Classical Pathways for the Transport of Macromolecular Drugs". *Expert Opin. Invest. Drugs*, **2000**. *9*, 2039-2050.

104. Fischer, P.M., Krausz, E., and Lane, D.P., "Cellular Delivery of Impermeable Effector Molecules in the Form of Conjugates with Peptides Capable of Mediating Membrane Translocation". *Bioconjugate Chem.*, **2001**. *12*, 825-841.

105. Hawiger, J., "Non-Invasive Intracellular Delivery of Functional Peptides and Proteins". *Curr. Opin. Chem. Biol.*, **1999**. *3*, 89-94.

106. Derossi, D., Chassaing, G., and Prochiantz, A., "Trojan Peptides: The Penetratin System for Intracellular Delivery". *Trends Cell Biol.*, **1998**. *8*, 84-87.

107. Schwarze, S.R., Hruska, K.A., and Dowdy, S.F., "Protein Transduction: Unrestricted Delivery into All Cells?" *Trends Cell Biol.*, **2000**. *10*, 290-295.

108. Prochiantz, A., "Messenger Proteins: Homeoproteins, Tat and Others". *Curr. Opin. Cell Biol.*, **2000**. *12*, 400-406.

109. Lindgren, M., Hallbrink, M., Prochiantz, A., and Langel, U., "Cell-Penetrating Peptides". *Trends Pharmacol. Sci.*, **2000**. *21*, 99-103.

110. Langel, U., *Cell-Penetrating Peptides: Processes and Applications*. 2002, Boca Raton, FL: CRC Press.

111. Lin, Y.Z., Yao, S.Y., Veach, R.A., Torgerson, T.R., and Hawiger, J., "Inhibition of Nuclear Translocation of Transcription Factor NF-Kappa B by a Synthetic Peptide Containing a Cell Membrane-Permeable Motif and Nuclear Localization Sequence". *J. Biol. Chem.*, **1995**. *270*, 14255-14258.

112. Liu, K.Y., Timmons, S., Lin, Y.Z., and Hawiger, J., "Identification of a Functionally Important Sequence in the Cytoplasmic Tail of Integrin Beta 3 by Using Cell-Permeable Peptide Analogs". *Proc. Natl. Acad. Sci. USA*, **1996**. *93*, 11819-11824.

113. Vives, E., Brodin, P., and Lebleu, B., "A Truncated HIV-1 Tat Protein Basic Domain Rapidly Translocates through the Plasma Membrane and Accumulates in the Cell Nucleus". *J. Biol. Chem.*, **1997**. *272*, 16010-16017.

114. Derossi, D., Calvet, S., Trembleau, A., Brunissen, A., Chassaing, G., and Prochiantz, A., "Cell Internalization of the Third Helix of the Antennapedia Homeodomain Is Receptor-Independent". *J. Biol. Chem.*, **1996**. *271*, 18188-18193.

115. Langel, U., Pooga, M., Kairane, C., Zilmer, M., and Bartfai, T., "A Galanin-Mastoparan Chimeric Peptide Activates the Na^+, K(+)-ATPase and Reverses Its Inhibition by Ouabain". *Regul. Pept.*, **1996**. *62*, 47-52.

116. Elliot, G. and O'Hare, P., "Intercellular Trafficking and Protein Delivery by a Herpesvirus Structural Protein". *Cell*, **1997**. *88*, 223-233.

117. Sheldon, K., Liu, D., Ferguson, J., and Gariepy, J., "Loligomers: Design of De Novo Peptide-Based Intracellular Vehicles". *Proc. Natl. Acad. Sci. USA*, **1995**. *92*, 2056-2060.

118. Futaki, S., Suzuki, T., Ohashi, W., Yagami, T., Tanaka, S., Ueda, K., and Sugiura, Y., "Arginine-Rich Peptides. An Abundant Source of Membrane Permeable Peptides Having Potential as Carriers for Intracellular Protein Delivery". *J. Biol. Chem.*, **2001**. *276*, 5836-5840.

119. Mitchell, D.J., Kim, D.T., Steinman, L., Fathman, C.G., and Rothbard, J.B., "Polyarginine Enters Cells More Efficiently Than Other Polycationic Homopolymers". *J. Pept. Res.*, **2000**. *56*, 318-325.

120. Waizenegger, T., Fischer, R., and Brock, R., "Intracellular Concentration Measurements in Adherent Cells: A Comparison of Import Efficiencies of Cell-Permeable Peptides". *Biol. Chem.*, **2002**. *383*, 291-299.

Chapter 2

Exploring the Extended Binding Determinants of Oligosaccharyl Transferase

Introduction

Asparagine-linked glycosylation is one of the most complex enzyme-catalyzed protein modifications.[1] This process is catalyzed by the multimeric membrane-associated glycoprotein, oligosaccharyl transferase (OT), and involves the transfer of a tetradecasaccharide from a dolichol pyrophosphate-linked donor to the side chain of an asparagine residue in an Asn-Xaa-Thr/Ser (NXT/S) consensus sequence in a nascent polypeptide. The function of the individual enzyme subunits and the details of the active site of this enzyme remain to be elucidated.[2-4]

Previously, peptide inhibitors were prepared in order to study the structural requirements for catalysis.[5-7] In these studies, a prototype inhibitor, with the asparagine in the consensus sequence substituted with α,γ-diaminobutanoic acid (Dab) was obtained.[8] Additionally, peptides structurally constrained in an Asx-turn conformation have greatly enhanced enzyme/ligand affinity.[3, 6] The tripeptide inhibitor c[Dab-Add]-Thr-NHMe, which contains the amino acid (S)-2-aminodecanedioic acid (Add), showed a K_i of 100 μM, while the linear analog Bz-Dab-Leu-Thr-NHMe showed a K_i ten times higher, 1 mM.[3]

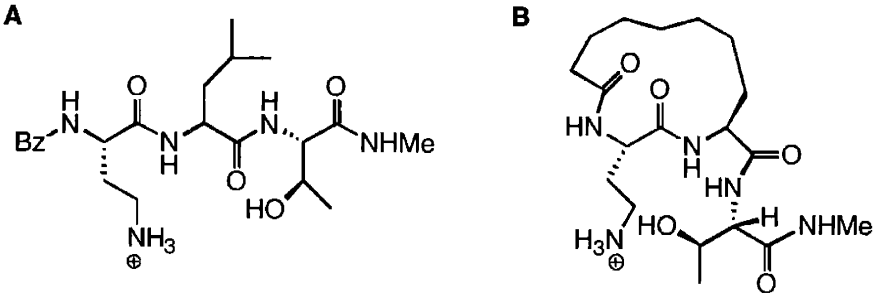

Figure 2.1.A. Linear inhibitor, K_i = 1mM. **B.** Inhibitor in a constrained Asx-turn, K_i = 100μM[3]

The central amino acid of the prototype inhibitor in Figure 2.1.B, Add, was substituted with a Cys(S-*t*Bu) residue to simplify the synthesis of the peptides (since Add is an unnatural amino acid and the macrocyclization was low yielding) and the peptides were capped with 6-bromohexanoic acid. The Cys(S-*t*Bu) was orthogonally deprotected under N_2 using

tributylphosphine. Cyclization between the thiolate of the cysteine and the 6-bromohexanoyl group was achieved in degassed DMF, using an excess of 1,1,3,3-tetramethylguanidine as a base.[9] This cyclization provides a constrained Asx-turn-type motif (see Figure 2.2). Also, previous studies showed that the use of a valine-threonine dipeptide at the *C*-terminus of the consensus sequence results in greatly enhanced binding to OT, relative to a variety of other dipeptide combinations.[3, 10] A *p*-nitrophenyl alanine was added at the *C*-terminus for quantitation purposes. For example, peptide **1** has a K_i of 37 nM.[3]

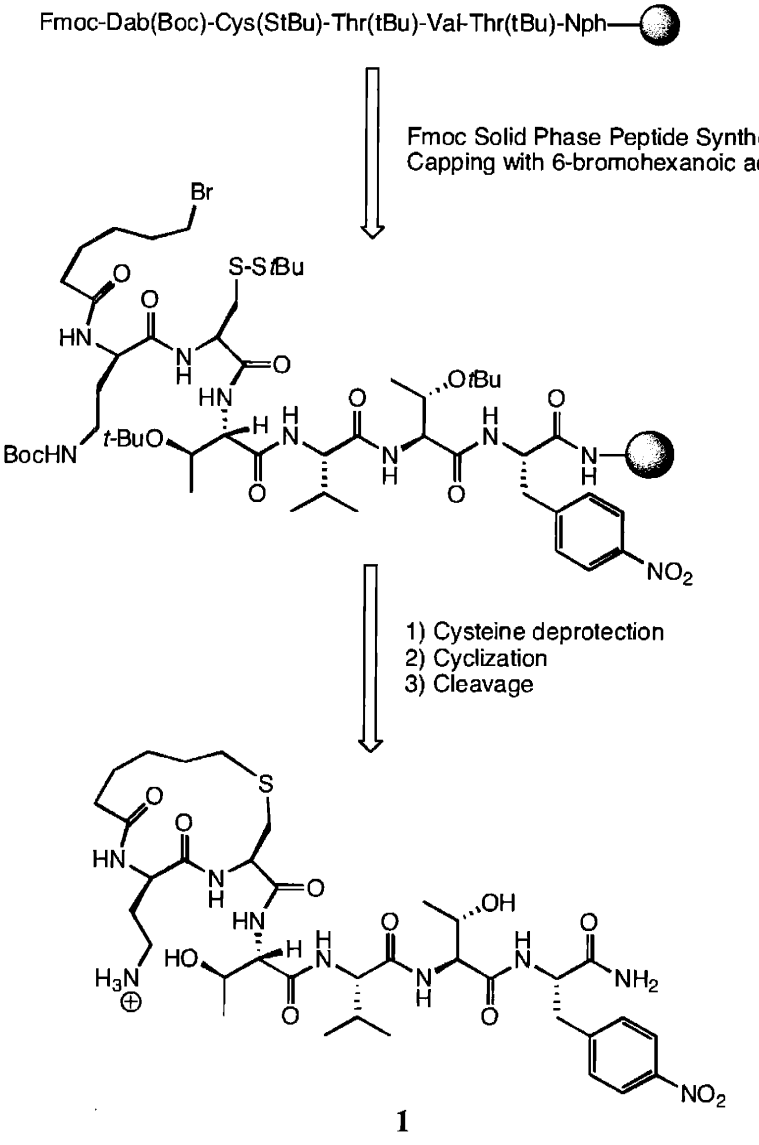

1

Figure 2.2. Synthesis of cyclized inhibitors on the solid phase through the use of orthogonal protecting groups.

The current study explores the effect of modifications in the structure of a pentapeptide on enzyme-inhibitor interactions. The modifications presented herein include *C*-terminus and Dab variations, as well as a comparison of linear analogs versus cyclized peptides. Also, linear peptides are tuned to obtain tight binding inhibitors in the low nanomolar range with K_i values comparable to the cyclic inhibitors.

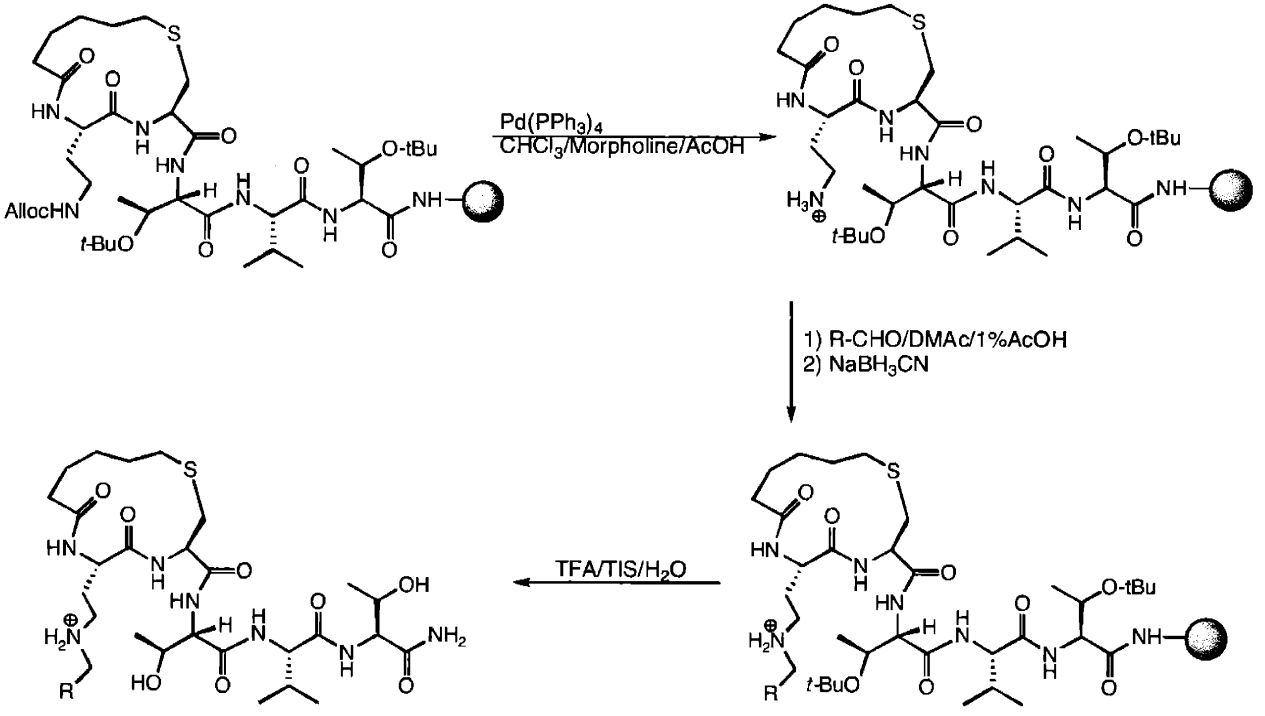

Figure 2.3. Modification of the side chain of Dab. The orthogonally protecting group Alloc is removed on the resin, after which reductive amination is performed using the desired aldehyde.

Peptides were synthesized using standard Fmoc-based solid phase synthesis methods on Fmoc-PAL-PEG-PS resin. In order to prepare peptides with modifications in the side chain of Dab, an allyloxycarbonyl protected (*N*-alloc) Dab was used (see Figure 2.3). The alloc group can be deprotected on the resin without affecting other protecting groups; deprotection was achieved using tetrakis(triphenylphosphine) palladium(0) in $CHCl_3$/morpholine/AcOH (37/1/2). Reductive amination was carried out by the addition of the desired aldehyde, followed by

reduction with $NaBH_3CN$, as described by Devraj and Cushman.[11] It is important to wash away any excess of the aldehyde before adding the sodium cyanoborohydride in order to avoid reductive alkylation of the secondary amine product.

Peptides with modifications at the *C*-terminus were synthesized on a 2-(4-formyl-3-methoxyphenoxy)ethyl polystyrene resin, as shown in Figure 2.4. The desired amine and sodium triacetoxyborohydride were added to the resin in a tenfold excess. Double addition to the resin is not observed due to steric hindrance. The first amino acid was coupled to the secondary amine using HOAt/DIPCDI as activators. Further elongation of the peptide was performed using HBTU/HOBt. The peptide was cleaved from the resin using TFA/triisopropylsilane/H_2O (95/2.5/2.5) to obtain the desired inhibitor.

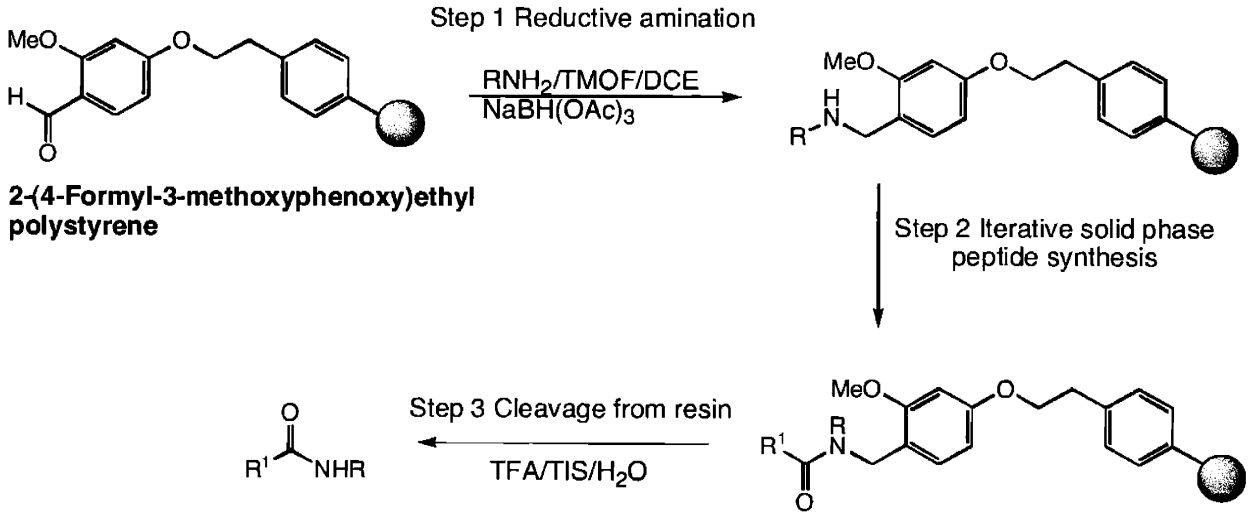

Figure 2.4. Synthesis of *C*-terminal-modified peptides. R = *C*-terminal amide introduced via reductive amination with RNH_2 in the Step 1; R^1 = polypeptide chain constructed in *N*-terminal direction in Step 2.

Dab modifications were peformed in cyclized inhibitors and also in linear peptides. All the *C*-terminus modified peptides were cyclized. Other modifications in linear peptides included changes in the central amino acid of the consensus sequence and the peptide backbone. These

modifications gave us information on the importance of the backbone amides for recognition by the enzyme.

Results

The *p*-nitrophenylalanine (Nph) residue in peptide **1** was originally introduced to allow facile concentration determination *via* the spectroscopic handle.[3, 10] Removal of this residue (peptide **2**) resulted in decreased enzyme-inhibitor affinity (K_i 82 nM *vs* 37 nM), but allowed the introduction of other hydrophobic groups while keeping a peptide of a relatively low molecular weight.

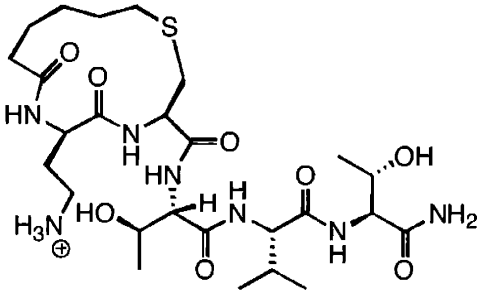

2

Dab Modifications

Modification of the Dab side chain, by reductive amination with either *n*-decyl or 2-naphthyl aldehyde resulted in a lower K_i and increased affinity of peptides **3** and **4** to OT (K_i 61 nM and 40 nM respectively). These derivatives were prepared to probe whether it was possible to exploit hydrophobic interactions that the enzyme might make with the glycosyl donor. Interestingly, the related 1-naphthyl analog (**5**) shows a higher K_i, which may be the result of unfavorable interactions, since the orientation of the naphthyl group is different in the two

peptides. The choice of these highly hydrophobic groups was based on the observation that aromatic amino acids have been implicated in carbohydrate binding sites.[12, 13]

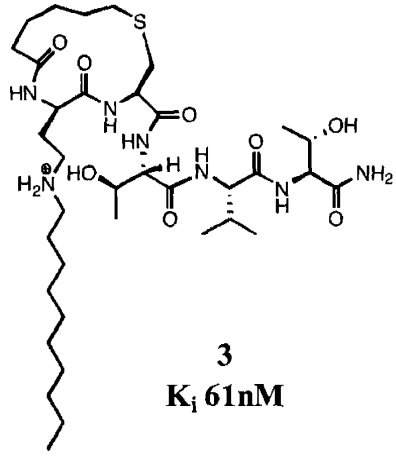

3
K_i 61nM

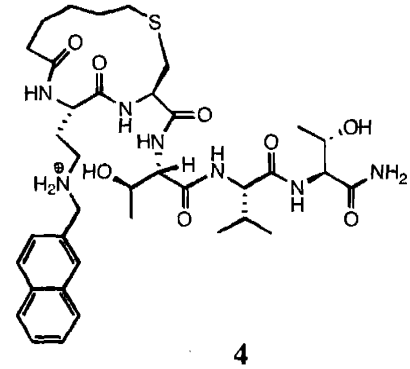

4
K_i 40nM

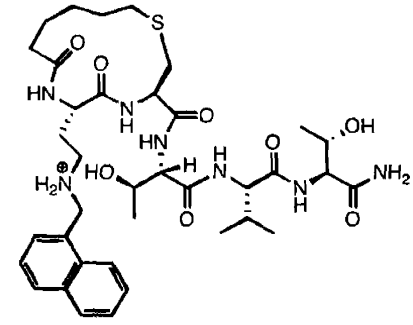

5
K_i 98nM

Linear analogs **6-8** were prepared in order to study the importance of groups attached to the Dab in unconstrained analogs. Also, the importance of electron withdrawing (peptide **7**) and electron donor (peptide **8**) groups in the benzyl ring attached to the Dab was explored. The addition of the nitro group (peptide **7**) and the methoxy group (peptide **8**) provided inhibitors which are approximately 70 times and 35 times better, respectively, than the unsubstituted aromatic benzyl group (peptide **6**). The diminished binding of these analogs emphasizes the importance of the constrained motif provided by the cyclization. Inhibitors **6-8** are all significantly less potent than the cyclic analogs, peptides **2-5**.

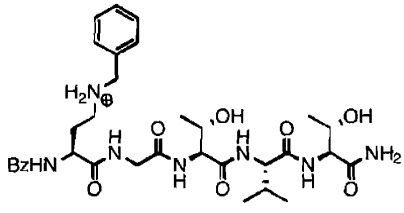

6
K_i = 11000nM

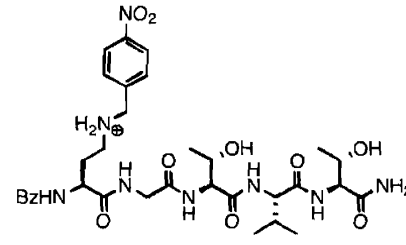

7
K_i = 154nM

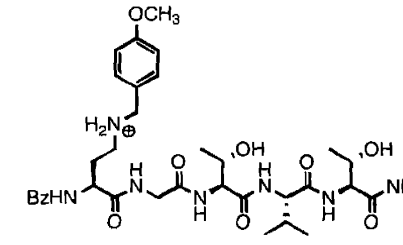

8
K_i = 305nM

Modifications at the carboxy terminus

As previously mentioned, the *p*-nitrophenylalanine (Nph) residue was initially introduced in the inhibitors to allow facile concentration determination. Removal of this residue resulted in an inhibitor (peptide **2**) with a two-fold decrease in affinity for OT (K_i 82 nM *vs* 37 nM). The *C*-terminus of peptide **2** was modified with different phenylalkyl derivatives, varying the length of the alkyl chain and the substituents on the phenyl ring. As illustrated below, varying the alkyl chain from two to four carbons barely affects binding (peptide **9** and **10**). However, in the interest of keeping the size of the inhibitor as short as possible, further modifications were performed in the smaller peptide **9**. The effect of electron donor or electron withdrawing groups was assessed with the use of a *p*-methoxyphenethyl- (peptide **11**) and a *p*-nitrophenethyl-derivative (peptide **12**). As shown below, the replacement of the terminal amino acid in **1** by appropriately spaced and substituted aryl derivatives compensates for the loss of the binding determinants in **1**. For example, the *p*-nitrophenethyl-modified derivative, **12**, shows a 20 nM K_i.

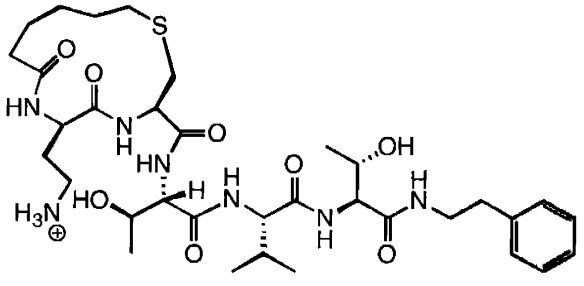

9
K_i 44nM

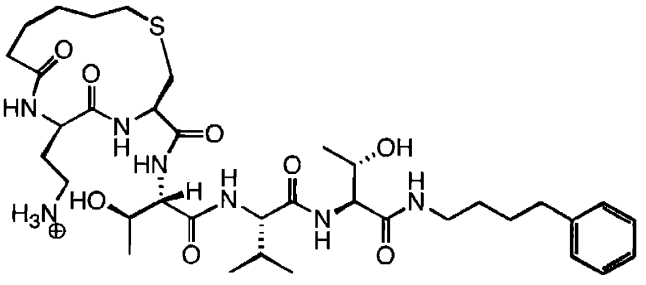

10
K_i 50nM

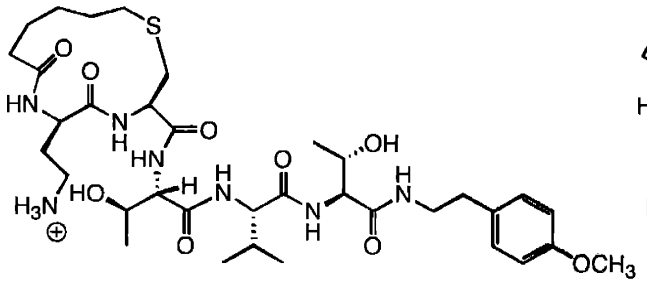

11
K_i 34nM

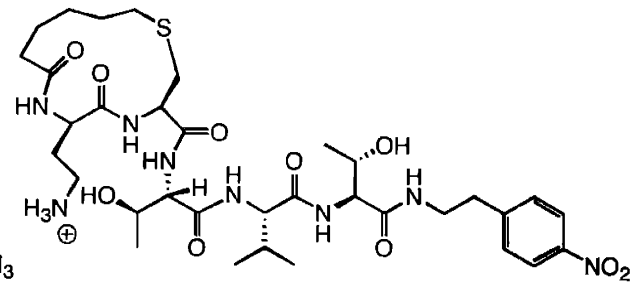

12
K_i 20nM

Additive effect

Modifications at the *C*-terminus provided inhibitors with a higher affinity for OT. The same effect was observed with modifications on the side chain of Dab, when performed on cyclized inhibitors. Peptides **13-15** were synthesized in order to determine if the addition of both Dab and *C*-terminus modifications would yield peptides with even a higher enzyme/peptide affinity. As shown below for peptide **14**, the introduction of a 2-naphthyl moiety at the side chain of Dab, which produced the best of the Dab-modified inhibitors, and a *p*-nitrophenethyl moiety at the *C*-terminus, generates the most potent inhibitor of OT to date, with a K_i of 10 nM. Peptide **13**, incorporating the 2-naphthyl moiety at the Dab and a phenethyl at the *C*-terminus, also has a low nanomolar K_i. A peptide containing the 2-naphthyl as well as the *p*-methoxyphenethyl modifications was also synthesized (peptide **15**), but the K_i could not be determined because of solubility problems.

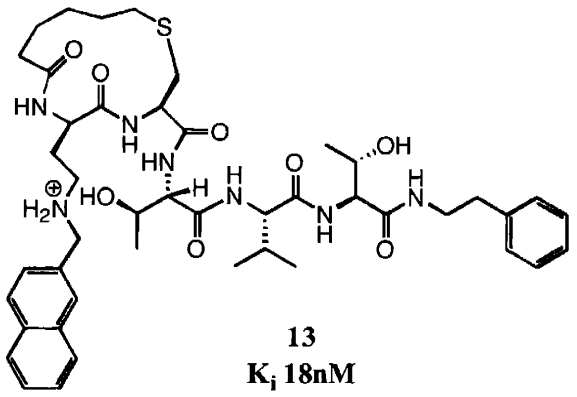

13
K_i 18nM

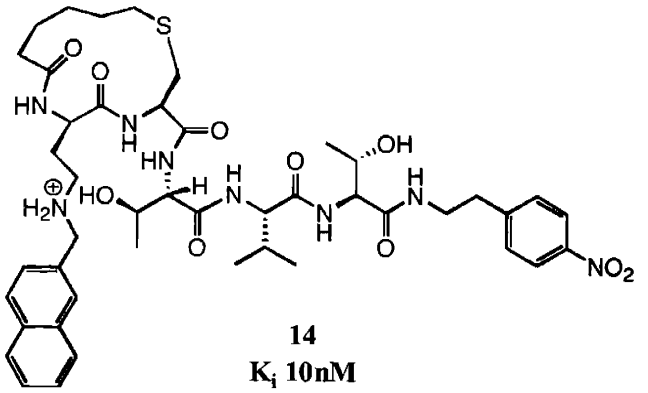

14
K_i 10nM

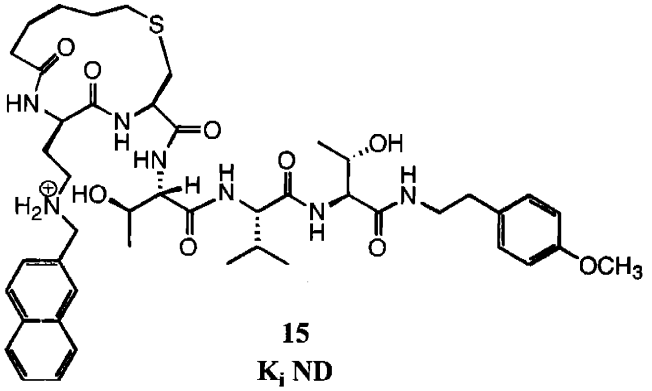

15
K_i ND

Summary

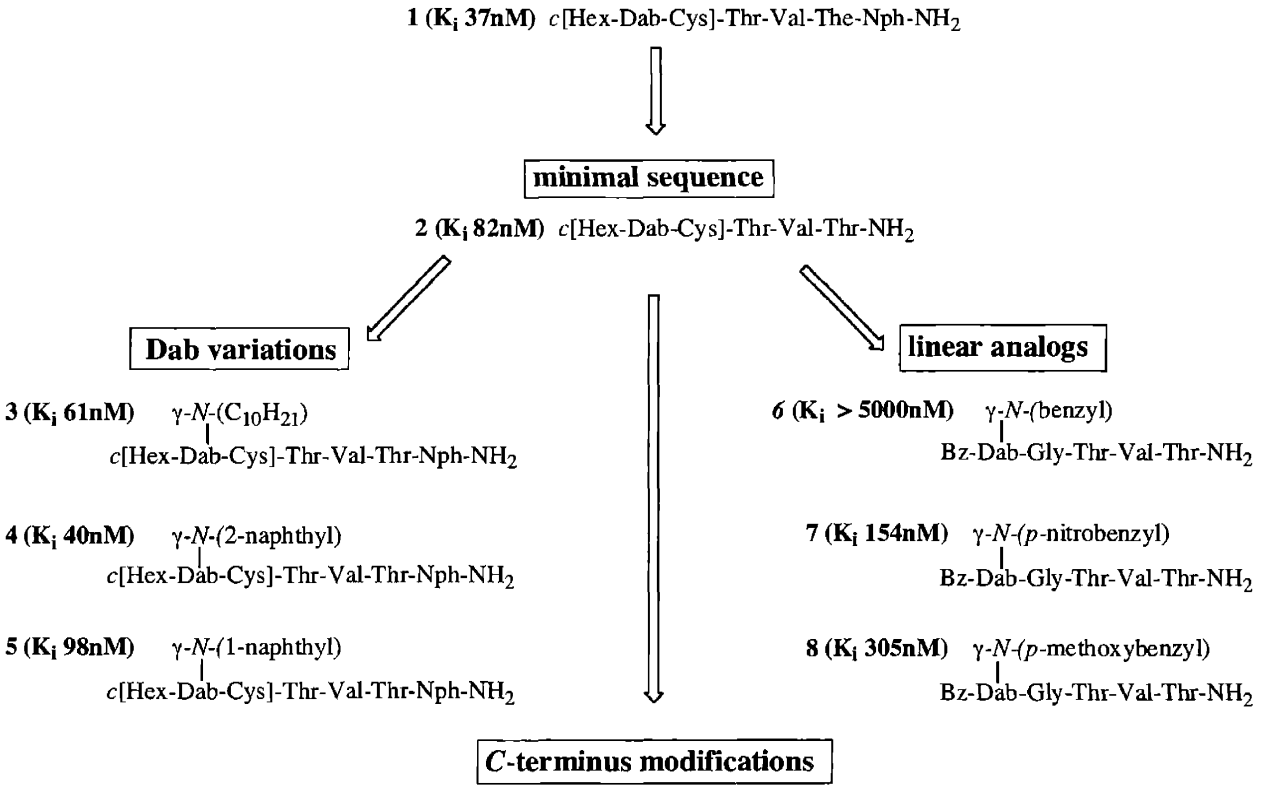

9 (K_i 44nM)

c[Hex-Dab-Cys]-Thr-Val-Thr-NH-CH_2-CH_2-Ph

10 (K_i 50nM)

c[Hex-Dab-Cys]-Thr-Val-Thr-NH-$(CH_2)_4$-Ph

11 (K_i 34nM)

c[Hex-Dab-Cys]-Thr-Val-Thr-NH-CH_2-CH_2-Ph-OCH_3

12 (K_i 20nM)

c[Hex-Dab-Cys]-Thr-Val-Thr-NH-CH_2-CH_2-Ph-NO_2

13 (K_i 18nM) γ-*N*-(2-naphthyl)

c[Hex-Dab-Cys]-Thr-Val-Thr-NH-CH_2-CH_2-Ph

14 (K_i 10nM) γ-*N*-(2-naphthyl)

c[Hex-Dab-Cys]-Thr-Val-Thr-NH-CH_2-CH_2-Ph-NO_2

Linear peptides

Cyclization has proven to provide a pre-organized structure that binds to OT with a higher affinity than unconstrained analogs. However, linear peptides are easier and faster to synthesize since no extra steps or manipulations on the resin are needed. Therefore, the use of linear peptides is more convenient to study the different binding determinants of OT, such as the importance of the backbone or residues in the sequence. It has been shown that the addition of the *C*-terminal residues Val-Thr-Nph enhances binding to OT by more than three orders of magnitude. The selection of an appropriate *N*-terminal capping moiety for the linear peptide produces inhibitors in the nanomolar range, as will be discussed in the following sections. The work described below was done in collaboration with Dr. S. Peluso.

A linear hexapeptide containing an Ala at the central position of the consensus sequence and a benzoyl capping at the *N*-terminus was synthesized as a model compound to compare with modified peptides (peptide **16**). This peptide was assayed against yeast OT and a K_i of 62 nM was obtained.

Modification of the peptide backbone

A major interest towards developing bioavailable OT inhibitors is the importance of the amides in the backbone of the peptide. One of the factors that contributes to the cell impermeable nature of peptides is their hydrophilicity, which is accentuated by the backbone amides. In general, compounds have to be desolvated to be able to cross membrane bilayers. The peptide backbone increases this desolvation energy, resulting in a lower propensity for the compound to cross the cellular membrane. Therefore, it is desirable to decrease the number of amides in the backbone of the inhibitors. Before doing this, it is necessary to verify that the backbone amides are not recognized by the enzyme.

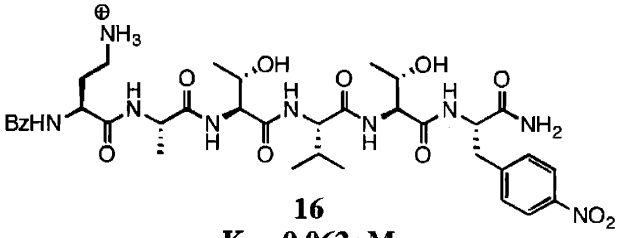

16
$K_i = 0.062\mu M$

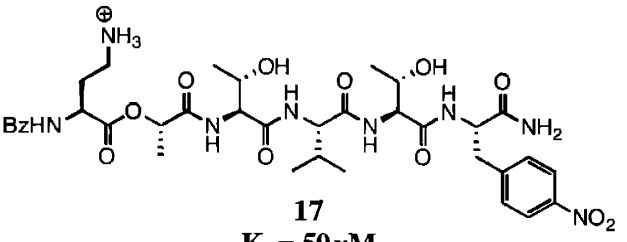

17
$K_i = 50\mu M$

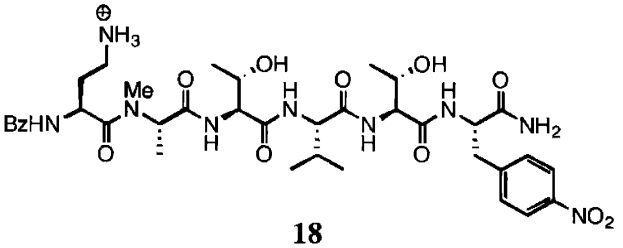

18
$K_i = 66\mu M$

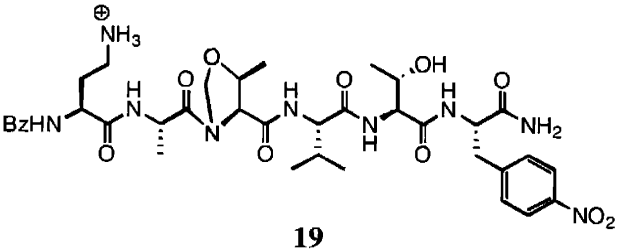

19
$K_i > 160\mu M$

The amide of the Ala in peptide **16** was substituted by a *N*-α-methylated Ala (peptide **18**). This modification produced an inhibitor with a K_i three orders of magnitude higher than the K_i for the parent hexapeptide **16**, 66 μM and 0.062 μM, respectively. The Ala was also substituted by a lactate, which has an ester in place of the amide (peptide **17**). The resulting inhibitor, with a measured K_i of 50 μM, is also three orders of magnitude worse than peptide **16**. Clearly, this amide is essential for enzyme recognition and no changes should be introduced at this position. This data suggests that the Pro is not accepted at this position not only because of conformational requirements, but also because of the lack of a hydrogen bond donor in the amide.

Considering that the α,γ-diaminobutanoic acid (Dab) cannot provide the carbonyl group of the natural asparagine to hydrogen bond with the hydroxyl or the amide of the threonine, we substituted the threonine of the triad with a ψ-Pro (peptide **19**), where the hydrogens of the hydroxyl and the amide are not present. Peptide **19** is not recognized by OT, suggesting that the hydroxyl amino acid and the amide of the essential Thr are involved in hydrogen bonding

interactions with the enzyme. Therefore, no changes that affect these features should be introduced in the sequence.

Inducing secondary structure

A series of inhibitors were synthesized based on a study performed by Imperiali *et al*[7] on tripeptide substrates. In this study, several tripeptides with different residues at the central position of the triad were synthesized to study the relationship between the substrate properties of the peptides and their conformation in solution. Some of the residues used at the Xaa position of the Bz-Asn-Xaa-Thr-NHMe sequence were Pro, D-Ala, and α-aminoisobutyric acid (Aib). It was found that peptide acceptors would acquire an Asx-turn conformation in solution, while tripeptides containing the residues mentioned could not adopt this conformation, and showed poor acceptor or nonacceptor properties.[7]

Dab containing peptides act as inhibitors of OT, but they lack the carbonyl group that mediates the formation of Asx-turns. However, the affinity provided by other binding determinants allows binding to the enzyme, which can mediate the formation of the required structural motif. We have synthesized inhibitors containing a Pro (peptide **20**), a D-Pro (peptide **21**), Aib (peptide **22**) or D-Ala (peptide **23**) at the central position of the consensus sequence to examine the behavior of these peptides with the enzyme.

Peptide **20** has an IC_{50} higher than 800 μM. The exact IC_{50} and K_i could not be determined because they were too high. However, the measured K_i for peptide **21**, which has D-Pro instead of a Pro, is 26 μM, which could be at least six times lower than the approximate K_i for the L-Pro. This K_i is lower than the kinetic data obtained for peptides **17** and **18**, in which the amide of the central residue is substituted by an ester or a tertiary amide, but it is still in the micromolar range. The conformation provided by the different stereocenter seems to be more

favorable towards interactions with OT compared to the conformation provided by L-Pro, but even if the conformation provided is more favorable, the peptide still has a tertiary amide, which is not favorable at this position, as seen for peptide **18**.

Aib, an unnatural amino acid that is known to induce the formation of α-helices, was introduced as the central amino acid of the triad (peptide **22**). The K_i obtained for this inhibitor (12 μM) was lower than any of the previously mentioned inhibitors, but it is still in the micromolar range. A D-Ala residue was introduced at this position to compare its effect on the enzyme affinity to the effect of the Aib inhibitor. The K_i for the D-Ala inhibitor **23** was twice that of the Aib inhibitor.

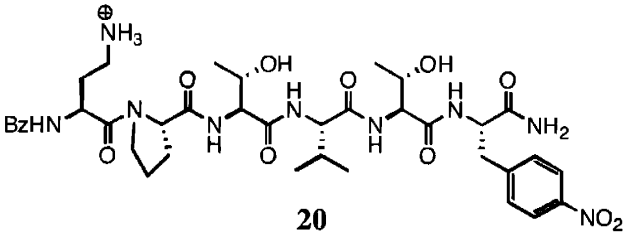

20
K_i > 120μM

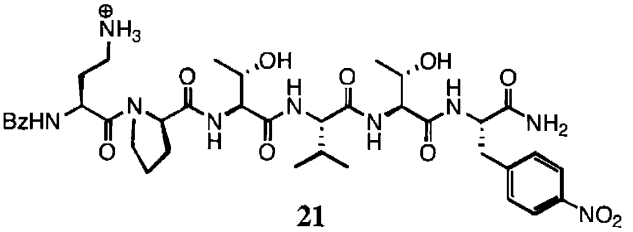

21
K_i = 26μM

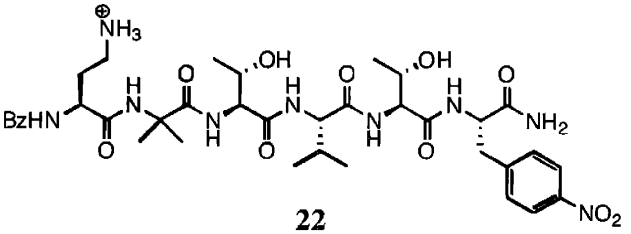

22
K_i = 12μM

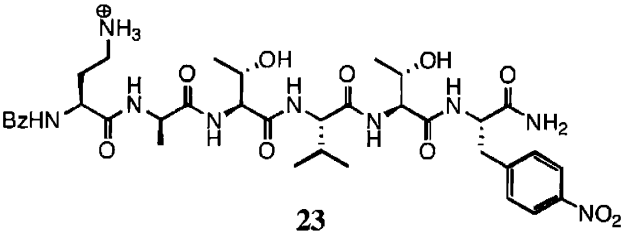

23
K_i = 24μM

Tuning of linear inhibitors

Several natural amino acids were introduced as the central residue of the triad based on the statistical studies of Gavel.[14] According to this study, the most probable residues at this position in naturally glycosylated proteins are Gly, Ser, Val, Ala and Leu, in that order, with Gly

being the most frequent. The K_i obtained for the glycine inhibitor (peptide **24**), 470 nM, was approximately ten times higher than the K_i for the alanine inhibitor (peptide **16**). The serine containing peptide (**25**) inhibited in the same order of magnitude as the alanine peptide (72 nM vs. 62 nM, respectively). Since the alanine peptide, a little bulkier than the glycine peptide, has a much stronger interaction with the enzyme we decided to introduce an unnatural amino acid, α-aminobutanoic acid (Abu) in place of the alanine (peptide **26**). The K_i measured for this inhibitor was 10 nM, the lowest K_i that we have obtained for a non-cyclized inhibitor. All of the inhibitors mentioned in this section are linear peptides, indicating that cyclization was not necessary to produce low nanomolar inhibitors. Even though constraining the structure of the peptide to an Asx-turn improves its ability to interact with the enzyme, it seems that the chosen amino acids in the sequence fit well in the binding pockets of the enzyme, so that the enzyme takes care of accommodating the flexible peptide into the desired conformation.

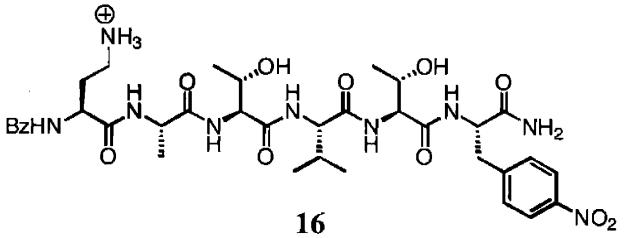

16
$K_i = 0.062\mu M$

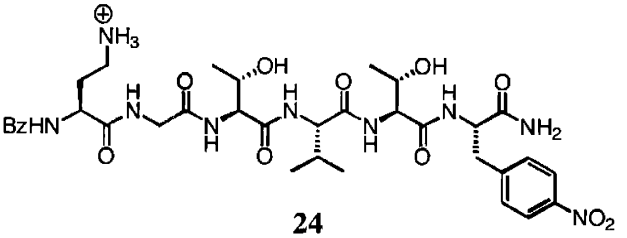

24
$K_i = 0.45\mu M$

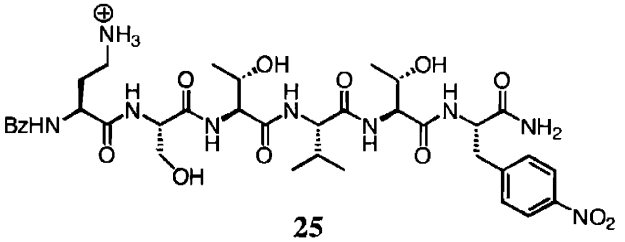

25
$K_i = 0.072\mu M$

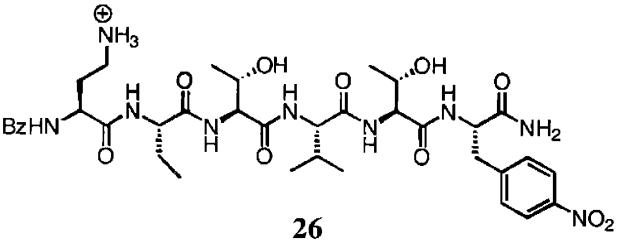

26
$K_i = 0.011\mu M$

Summary

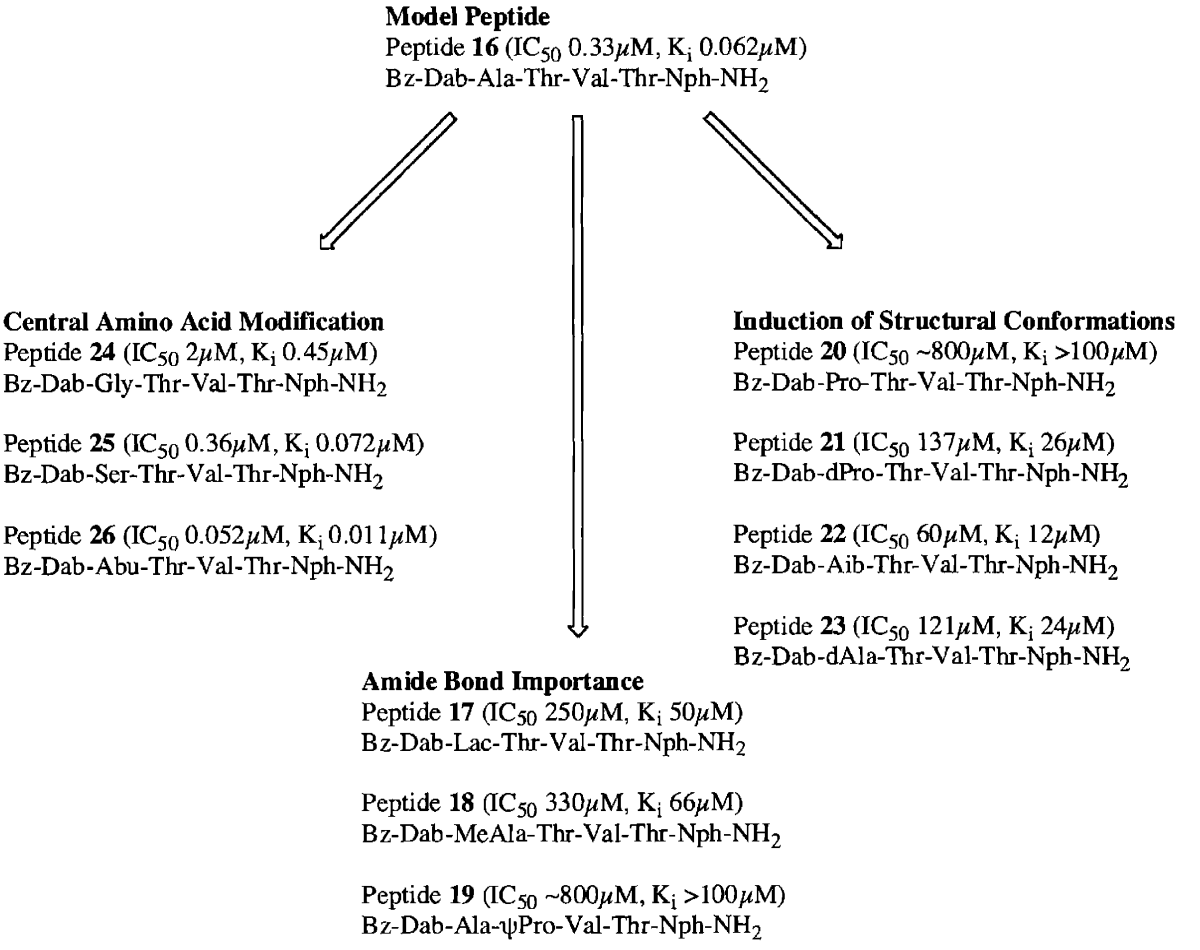

Discussion

Several modifications were introduced at the *C*-terminus and the side chain of the Dab on cyclized inhibitors. These modifications improved enzyme/ligand binding affinities. When the best of both modifications were introduced in a single peptide an additive effect in enzyme affinity was observed, resulting in the most potent OT cyclized inhibitor to date.

Dab side chain modifications were also introduced in linear inhibitors. However, these inhibitors were weak compared to the cyclized analogs, emphasizing the importance of the Asx-turn conformation provided by the cyclization. Nevertheless, linear peptides were synthesized to

study the effect of sequence variations on enzyme affinity, since these are easier to prepare than the cyclized analogs. We were able to show that it is possible to obtain tight binding inhibitors of OT that bind in the low nanomolar range when the appropriate residue is located at the central position of the consensus sequence. It was also shown that the amide of the central residue and the Thr of the recognition sequence are required for enzyme recognition. The introduction of residues that induce structural conformations other than the Asx-turn is also detrimental to peptide/enzyme interactions.

Acknowledgements

This work was supported by a grant from NIH (GM-39334) and by a Ford Foundation predoctoral fellowship to M. L. Ufret. Part of this work appears in Ufret, M. L. and Imperiali, B. "Probing the Extended Binding Determinants of Oligosaccharyl Transferase with Synthetic Inhibitors of Asparagine-Linked Glycosylation" *Bioorg. Med. Chem. Lett.* **2000**, 10, 281-284.

Experimental section

General Procedure for Fmoc-Based Solid-Phase Peptide Synthesis

Peptides were synthesized manually on a column glass vessel with a frit. Mixing was accomplished by bubbling N_2 through the frit. Discharge of solvent and excess reagents was accomplished by the use of vacuum or N_2 pressure, in the case of reactions performed under a N_2 atmosphere. The resin was swelled in DMF for 10min. Fmoc deprotection was effected with 20% piperidine in DMF (3 x 3min). Coupling of the amino acids was performed in DMF using 4 equivalents of amino acids and HOBt/HBTU, and 8 equivalents of DIPEA. The success of each coupling reaction was determined using either a Kaiser test or a TNBS test. A capping step

(Ac_2O/DIPEA 2:3 in DMF/DCM 4:1) was done after each successful coupling to ensure that any remaining undetected, unreacted peptide was capped to avoid deletion peptides. For cyclized peptides, the *N*-terminus was capped with 6-bromohexanoic acid, as described below. For linear peptides, the *N*-terminus was capped using 10 equivalents of benzoic anhydride and 10 equivalents of DIPEA in DMF. The resin was rinsed with DMF, DCM and ethyl ether and dried under vacuum. Peptides were cleaved from the resin using TFA/TIS/H_2O (95:2.5:2.5), precipitated with ice-cold ether, rinsed twice with ether, analyzed and purified by HPLC, and characterized by ES-MS.

Synthesis of cyclized peptides

In general, peptides were synthesized manually using standard Fmoc-based SPPS on PAL-PEG-PS resin (substitution 0.2mmole/g); HOBt/HBTU (4 equivalents) were used as activators. Fmoc-L-Cys(S-tBu)-OH was used as the central amino acid of the enzyme recognition sequence. The amino terminus was capped with 6-bromohexanoic acid, followed by deprotection of the Cys(S-tBu) under N_2, with a large excess of tri-*n*-butylphosphine in degassed DMF (2 x 3 h). The resin was rinsed with degassed DMF and cyclization from the thiolate of the Cys to the 6-bromohexanoyl was performed under N_2 in the presence of a large excesss of 1,1,3,3-tetramethylguanidine in degassed DMF (shaken overnight). The resin was rinsed with DMF, DCM and ether, and dried, followed by cleavage of the peptide with TFA/H_2O/TIS (95:2.5:2.5). Peptides were precipitated with ice-cold ether and analyzed and purified by HPLC on reverse phase, using C18 columns. The peptides were characterized by ES-MS. Peptides without a chromophore were quantified by quantitative amino acid analysis (QAA). Peptides with a chromophore were quantitated using UV.

Synthesis of Dab modified peptides

In general, peptides were synthesized manually using standard Fmoc-based SPPS on PAL-PEG-PS resin (substitution 0.2 mmole/g); HOBt/HBTU (4 equivalents) were used as activators. In the case of cyclized peptides, cyclization was performed prior to Dab modification. An allyloxycarbonyl-protected Dab was used since it can be deprotected on the resin without affecting other protecting groups. The alloc was removed using tetrakis(triphenylphosphine) palladium in $CHCl_3$/morpholine/AcOH (37/1/2); the deprotection was carried out over 18 h. Reductive amination was carried out by adding the desired aldehyde in excess in DMAc/1%AcOH. The excess aldehyde was rinsed off the resin to avoid double alkylation, and reduction was effected with $NaBH_3CN$ in DMAc/1%AcOH overnight. The peptide was cleaved off the resin and analyzed as described in the previous section.

Synthesis of C-terminus modified inhibitors

C-terminus modified peptides were synthesized manually using standard Fmoc-based SPPS on a 2-(4-formyl-3-methoxyphenoxy)ethyl polystyrene resin. Reductive amination was carried out by adding a ten-fold excess of the desired amine and sodium triacetoxyborohydride ($NaBH(OAc)_3$) in trimethylorthoformate (TMOF) and dichloroethane (DCE). The reaction was allowed to proceed overnight; double addition to the resin is not observed in this case because of steric hindrance. The first amino acid was coupled to the resulting secondary amine using HOAt/DIPCDI as activators. The coupling efficiency of the first amino acid was monitored by measurement of the Fmoc deblocked from a small portion of the resin. Coupling of subsequent residues was carried out using HOBt/HBTU as activators. The peptides were cyclized as

described above, followed by Dab modifications for peptides **13-15** as described earlier. Peptides were cleaved from the resin, analyzed by HPLC and characterized by ES-MS, as described above.

*c[Hex-Dab-Cys]-Thr-Val-Thr-NH_2 (**2**)*

Purified peptide was dissolved in DMSO and the solution was quantified by QAA. The peptide was assayed for inhibition against yeast microsomes as described below. IC_{50} = 0.266 μM. The reported K_i, 0.082 μM, is a mean value and the observed deviation is less than 15% of the mean value.

HPLC: t_R = 19.3 min (C_{18}, 0%–70% B over 25 min); ES-MS: Calculated for $C_{26}H_{47}N_7O_8S$ 617, observed 618 (MH^+)

*c[Hex-Dab(γ-N-$C_{10}H_{21}$)-Cys]-Thr-Val-Thr-NH_2 (**3**)*

The purified peptide was dissolved in DMSO and the solution was quantified by QAA. The peptide was assayed for inhibition against yeast microsomes as described below. IC_{50} = 0.322 μM. The reported K_i, 0.062 μM, is a mean value and the observed deviation is less than 10% of the mean value.

HPLC: t_R = 46 min (C_{18}, 15%–85% B over 85 min); ES-MS: Calculated for $C_{36}H_{67}N_7O_8S$ 757, observed 758 (MH^+)

*c[Hex-Dab(γ-N(2-naphthyl))-Cys]-Thr-Val-Thr-NH_2 (**4**)*

The purified peptide was dissolved in DMSO and the solution was quantified by QAA. Using the obtained concentration, the ε_{max} was calculated for the naphthyl group and used to

quantify other naphthyl-containing peptides. The peptide was assayed for inhibition against yeast microsomes as described below. IC_{50} = 0.230 μM; the reported K_i, 0.040 μM, is a mean value and the observed deviation is 5% of the mean value.

HPLC: t_R = 24.9 min (C_{18}, 0%–70% B over 25 min); ES-MS: Calculated for $C_{37}H_{55}N_7O_8S$ 757, observed 758 (MH^+)

*c[Hex-Dab(γ-N(1-naphthyl))-Cys]-Thr-Val-Thr-NH_2 (**5**)*

The purified peptide was dissolved in DMSO and the solution was quantified using the absorbance of the naphthyl group. The peptide was assayed for inhibition against yeast microsomes as described below. IC_{50} = 0.440 μM; the reported K_i, 0.098 μM, is a mean value and the observed deviation is 25% of the mean value.

HPLC: t_R = 25.2 min (C_{18}, 0%–70% B over 25 min); ES-MS: Calculated for $C_{37}H_{55}N_7O_8S$ 757, observed 758 (MH^+)

*Bz-Dab(γ-N(benzyl))-Gly-Thr-Val-Thr-NH_2 (**6**)*

The purified peptide was dissolved in DMSO and the solution was quantified by QAA. The peptide was assayed for inhibition against yeast microsomes as described below. The K_i is estimated to be higher than 5 μM.

HPLC: t_R = 24.1 min (C_{18}, 0%–70% B over 25 min); ES-MS: Calculated for $C_{33}H_{47}N_7O_8$ 669, observed 670 (MH^+)

*Bz-Dab(γ-N(p-nitrobenzyl))-Gly-Thr-Val-Thr-NH_2 (**7**)*

The purified peptide was dissolved in DMSO and the solution was quantified by QAA. The peptide was assayed for inhibition against yeast microsomes as described below. IC_{50} = 0.810 μM. The reported K_i, 0.154 μM, is a mean value and the observed deviation is 30% of the mean value.

HPLC: t_R = 24.1 min (C_{18}, 0%–70% B over 25 min); ES-MS: Calculated for $C_{33}H_{46}N_8O_{10}$ 714, observed 715 (MH^+)

*Bz-Dab(γ-N(p-methoxybenzyl))-Gly-Thr-Val-Thr-NH_2 (**8**)*

The purified peptide was dissolved in DMSO and the solution was quantified by QAA. The peptide was assayed for inhibition against yeast microsomes as described below. IC_{50} = 1.3 μM. The reported K_i, 0.305 μM, is a mean value and the observed deviation is 10% of the mean value.

HPLC: t_R = 24 min (C_{18}, 0%–70% B over 25 min); ES-MS: Calculated for $C_{34}H_{49}N_7O_9$ 699, observed 700 (MH^+)

*c[Hex-Dab-Cys]-Thr-Val-Thr-NH-CH_2-CH_2-Ph (**9**)*

The purified peptide was dissolved in DMSO and the solution was quantified by QAA. The peptide was assayed for inhibition against yeast microsomes as described below. IC_{50} = 0.198 μM. The reported K_i, 0.044 μM, is a mean value and the observed deviation is 11% of the mean value.

HPLC: t_R = 25.2 min (C_{18}, 0%–70% B over 25 min); ES-MS: Calculated for $C_{34}H_{55}N_7O_8S$ 721, observed 722 (MH^+)

c[Hex-Dab-Cys]-Thr-Val-Thr-NH-$(CH_2)_4$-Ph ***(10)***

The purified peptide was dissolved in DMSO and the solution was quantified by QAA. The peptide was assayed for inhibition against yeast microsomes as described below. IC_{50} = 0.231 μM. The reported K_i, 0.047 μM, is a mean value and the observed deviation is 5% of the mean value.

HPLC: t_R = 27 min (C_{18}, 0%–70% B over 25 min); ES-MS: Calculated for $C_{36}H_{59}N_7O_8S$ 749, observed 750 (MH^+)

c[Hex-Dab-Cys]-Thr-Val-Thr-NH-CH_2-CH_2-Ph-OCH_3 ***(11)***

The purified peptide was dissolved in DMSO and the solution was quantified by QAA. The peptide was assayed for inhibition against yeast microsomes as described below. IC_{50} = 0.183 μM. The reported K_i, 0.034 μM, is a mean value and the observed deviation is 6% of the mean value.

HPLC: t_R = 25.3 min (C_{18}, 0%–70% B over 25 min); ES-MS: Calculated for $C_{35}H_{58}N_7O_9S$ 752, observed 753 (MH^+)

c[Hex-Dab-Cys]-Thr-Val-Thr-NH-CH_2-CH_2-Ph-NO_2 ***(12)***

The purified peptide was dissolved in DMSO and the solution was quantified by QAA. The peptide was assayed for inhibition against yeast microsomes as described below. IC_{50} = 0.100 μM. The reported K_i, 0.020 μM, is a mean value and the observed deviation is 10% of the mean value.

HPLC: t_R = 25.2 min (C_{18}, 0%–70% B over 25 min); ES-MS: Calculated for $C_{34}H_{54}N_8O_{10}S$ 766, observed 767 (MH^+)

c[Hex-Dab(γ-N(2-naphthyl))-Cys]-Thr-Val-Thr-NH-CH_2-CH_2-Ph ***(13)***

The purified peptide was dissolved in DMSO and the solution was quantified by QAA. The peptide was assayed for inhibition against yeast microsomes as described below. IC_{50} = 0.097 μM; the reported K_i, 0.018 μM, is a mean value and the observed deviation is 1% of the mean value.

HPLC: t_R = 31.4 min (C_{18}, 0%–70% B over 25 min); ES-MS: Calculated for $C_{45}H_{63}N_7O_8S$ 861, observed 862 (MH^+)

c[Hex-Dab(γ-N(2-naphthyl))-Cys]-Thr-Val-Thr-NH-CH_2-CH_2-Ph-NO_2 ***(14)***

The purified peptide was dissolved in DMSO and the solution was quantified by QAA. The peptide was assayed for inhibition against yeast microsomes as described below. IC_{50} = 0.045 μM. The reported K_i, 0.010 μM, is a mean value and the observed deviation is 20% of the mean value.

HPLC: t_R = 28.6 min (C_{18}, 0%–70% B over 25 min); ES-MS: Calculated for $C_{45}H_{62}N_8O_{10}S$ 906, observed 907 (MH^+)

c[Hex-Dab(γ-N(2-naphthyl))-Cys]-Thr-Val-Thr-NH-CH_2-CH_2-Ph-OCH_3 ***(15)***

The purified peptide was dissolved in DMSO and the solution was quantified by QAA. The peptide was assayed for inhibition against yeast microsomes as described below. The K_i could not be measured due to the insoluble character of the peptide.

HPLC: t_R = 28.7 min (C_{18}, 0%–70% B over 25 min); ES-MS: Calculated for $C_{46}H_{65}N_7O_9S$ 892, observed 893 (MH^+)

Bz-Dab-Ala-Thr-Val-Thr-Nph-NH_2 (16)

The purified peptide was dissolved in DMSO and the solution was quantified by measuring the absorbance of the *p*-nitrophenyl moiety[10]. The peptide was assayed for inhibition against yeast microsomes as described below. IC_{50} = 0.330 μM; the reported K_i, 0.062 μM, is a mean value and the observed deviation is 13% of the mean value.

HPLC: t_R = 17.6 min (C_{18}, 7%–100% B over 28 min); ES-MS: Calculated for $C_{36}H_{51}N_9O_{11}$ 785, observed 786 (MH^+)

Bz-Dab-Lac-Thr-Val-Thr-Nph-NH_2 (17)

The formation of the ester bond involved coupling of lactic acid using PyAOP as activating reagent and collidine as base. *N*-α-Alloc-Dab(γ-Boc)-OH was coupled using DIC as activating agent and a catalytic amount of DMAP as base, to avoid transesterification and racemization of the lactic residue. The alloc was removed with $Pd(PPh_3)_4$ using phenylsilane as a scavenger. The *N*-terminus was capped with benzoic anhydride and pyridine. The purified peptide was dissolved in DMSO and the solution was quantified by measuring the absorbance of the *p*-nitrophenyl moiety[10]. The peptide was assayed for inhibition against yeast microsomes as described below. IC_{50} = 252 μM; the reported K_i, 50 μM, is a mean value and the observed deviation is 2% of the mean value.

HPLC: t_R = 18.8 min (C_{18}, 7%–100% B over 28 min); ES-MS: Calculated for $C_{36}H_{50}N_8O_{12}$ 786, observed 787 (MH^+)

Bz-Dab-N-α-Me-Ala-Thr-Val-Thr-Nph-NH_2 (18)

The purified peptide was dissolved in DMSO and the solution was quantified by measuring the absorbance of the *p*-nitrophenyl moiety[10]. The peptide was assayed for inhibition against yeast microsomes as described below. IC_{50} = 333 μM; the reported K_i, 66 μM, is a mean value and the observed deviation is 2% of the mean value.

HPLC: t_R = 18 min (C_{18}, 7%–100% B over 28 min); ES-MS: Calculated for $C_{37}H_{53}N_9O_{11}$ 799, observed 800 (MH^+)

Bz-Dab-Ala-ψPro-Val-Thr-Nph-NH_2 (19)

Peptide 19 was synthesized using standard Fmoc-based SPPS. Introduction of the ψPro was achieved by coupling of the building block Fmoc-Ala-ψPro-OH using PyAOP as activating agent and DIPEA as base. The purified peptide was dissolved in DMSO and the solution was quantified by measuring the absorbance of the *p*-nitrophenyl moiety[10]. The peptide was assayed for inhibition against yeast microsomes as described below. $IC_{50} > 800$ μM; $K_i > 150$ μM.

HPLC: t_R = 18.1 min (C_{18}, 7%–100% B over 28 min); ES-MS: Calculated for $C_{37}H_{51}N_9O_{11}$ 797, observed 798 (MH^+)

Bz-Dab-Pro-Thr-Val-Thr-Nph-NH_2 (20)

The purified peptide was dissolved in DMSO and the solution was quantified by measuring the absorbance of the *p*-nitrophenyl moiety[10]. The peptide was assayed for inhibition against yeast microsomes as described below. $IC_{50} > 800$ μM; $K_i > 120$ μM.

HPLC: t_R = 18.12 min (C_{18}, 7%–100% B over 28 min); ES-MS: Calculated for $C_{38}H_{53}N_9O_{11}$ 811, observed 812 (MH^+)

Bz-Dab-dPro-Thr-Val-Thr-Nph-NH_2 (21)

The purified peptide was dissolved in DMSO and the solution was quantified by measuring the absorbance of the *p*-nitrophenyl moiety[10]. The peptide was assayed for inhibition against yeast microsomes as described below. IC_{50} = 137 μM; the reported K_i, 26 μM, is a mean value and the observed deviation is less than 20% of the mean value.

HPLC: t_R = 18.01 min (C_{18}, 7%–100% B over 28 min); ES-MS: Calculated for $C_{38}H_{53}N_9O_{11}$ 811, observed 812 (MH^+)

Bz-Dab-Aib-Thr-Val-Thr-Nph-NH_2 (22)

The purified peptide was dissolved in DMSO and the solution was quantified by measuring the absorbance of the *p*-nitrophenyl moiety[10]. The peptide was assayed for inhibition against yeast microsomes as described below. IC_{50} = 60 μM; the reported K_i, 12 μM, is a mean value and the observed deviation is less than 10% of the mean value.

HPLC: t_R = 18.11 min (C_{18}, 7%–100% B over 25 min); ES-MS: Calculated for $C_{37}H_{53}N_9O_{11}$ 799, observed 800 (MH^+)

Bz-Dab-dAla-Thr-Val-Thr-Nph-NH_2 (23)

The purified peptide was dissolved in DMSO and the solution was quantified by measuring the absorbance of the *p*-nitrophenyl moiety[10]. The peptide was assayed for inhibition against yeast microsomes as described below. IC_{50} = 121 μM; the reported K_i, 24 μM, is a mean value and the observed deviation is 4% of the mean value.

HPLC: t_R = 17.4 min (C_{18}, 7%–100% B over 28 min); ES-MS: Calculated for $C_{36}H_{51}N_9O_{11}$ 785, observed 786 (MH^+)

Bz-Dab-Gly-Thr-Val-Thr-Nph-NH_2 (24)

The purified peptide was dissolved in DMSO and the solution was quantified by measuring the absorbance of the *p*-nitrophenyl moiety[10]. The peptide was assayed for inhibition against yeast microsomes as described below. IC_{50} = 2 μM; the reported K_i, 0.47 μM, is a mean value and the observed deviation is 4% of the mean value.

HPLC: t_R = 17.3 min (C_{18}, 7%–100% B over 28 min); ES-MS: Calculated for $C_{35}H_{49}N_9O_{11}$ 771, observed 772 (MH^+)

Bz-Dab-Ser-Thr-Val-Thr-Nph-NH_2 (25)

The purified peptide was dissolved in DMSO and the solution was quantified by measuring the absorbance of the *p*-nitrophenyl moiety[10]. The peptide was assayed for inhibition against yeast microsomes as described below. IC_{50} = 0.358 μM; the reported K_i, 0.072 μM, is a mean value and the observed deviation is 4% of the mean value.

HPLC: t_R = 17.1 min (C_{18}, 7%–100% B over 28 min); ES-MS: Calculated for $C_{36}H_{51}N_9O_{12}$ 801, observed 802 (MH^+)

Bz-Dab-Abu-Thr-Val-Thr-Nph-NH_2 (26)

The purified peptide was dissolved in DMSO and the solution was quantified by measuring the absorbance of the *p*-nitrophenyl moiety[10]. The peptide was assayed for inhibition against yeast microsomes as described below. IC_{50} = 0.052 μM; the reported K_i, 0.010 μM is a mean value and the observed deviation is 10% of the mean value.

HPLC: t_R = 18.5 min (C_{18}, 7%–100% B over 28 min); ES-MS: Calculated for $C_{37}H_{53}N_9O_{11}$ 799, observed 800 (MH^+)

Determination of IC_{50} and K_i

The radiolabeled carbohydrate substrate Dol-P-P-GlcNAc-[^{3}H]-GlcNAc was dissolved in DMSO for the control measurements, or, DMSO containing the inhibitor for the inhibition studies. Assay buffer (50 mM Hepes, pH 7.5, 140 mM sucrose, 1.2% Triton X-100, 0.5 mg/mL PC, 10 mM $MnCl_2$) and crude OT-containing microsomes from *S. cerevisiae*[15, 16] were added to the carbohydrate substrate. After incubation for 30 minutes, the assay was initiated by adding the Bz-NLT-NHMe peptide substrate (100 μM). Reaction aliquots (4 x 40 μL) were removed at two minute intervals and quenched into 3:2:1 chloroform:methanol:4 mM $MgCl_2$. The tritiated glycopeptide in the upper aqueous layer was separated from the unreacted glycolipid through a series of extractions. The combined aqueous layers were quantitated for tritium content. The disintegrations per minute (dpm) were plotted as a function of time for the control and 3-5 different inhibitor concentrations. The percentage of inhibition was determined from this plot in order to estimate the IC_{50}. Three concentrations were then selected to give between 30% and 70% inhibition. All experiments were run in duplicate. In each case, the approximate K_i was determined using the following equation:[17]

$$K_i = \frac{[I] \times (1-i)}{i + \left(\frac{[S]}{K_M} \times i \right)}$$

References

1. Varki, A., "Biological Roles of Oligosaccharides: All of the Theories Are Correct". *Glycobiology*, **1993**. *3*, 97-130.

2. Imperiali, B., "Protein Glycosylation: The Clash of the Titans". *Acc. Chem. Res.*, **1997**. *30*, 452-459.

3. Hendrickson, T.L., Spencer, J.R., Kato, M., and Imperiali, B., "Design and Evaluation of Potent Inhibitors of Asparagine-Linked Glyosylation". *J. Am. Chem. Soc.*, **1996**. *118*, 7636-7637.

4. Eason, P.D. and Imperiali, B., "A Potent Oligosaccharyl Transferase Inhibitor That Crosses the Intracellular Endoplasmic Reticulum Membrane". *Biochemistry*, **1999**. *38*, 5430-5437.

5. Imperiali, B., Shannon, K.L., and Rickert, K.W., "Role of Peptide Conformation in Asparagine-Linked Glycosylation". *J. Am. Chem. Soc.*, **1992**. *114*, 7942-7944.

6. Imperiali, B., Spencer, J.R., and Struthers, M.D., "Structural and Functional Characterization of a Constrained Asx-Turn Motif". *J. Am. Chem. Soc.*, **1994**. *116*, 8424-8425.

7. Imperiali, B. and Shannon, K.L., "Differences between Asn-Xaa-Thr-Containing Peptides: A Comparison of Solution Conformation and Substrate Behavior with Oligosaccharyltransferase". *Biochemistry*, **1991**. *30*(18), 4374-4380.

8. Imperiali, B., Shannon, K.L., Unno, M., and Rickert, K.W., "A Mechanistic Proposal for Asparagine-Linked Glycosylation". *J. Am. Chem. Soc.*, **1992**. *114*, 7944-7945.

9. Virgilio, A.A. and Ellman, J.A., "Simultaneous Solid Phase Synthesis of β-Turn Mimetics Incorporating Side Chain Functionality". *J. Am. Chem. Soc.*, **1994**. *116*, 11580-11581.

10. Kellenberger, C., Hendrickson, T.L., and Imperiali, B., "Structural and Functional Analysis of Peptidyl Oligosaccharyl Transferase Inhibitors". *Biochemistry*, **1997**. *36*, 12554-12559.

11. Devraj, R. and Cushman, M., "A Versatile Solid Phase Synthesis of Laventuctin A and Certain Biologically Active Analogs". *J. Org. Chem.*, **1996**. *61*, 9368-9373.

12. Wiesmann, C., Hengstenberg, W., and Schulz, G.E., "Crystal Structure and Mechanism of 6-Phosphogalactosidase from *Lactococcus Lactis*". *J. Mol. Biol.*, **1997**. *269*, 851-860.

13. Johnson, P.E., Tomme, P., Joshi, M.D., and McIntosh, L.P., "Interaction of Soluble Cellooligosaccharides with *N*-Terminal Cellulose-Binding Domain of Cellulomonas Fimi Cenc. 2. NMR and Ultraviolet Absorption Spectroscopy". *Biochemistry*, **1996**. *35*, 13895-13906.

14. Gavel, Y. and von Heijne, G., "Sequence Differences between Glycosylated and Non-Glycosylated Asn-X-Thr/Ser Acceptor Sites: Implications for Protein Engineering". *Protein Eng.*, **1990**. *3*(5), 433-442.

15. Pathak, R., Hendrickson, T.L., and Imperiali, B., "Sulfydryl Modification of the Yeast Wbp1p Inhibits Oligosaccharyl Tranferase Activity". *Biochemistry*, **1995**. *34*, 4179-4185.

16. Pathak, R., Parker, C.S., and Imperiali, B., "The Essential Yeast Nlt1 Gene Encodes the 64kDa Glycoprotein Subunit of the Oligosaccharyl Tranferase". *FEBS Lett.*, **1995**. *362*, 229-234.

17. Segel, I.H., *Enzyme Kinetics*. 1975, New York: John Wiley and Sons.

Chapter 3

Neoglycopeptides as Product Inhibitors of OT

Introduction

Asparagine-linked glycosylation is a crucial event that takes place in eukaryotic cells and affects secretory and membrane bound proteins.[1] This process, catalyzed by the multimeric, membrane-bound enzyme OT, involves the en bloc transfer of a preassembled triantennary tetradecasaccharide $Glc_3Man_9GlcNAc_2$ from a dolichyl-pyrophosphate-linked donor to selected Asn-Xaa-Thr/Ser acceptor sites within nascent polypeptides.[2] One of the remarkable features of this event is that the enzyme appears to simultaneously associate with both substrates, the polypeptide and the dolichol-linked oligosaccharide, in a ternary complex. It is surprising that OT can accommodate these large substrates, while still being able to efficiently turn over at a rate that is consistent with the rate of protein synthesis.[3,4] Little is known about the active site of OT due to the challenges associated with overexpression and purification of membrane-bound protein complexes. Currently, substrate and product-based probes of OT represent the most valuable tools for providing insight into the mechanism of *N*-linked glycosylation.[5]

To date, there are three proposed mechanisms for the reaction catalyzed by oligosaccharyl transferase. Two of the proposed mechanisms, those proposed by Marshall[6] and Bause[7], involve the formation of a transition state with a negative charge in the nitrogen of the Asn side chain (see Figure 3.1). However, peptides with an Asp in place of the Asn, which should mimic such a transition state, are not recognized by the enzyme.[8,9]

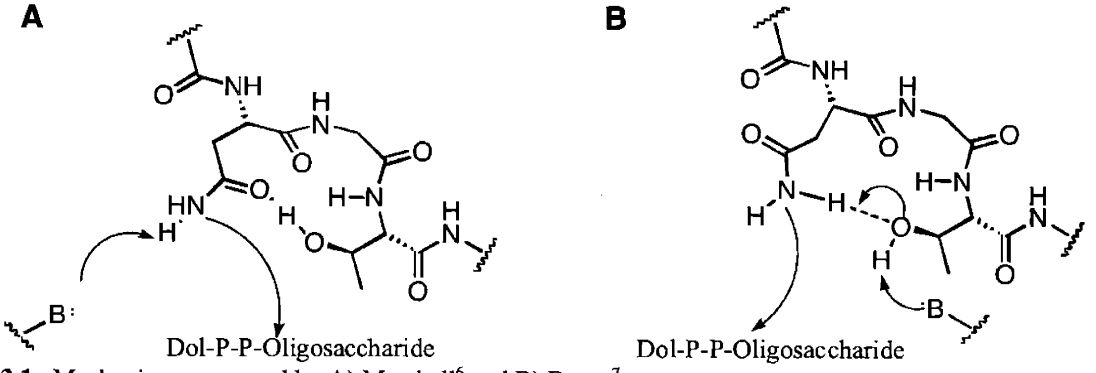

Figure 3.1. Mechanisms proposed by A) Marshall[6] and B) Bause[7].

The third mechanism, proposed by Imperiali et al[8], involves the activation of the side chain of the Asn, assisted by the hydrogen bonding interactions provided by an Asx-turn conformation[10] (see Figure 3.2). Evidence supporting this mechanism was presented when a peptide constrained in an Asx-turn conformation showed to be a better substrate than the linear analog.[11] Further evidence was presented from NMR data, which supports this proposed mechanism by showing that unglycosylated peptides acquire an Asx-turn conformation in solution, while the glycosylated analog shows a β-turn conformation.[12]

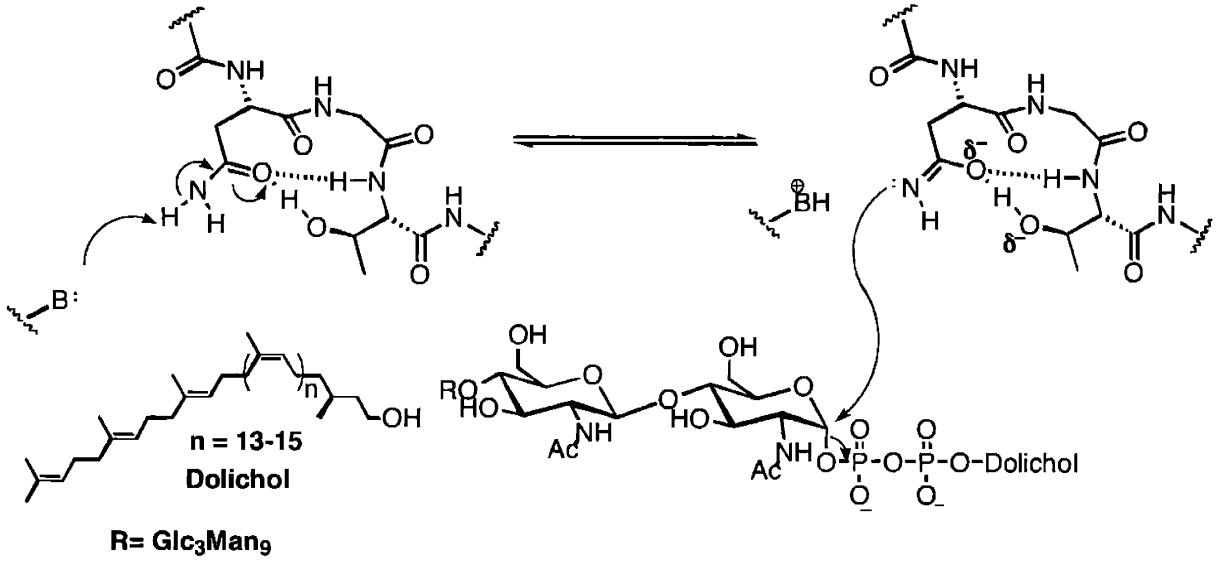

Figure 3.2. Mechanism proposed by Imperiali et al.[8]

Previous research efforts resulted in the development of a potent and specific cyclic inhibitor of OT, c[Hex-Dab-Cys]-Thr-Val-Thr-Nph-NH_2 (Peptide **1**, Figure 3.3, K_i = 37 nM), where the consensus sequence for glycosylation is constrained to an Asx-turn motif and bears a Dab in place of Asn.[11, 13, 14] In the previous chapter we showed that linear peptides that retain the inhibitor nanomolar potency can be obtained when the appropriate residues are selected (Peptide **3**, Figure 3.3, K_i = 11 nM). Also, efforts to improve the potency of the cyclic inhibitor led to the discovery that *N*-δ-alkylation of the Dab side chain with a bulky, aromatic naphthyl group in the

right orientation improves inhibitory activity (Peptide **2**, Figure 3.3, K_i = 10 nM).[15] This effect is in stark contrast with modification of the native asparagine side chain of OT substrates, where a simple *N*-δ-methylation is known to eliminate binding to the enzyme.[16] As aromatic amino acids are often implicated in carbohydrate/protein binding interactions,[17, 18] we reasoned that the naphthyl group might be involved in π-stacking interactions within the saccharide binding pocket of the active site of the enzyme.[19, 20] This hypothesis led us to investigate neoglycopeptides as potential product analog inhibitors of OT. Product analogs would be anticipated to exhibit better affinity and specificity for the enzyme than compounds that mimic either substrate alone. Furthermore, such constructs might provide insights into the geometry of the active site as well as the mechanism of the enzyme.[21]

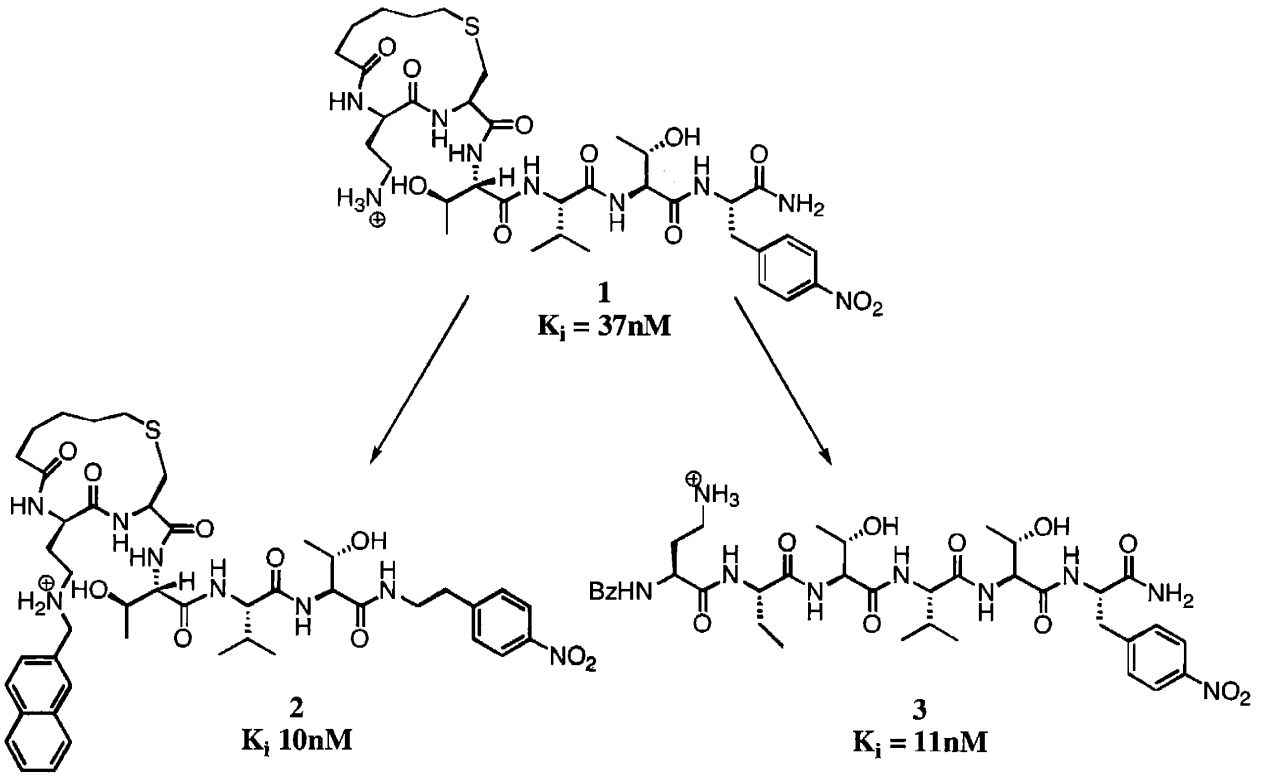

Figure 3.3. Nanomolar inhibitors of *N*-linked glycosylation.

The synthesis of glycopeptide mimetics (or "neoglycopeptides") has received considerable attention recently with the development of *C*- and *S*-glycoside analogs as well as

targets prepared by chemoselective ligation techniques.[22] These neoglycopeptides show similar solution conformation and biological activities to the native *N*- or *O*-linked glycopeptides.[23, 24] Furthermore, it has been shown that substituting the native *N*-*C* or *O*-*C* of *N*-linked or *O*-linked glycopeptides with *S*-*C* or *C*-*C* bonds increases the stability of the glycopeptides against enzymatic hydrolysis.[25, 26]

The strategy for the assembly of product analog inhibitors of OT described herein is based on the use of alanine β-hydroxylamine (Aβx)[27], alanine β-hydrazide (Aβz)[27], and Dab[8, 13-15] as asparagine surrogates (Figure 3.4). These residues have been chosen because the side chain functionality reacts chemoselectively with reducing sugars, without the need for protecting groups or activating agents, to afford *N*-linked glycoconjugates in highly convergent synthetic routes. The work presented here was done in collaboration with Dr. S. Peluso and M. O'Reilly.

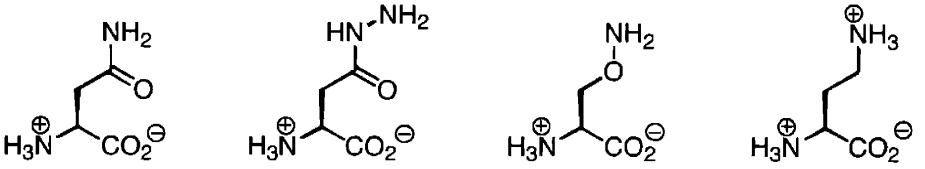

Figure 3.4. Asparagine and asparagine analogs used in this study.

In the present work, we have designed linear hexapeptides of the general sequence Bz-Xaa-Ala-Thr-Val-Thr-Nph-NH_2, featuring the natural substrate, Asn (**4**), as well as Aβz (**5**), Aβx (**6**), and Dab (**7**) at the Xaa position (Figure 3.5). Peptides of this general sequence show good affinity for OT.[13-15, 28] Glycoconjugates of **5**, **6**, and **7** with *N*-acetylglucosamine (**5a**, **6a**, **6b**, and **7a**) were also prepared as potential product analog inhibitors of OT. Glycopeptide **4a** was prepared as a reference compound. The four nonnatural glycopeptides exhibited binding affinities that are similar to those of their respective parent peptides, while the natural glycopeptide has significantly diminished binding compared to its parent peptide. The contrast

between the binding affinity of the glycopeptide bearing a natural amide linkage and those with nonnatural linkages is discussed in the context of the conformational preferences of the polypeptide substrate and glycopeptide product in the active site of OT.

Results

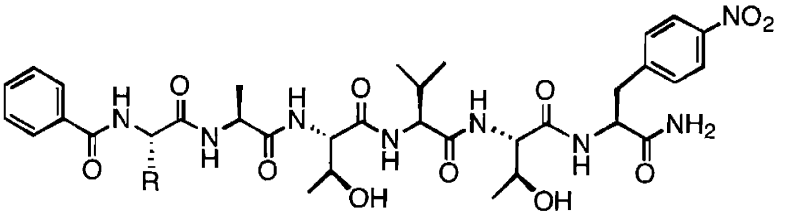

R =

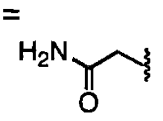

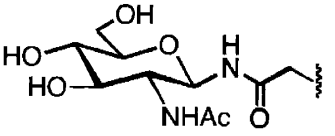

4 $K_m = 0.31\ \mu M$ **4a** $K_i = 100 \pm 5\ \mu M$

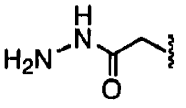

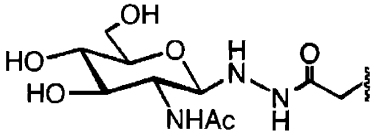

5 $K_i = 2.5 \pm 0.2\ \mu M$ **5a** $K_i = 4.5 \pm 0.5\ \mu M$

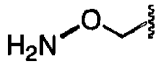

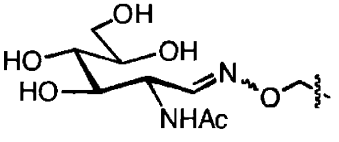

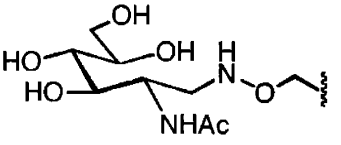

6 $K_i = 34 \pm 3\ \mu M$ **6a** $K_i = 1.10 \pm 0.05\ \mu M$ **6b** $K_i = 4.0 \pm 0.9\ \mu M$

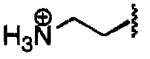

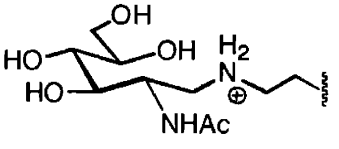

7 $K_i = 0.062 \pm 0.005\ \mu M$ **7a** $K_i = 0.041 \pm 0.002\ \mu M$

Figure 3.5. Peptide and glycopeptide conjugates

Synthesis of Peptides and Glycopeptides

Peptides **4–7** were assembled using a combination of solid-phase and solution-state methods. An Asn(GlcNAc) building block was employed for the synthesis of **4a**. The hydrazide functionality in **5** was prepared from an orthogonally protected aspartic acid derivative, which enabled deprotection and coupling of *t*-butylcarbazate onto the side chain prior to cleavage from the resin as described previously.[27] Formation of the glycosyl-hydrazide (**5a**) was carried out in solution by chemoselective ligation of peptide **5** with unprotected *N*-acetylglucosamine. For the preparation of the hydroxylamine analog (**6**), the corresponding phthalimide-protected derivative was prepared and integrated into polypeptide sequences via standard solid-phase synthesis methods.[27] After deprotection, reaction of **6** with *N*-acetylglucosamine gave the glycosyl-oxime (**6a**) as a mixture of cyclic and acyclic saccharide derivatives. Subsequent reduction of **6a** with sodium cyanoborohydride resulted in the glycosyl-hydroxylamine (**6b**). Reduction fixes the sugar in the acyclic form. For the synthesis of **7**, commercially available *N*-α-Fmoc-Dab(Boc)-OH was employed. Neoglycopeptide **7a** was prepared through treatment with *N*-acetylglucosamine followed by reduction with sodium cyanoborohydride.

Kinetic Analysis of the Natural Substrate and Corresponding Glycoconjugate

Each of the compounds was evaluated for inhibition with *S. cerevisiae* OT in competition assays with the tritium labeled disaccharide donor Dol-P-P-$(GlcNAc)_2$ and the tripeptide substrate Bz-Asn-Leu-Thr-NHMe.[29] The inhibition constants are summarized in Figure 3.5. The K_m of the asparagine-containing peptide (**4**) was determined by measuring the rate of reaction over a range of peptide concentrations. Kinetic parameters were determined using a Hanes plot. The glycopeptide featuring a secondary glycosyl amide at the glycosidic linkage, **4a**, is a very

poor product inhibitor of OT (K_i ~100 μM), reflecting a significant change in binding affinity from the peptide featuring asparagine in the same site (K_m = 0.31 μM). This dramatic decrease in affinity may account for the lack of product inhibition that is necessary for the turnover of OT to keep up with the rate of protein translation and translocation. While these model systems are significantly smaller than the actual substrate and product that they represent, a direct comparison is being made between two peptides that are the same in length, only differing by the presence or absence of a single saccharide unit. It is postulated that the effect observed in the native system may be even more pronounced.

Kinetic Analysis of Nonnatural Peptides and Glycoconjugates

Each of the substrate mimetics (**5**–**7**) displays inhibition of OT (Figure 3.5). The estimated pK_a values of each nonnatural side chain functionality (based on model compounds in which the methylene adjacent to the α-carbon has been replaced by a methyl substituent) are 3.2, 4.6, and 10.6 for **5**, **6**, and **7**, respectively (pK_a values were determined with the software ACD/pKDB v. 4.59 [Advanced Chemistry Development Inc., Toronto, Canada]), suggesting that only **7** is protonated in the pH range of 6–8 where OT is active. As peptide **7** is notably more potent than peptides **5** and **6**, it is clear that the positive charge on the γ-nitrogen at neutral pH imparts additional binding affinity, potentially via interactions that may develop between high energy intermediates and the enzyme in the transition state of the reaction.[30] Since the enzyme is active only at pH 6-8, a detailed study of the pH dependence of the inhibition constants is not feasible; therefore, the focus of the following analysis will be on the relative effects of saccharide modification within each peptide and neoglycopeptide family.

In contrast to the naturally occurring glycoside (**4a**), replacement of the glycosyl-amide bond with a glycosyl-hydrazide (**5a**), a glycosyl-oxime (**6a**), a glycosyl-hydroxylamine (**6b**), or a glycosyl amine (**7a**) affords low micromolar-nanomolar inhibitors of OT. Therefore, replacing the native amide bond between the peptide and the *N*-acetylglucosamine moiety with a more flexible linkage allows the neoglycopeptide to retain, and in some cases improve, binding affinity over that of the parent peptide.

A possible rationale for these observations lies in the conformational preferences of the various glycosidic linkages examined, together with previous proposals for the mechanism of OT.[10] A statistical survey of crystalline *N*-linked glycoproteins reveals that native glycosyl-amide bonds preferentially adopt a stable *trans* conformation (Figure 3.6), as would be expected for a secondary amide linkage.[31] However, as shown by studies on peptide **1a**, this *trans* conformation appears to be poorly accommodated by the enzyme (K_i = 100 μM). This observation is further underscored by studies with a simple peptide featuring a δ-methylasparagine[16] which would also preferentially adopt a *trans* conformation and is neither a substrate nor an inhibitor. Thus, these studies suggest that even a minimal methyl group is not accommodated in the enzyme active site when the substituent favors a *trans* orientation relative to the asparagine side chain. Therefore, the conformation of the nascent glycopeptide product at the OT active site is likely to be represented by a relatively unstable species, such as a *cis* glycosyl amide or a product with a pyramidalized nitrogen, which would undergo a favorable equilibration to a more stable species such as the *trans* glycosyl amide. That ultimate species would no longer present the peptide and saccharide moieties in an appropriate orientation to bind to the enzyme, due to unfavorable steric interactions. In contrast with the native glycosyl amide (**4a**), the Aβz(GlcNAc) featuring peptide, **5a**, shows a K_i of 4.5 μM. Modification of the parent

peptide with the monosaccharide moiety effects a slight decrease in the affinity of the neoglycopeptide for the enzyme; however, compared with **4a** the effect is modest. The reaction of hydrazides at the anomeric center of saccharides is known to lead essentially to the β-pyranosidic form of the saccharide.[32, 33] Crystallographic studies show that substituted hydrazides feature a *trans* planar C-CO-NH-N fragment, the terminal nitrogen having a pyramidal sp^3 character with the substituents out of the hydrazide plane (Figure 3.6).[34, 35] Additionally, a theoretical study of the conformational preferences of the hydrazide linkage in *N,N'*-diacetylhydrazide shows that the CO-NH bonds do not show resonance comparable with *N*-methyl acetamide, and therefore the barrier to rotation about these bonds would be low[36]. Therefore, the hydrazide neoglycopeptide may be able to make similar binding interactions with the peptidyl portion of the OT active site, but the length of the hydrazido side chain may preclude the saccharide moiety from engaging in additional binding. The freedom of rotation around the hydrazido linkage, however, is sufficiently flexible to enable the saccharide to move to a "neutral" position with respect to OT binding.

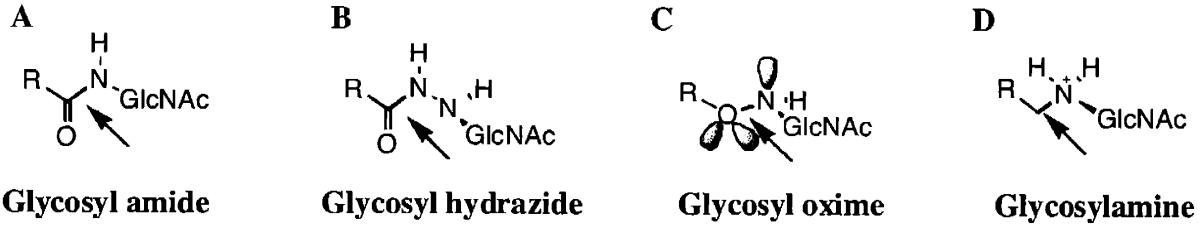

Figure 3.6. Conformational preferences of glycopeptide and neoglycopeptides. **A.** The **glycosyl amide** bond is locked in a trans conformation, and the rotational barrier of this bond is high. The addition of the saccharide in this trans conformation greatly affects binding to OT. **B.** For the **glycosyl hydrazide** a *trans/trans* conformation is favored, but the rotational barrier is low. However, the saccharide is one bond removed from the native product position. **C.** The **glycosyl oxime** dipole/dipole interactions favor an eclipsed conformation, but the rotational barrier is low. Addition of the saccharide significantly enhances binding to OT. **D.** The rotational barrier for the **glycosylamine** is minimal and binding to OT is dominated by the charged nature of the glycoconjugate. Only a slight increase in binding affinity is observed with the addition of the saccharide.

Replacing the native glycosyl-amide bond with a glycosyl-oxime bond in **6a** dramatically affects inhibitory potency of the hydroxylamine-peptide; the K_i is 1.1 μM (compared with 34 μM

for the unmodified peptide). Glycosyl-oxime derivatives have been shown to exist in an equilibrium mixture involving E and Z acyclic isomers as well as the cyclic β-pyranosidic glycosyl-hydroxylamine.[37] Reducing the glycosyl-oxime **6a** to the linear glycosyl-hydroxylamine **6b** resulted in a 4-fold weaker OT inhibition. This observation suggests that the most active species of **6a** is the β-pyranosidic form. The hydroxylamine bond is known to adopt unusual conformational preferences due to the lone pair electrons on both oxygen and nitrogen. Thus *N,O*-disubstituted hydroxylamines like **6a** and **6b** preferentially adopt a conformation where $\omega_{C\text{-}N\text{-}O\text{-}C} = 240°$ (Figure 3.6); however, the barrier to rotation in these species is low[38]. Thus, in the case of the glycosyl oxime derivatives a 30-fold improvement in binding is observed with the neoglycopeptide derivative.

Finally, the conjugate with Dab, **7a**, shows the most potent inhibition ($K_i = 0.041\ \mu M$). In this case, it should be noted that the parent peptide without the glycosyl modification is also a potent inhibitor ($K_i = 0.061\ \mu M$); thus, inhibitory effects are dominated by the charged state of the analog and only slightly effected by the glycosylation.

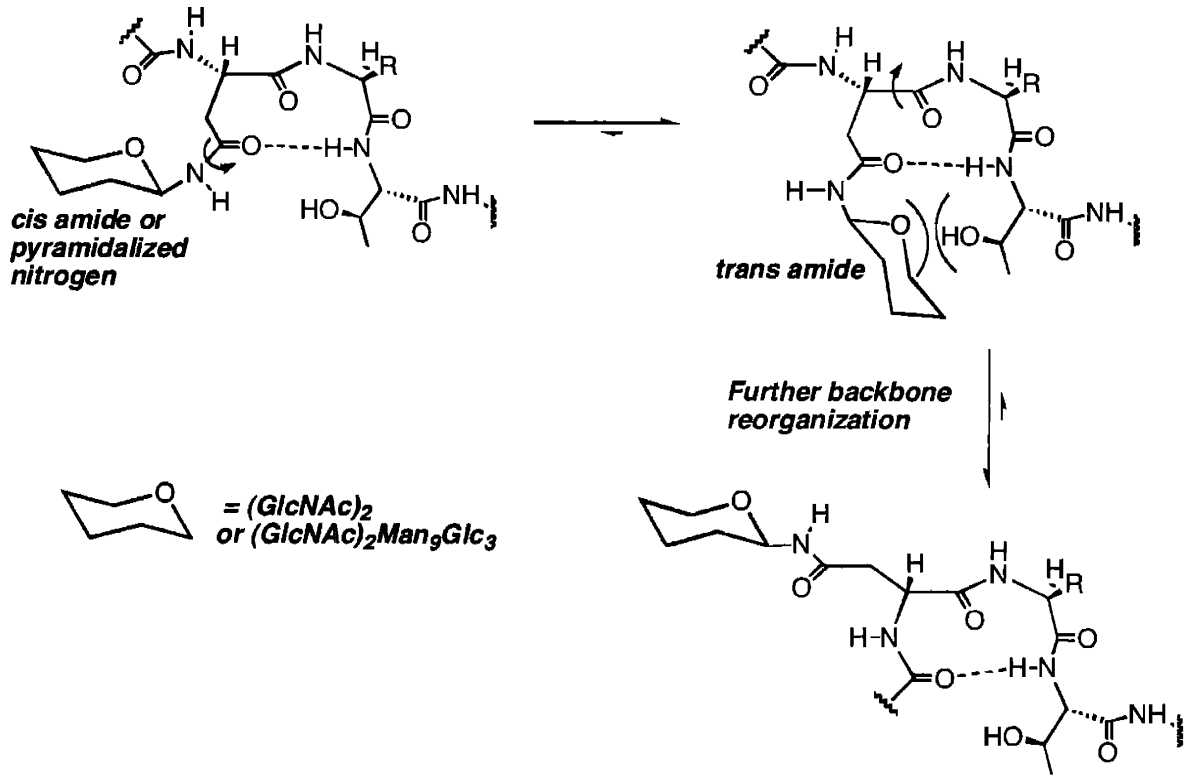

Figure 3.7. Proposal for the role of isomerization in promoting product release. Initially, the glycosyl amide bond is in a *cis* amide conformation and rapidly switches to a more energetically favorable *trans* conformation that promotes product release from the active site. The backbone then experiences a complete chain reversal to a more favorable β-turn conformation.

These conformational considerations suggest that neoglycopeptides can be accommodated in the OT binding site only when the nitrogen carrying the glycosyl moiety is not "locked" into a *trans* orientation relative to the asparagine side chain. In this context, we propose a mechanistic model in which the initial glycoconjugate formed in the OT active site may be represented by a species with *cis* or twisted amide geometry. Thus, an energetically favorable equilibration to the *trans* amide species may participate in the release of the *N*-glycosylated peptide from the OT active site and effectively eliminate product inhibition due to the greatly reduced binding affinity of the *trans* amide isomer for the OT active site (Figure 3.7). It should be noted that a great deal more energy would be required for such a conformational change in the

case of the natural tetradecasaccharide as compared to a monosaccharide; however, the strain in the native product would also be significantly greater in this scenario.

In summary, the results of these studies reveal that binding in the OT active site depends heavily on both the geometry and electronics of the linkage between the peptide and saccharide components of the inhibitor. These product analog inhibitors also suggest a model for understanding the lack of product inhibition in the enzyme-catalyzed transformation. Current work in our laboratory is focused on the further study of this proposal.

Discussion

Asparagine-linked glycosylation is a ubiquitous modification of eukaryotic secretory and membrane-bound proteins. This reaction is catalyzed by the heteromeric membrane-associated complex oligosaccharyl transferase during translocation of nascent polypeptides into the endoplasmic reticulum. As this is a cotranslational process occurring between two large substrates, each with significant affinity for the enzyme, insight into understanding how an enzyme such as OT may negotiate product inhibition is of significant interest. Herein we have shown, in contrast to the native glycosyl amide linkage, that some neoglycopeptides retain or even gain affinity for OT relative to the unglycosylated counterparts. We propose that this effect may be due to the fact that the nascent glycopeptide is initially synthesized in a metastable conformation that equilibrates to a stable *trans* amide isomer that is no longer accommodated at the enzyme active site. Such an event may represent a useful mechanism for prevention of product inhibition, as it would result in a "mismatch" between the binding determinants in the product with those at the active site. Furthermore, these studies have led to the development of

neoglycopeptides with flexible linkages that are accepted into the binding site, thus introducing the first product inhibitors of OT.

Acknowledgements

This research was supported by the NIH (GM-39334) and Merck Research Laboratories. Support to M.K.O. (NIH traineeship in Biotechnology) and M.L.U. (NIH Cancer Training Grant) is also gratefully acknowledged.

Experimental Section

General Procedure for Fmoc-Based Solid-Phase Peptide Synthesis

All peptides were prepared manually using a glass reaction vessel fitted with a sintered glass frit. The resin was washed and swollen in CH_2Cl_2 (2 x 10 ml/g resin x 15 min) and dimethylformamide (DMF) (1 x 10 ml/g resin x 15 min). *N*-α-Fmoc was removed by treatment with piperidine: DMF 1:5 (3 x 10 ml/g resin x 5 min) followed by washing with DMF (5 x 10 ml/g resin x 1 min). The number of equivalents was determined by quantification of Fmoc release. This was accomplished by measuring the UV absorbance at 300 nm of the pooled deprotection rinses and DMF washes. Coupling reactions were performed using 1.5 equivalents of *N*-α-Fmoc-protected amino acids activated in situ with 1.5 equivalents of PyBOP and 3 equivalents of diisopropylethylamine (DIPEA) in DMF (10 ml/g resin) for 1 hr. The success of each coupling and deprotection was verified by a trinitrobenzene sulfonic acid (TNBS) test, whereby approximately a milligram of resin was removed and added to a solution of TNBS in DMF. TNBS reacts with free amines to form a bright pink product. *N*-terminal capping was

accomplished by adding 10 equivalents of benzoic anhydride and 10 equivalents of pyridine in DMF (2.5 ml/g resin) to resin-bound peptides and shaking at room temperature for 1 hr. This capping step was followed by washing with DMF (5 x 10 ml/g resin x 1 min) and CH_2Cl_2 (2 x 10 ml/g resin x 1 min). Cleavage of peptides from resin with concomitant removal of side-chain-protecting groups was performed using 10 ml/g resin of trifluoroacetic acid (TFA):CH_2Cl_2: triisopropylsilane:H_2O (90:5:2.5:2.5). The cleavage reaction was allowed to proceed for 1 hr, then the beads were filtered and rinsed with TFA (2 x 1 ml). Filtrate was concentrated to 1 ml under a stream of nitrogen, then triturated with 14 ml of diethyl ether. The white solid obtained was isolated by centrifugation, washed twice with diethyl ether, and dried. All peptides were purified by preparative HPLC with a gradient of increasing acetonitrile/0.1% TFA (B) in water/0.1% TFA.

*BzAsnAlaThrValThrNphNH$_2$ (**4**)*

For kinetic comparison, a natural OT substrate was synthesized by standard Fmoc-based solid-phase peptide synthesis on PAL-PEG-PS resin. K_m was determined by measuring the rate of reaction at 5 nM, 50 nM, 125 nM, 250 nM, 500 nM, 1 μM, 2 μM, 3 μM, and 4 μM peptide. These results were fit to a Hanes plot. The assay was performed as described below, using the hexapeptide, **4**, as the substrate.

$C_{36}H_{49}N_9O_{12}$; HPLC: t_R = 20 min (C_{18}, 7%–100% B over 28 min); exact mass, 799.35; mol. wt., 799.83; ES-MS: $[MH]^+$ = 800.26.

*BzAsn(GlcNAc)AlaThrValThrNphNH$_2$ (**4a**)*

BzAsn(Ac_3GlcNAc)AlaThrValThrNphNH$_2$ was prepared by standard methods on PAL-PEG-PS resin, with the exception that coupling of the building block, Fmoc-Asn(Ac_3 GlcNAc)-OPfp, proceeded without activating agent or base. Following deprotection and cleavage, the peptide was taken up in methanol (20 ml). Removal of the *O*-acetyl groups was accomplished by adding sodium methoxide (180 μmol, 9.7 mg). The reaction was monitored by HPLC and was 92% complete after 22 hr. The product was purified by preparative HPLC for an overall yield of 56%. The K_i was determined as described below and is reported as an average from seven measurements. The standard deviation was less than 10%.

$C_{44}H_{62}N_{10}O_{17}$; HPLC: t_R = 20 min (C_{18}, 7%–100% B over 28 min); exact mass, 1002.43; mol. wt., 1003.2; ES-MS: $[MH]^+$ = 1003.42.

*BzAβzAlaThrValThrNphNH$_2$ (**5**)*

Preparation of **5** began with the synthesis of BzAsp(OAll)AlaThrValThrNphNH$_2$ by standard Fmoc-based solid-phase peptide synthesis on Fmoc-XAL-PS resin. Removal of the allyl ester protecting group from Asp was done on the solid support using catalytic Pd(PPh_3)$_4$ (0.2 equivalents) and phenylsilane (25 equivalents) as a scavenger. Coupling of *t*-butylcarbazate (1.5 equivalents) onto the Asp side chain in the presence of PyAOP (3 equivalents) and collidine (15 equivalents) on the solid support led to **5** after standard cleavage, deprotection, and HPLC purification for an overall yield of 24%. The K_i was determined as described below and is reported as an average from three measurements. The standard deviation was less than 10%.

$C_{36}H_{50}N_{10}O_{12}$; HPLC: t_R = 18 min (C_{18}, 7%–100% B over 28 min); exact mass, 814.36; mol. wt., 814.84; ES-MS: $[MH]^+$ = 815.30.

*BzAβz(GlcNAc)AlaThrValThrNphNH$_2$ (**5a**)*

Chemoselective ligation was used to prepare **5a** in solution by adding 5 equivalents of GlcNAc (22.5 μmol) to one equivalent of **5** (4.5 μmol) in DMSO (100 μL). After 18 hr at room temperature followed by concentration under reduced pressure, the HPLC trace showed 80% conversion to **5a**. Preparative HPLC was used to purify the product. The K_i was determined as described below and is reported as an average from three measurements. The standard deviation was less than 10%.

$C_{44}H_{63}N_{11}O_{17}$; HPLC: t_R = 19 min (C_{18}, 20%–70% B over 25 min); exact mass, 1017.44; mol. wt., 1018.03; ES-MS: $[MH]^+$ = 1221.29, $[M\text{-}H_2O]^+$ = 1018.31.

*BzAβxAlaThrValThrNphNH$_2$ (**6**)*

Preparation of **6** began with the synthesis of a phthalimide-protected serine building block, Fmoc-Aβx(Pht)-OH, as reported[27]. The peptide was synthesized by standard Fmoc-based solid-phase peptide synthesis on Fmoc-XAL-PS resin, with the exception that coupling of the building block was accomplished using 2 equivalents of PyAOP as the activating agent and 3.7 equivalents of 2,4,6-collidine as the base. Removal of the phthalimide-protecting group with hydrazine: allyl alcohol: trifluoroethanol (1:3:46) (10 ml) was performed on the solid phase for 20 hr with 90% conversion by HPLC. Standard cleavage, deprotection, and purification led to **6**.

$C_{35}H_{49}N_9O_{12}$; HPLC: t_R = 20 min (C_{18}, 20%–70% B over 25 min); exact mass, 787.35; mol. wt., 787.82; ES-MS: $[MH]^+$ = 788.13.

*BzAβx(GlcNAc)AlaThrValThrNphNH$_2$ (**6a**)*

To a solution of **6** (15 μmol) in DMSO (30 μL) was added 30 μmol of GlcNAc (1 M) in 0.1 M sodium acetate buffer (pH 5.6, 30 μL). Additional DMSO (60 μL) was added to obtain a clear solution, then the reaction mixture was concentrated overnight under reduced pressure to obtain **6a** in 80% conversion by HPLC. Preparative HPLC was used to purify the product. The K_i was determined as described below and is reported as an average from three measurements. The standard deviation was less than 5%.

$C_{43}H_{62}N_{10}O_{17}$; HPLC: t_R = 16 min (C_{18}, 20%–70% B over 25 min); exact mass, 990.43; mol. wt., 991.01; ES-MS: $[MH]^+$ = 991.41.

*BzAβx(rGlcNAc)AlaThrValThrNphNH$_2$ (**6b**)*

To a solution of **6a** (15 μmol) in acetic acid (700 μL) was added sodium cyanoborohydride (120 μmol, 7.5 mg), and the progress of the reduction was monitored by analytical HPLC. After 10 min, the reaction was complete and the product was purified by preparative HPLC. Overall yield was approximately 20%. The K_i was determined as described below and is reported as an average of four measurements. The standard deviation was less than 20%.

$C_{43}H_{64}N_{10}O_{17}$; HPLC: t_R = 21 min (C_{18}, 7%–100% B over 28 min); exact mass, 992.45; mol. wt., 993.03; ES-MS: $[MH]^+$ = 993.29.

BzDabAlaThrValThrNphNH$_2$ (7)

Standard Fmoc-based solid-phase peptide synthesis procedures were used to obtain **7** on Fmoc-XAL-PS resin. The K_i was determined as described below and is reported as an average from five measurements. The standard deviation was less than 10%.

$C_{36}H_{51}N_9O_{11}$; HPLC: t_R = 18 min (C_{18}, 7%–100% B over 28 min); exact mass, 785.37; mol. wt., 785.84; ES-MS: $[MH]^+$ = 786.3.

*BzDab(GlcNAc)AlaThrValThrNphNH$_2$ (**7a**)*

A 25 μmol portion of GlcNAc (1 M in phosphate buffer, pH 7.5) was added to **7** (25 μmol in 100 μL DMF) and heated to 65°C. Sodium cyanoborohydride (250 μmol of a 0.25 mg/ml solution in DMF) was then added, and the mixture was stirred at 65°C for 2.5 hr. Finally, the reaction mixture was diluted in 1:1 water: acetonitrile (10 ml) and purified by preparative HPLC. Overall yield was 20%. The K_i was determined as described below and is reported as an average from three measurements. The standard deviation was less than 5%.

$C_{44}H_{66}N_{10}O_{16}$; HPLC: t_R = 19 min (C_{18}, 7%–100% B over 28 min); exact mass, 990.47; mol. wt., 991.05; ES-MS: $[MH]^+$ = 991.39.

Determination of IC_{50} and K_i

The radiolabeled carbohydrate substrate Dol-PP-GlcNAc-[^{3}H]-GlcNAc was dissolved in DMSO for the control measurements or DMSO containing the inhibitor for the inhibition studies. Assay buffer (50 mM HEPES [pH 7.5], 140 mM sucrose, 1.2% Triton X-100, 0.5 mg/ml PC, 10 mM $MnCl_2$) and OT-containing solubilized microsomes from *S. cerevisiae*[39, 40] were added to the carbohydrate substrate. After incubation for 30 min, the assay was initiated by adding the Bz-Asn-Leu-Thr-NHMe peptide substrate. Reaction aliquots (4 x 40 μL) were removed at 2 min intervals and quenched into 3:2:1 chloroform: methanol: 4 mM $MgCl_2$. The tritiated glycopeptide in the upper aqueous layer was separated from the unreacted glycolipid through a series of extractions. The combined aqueous layers were quantitated for tritium content. The disintegrations per minute (dpm) were plotted as a function of time for the control and three to five different inhibitor concentrations. The percentage of inhibition was determined from this plot in order to estimate the IC_{50}. Three concentrations were then selected to give between 30% and 70% inhibition. All experiments were run a minimum of three times. In each case, the approximate K_i was determined using the following equation:[41]

$$K_i = \frac{[I] \times (1-i)}{i + \left(\frac{[S]}{K_M} \times i \right)}$$

Determination of K_m of Bz-Asn-Ala-Thr-Val-Thr-Nph-NH_2

OT assays were performed as described above, except that instead of Bz-Asn-Leu-Thr-NHMe, Bz-Asn-Ala-Thr-Val-Thr-Nph-NH_2 was used as the disaccharide acceptor. The K_m of the tripeptide substrate, 0.25 μM, is similar to that of the hexapeptide containing asparagine that is used for comparison in this study, which has a K_m of 0.31 μM. The following concentrations

were assayed: 5 nM, 50 nM, 125 nM, 250 nM, 500 nM, 1 μM, 2 μM, 3 μM, and 4 μM. From the slope of the dpm versus time plots, velocity (nmol/s) was calculated. Velocity versus substrate concentration was plotted to confirm saturation, and a Hanes plot ([S]/V versus [S]) was used to determine the K_m, with a linear regression of 0.99447. From the Hanes plot, the x intercept is equal to (-)K_m.

References

1. Kornfeld, R. and Kornfeld, S., "Assembly of Asparagine-Linked Oligosaccharides". *Ann. Rev. Biochem.*, **1985**. *54*, 631-664.

2. Varki, A., "Biological Roles of Oligosaccharides: All of the Theories Are Correct". *Glycobiology*, **1993**. *3*, 97-130.

3. Knauer, R. and Lehle, L., "The Oligosaccharyltransferase Complex from Yeast". *Biochim. Biophys. Acta*, **1999**. *1426*, 259-273.

4. Yan, Q., Prestwich, G.D., and Lennarz, W.J., "The Ost1p Subunit of Yeast Oligosaccharyl Transferase Recognizes the Peptide Glycosylation Site Sequence, -Asn-X-Ser/Thr-". *J. Biol. Chem.*, **1999**. *274*, 5021-5025.

5. Imperiali, B., "Protein Glycosylation: The Clash of the Titans". *Acc. Chem. Res.*, **1997**. *30*, 452-459.

6. Marshall, R.D., "The Nature and Metabolism of the Carbohydrate-Peptide Linkages of Glycoproteins". *Biochem. Soc. Symp.*, **1974**. *40*, 17-26.

7. Bause, E., "Model Studies on *N*-Glycosylation of Proteins". *Biochem. Soc. Trans.*, **1984**. *12*, 514-517.

8. Imperiali, B., Shannon, K.L., Unno, M., and Rickert, K.W., "A Mechanistic Proposal for Asparagine-Linked Glycosylation". *J. Am. Chem. Soc.*, **1992**. *114*, 7944-7945.

9. Bause, E., Breuer, W., and Peters, S., "Investigation of the Active Site of Oligosaccharyltransferase from Pig Liver Using Synthetic Tripeptides as Tools". *Biochem. J.*, **1995**. *312*, 979-985.

10. Imperiali, B., Shannon, K.L., and Rickert, K.W., "Role of Peptide Conformation in Asparagine-Linked Glycosylation". *J. Am. Chem. Soc.*, **1992**. *114*, 7942-7944.

11. Imperiali, B., Spencer, J.R., and Struthers, M.D., "Structural and Functional Characterization of a Constrained Asx-Turn Motif". *J. Am. Chem. Soc.*, **1994**. *116*, 8424-8425.

12. O'Connor, S.E. and Imperiali, B., "Conformational Switching by Asparagine-Linked Glycosylation". *J. Am. Chem. Soc.*, **1997**. *119*, 2295-2296.

13. Hendrickson, T.L., Spencer, J.R., Kato, M., and Imperiali, B., "Design and Evaluation of Potent Inhibitors of Asparagine-Linked Glyosylation". *J. Am. Chem. Soc.*, **1996**. *118*, 7636-7637.

14. Kellenberger, C., Hendrickson, T.L., and Imperiali, B., "Structural and Functional Analysis of Peptidyl Oligosaccharyl Transferase Inhibitors". *Biochemistry*, **1997**. *36*, 12554-12559.

15. Ufret, M.d.L., Imperiali, B., "Probing the Extended Binding Determinants of Oligosaccharyl Transferase with Synthetic Inhibitors of Asparagine-Linked Glycosylation". *Bioorg. Med. Chem. Lett.*, **2000**. *10*, 281-284.

16. Welpy, J.K., Shenbagamurthi, P., Lennarz, W.J., and Naider, F., "Substrate Recognition by Oligosaccharyltransferase: Studies on Glycosylation of Modified Asn-X-Thr/Ser Tripeptides". *J. Biol. Chem.*, **1983**. *258*, 11856-11863.

17. Wiesmann, C., Hengstenberg, W., and Schulz, G.E., "Crystal Structure and Mechanism of 6-Phosphogalactosidase from *Lactococcus Lactis*". *J. Mol. Biol.*, **1997**. *269*, 851-860.

18. Johnson, P.E., Tomme, P., Joshi, M.D., and McIntosh, L.P., "Interaction of Soluble Cellooligosaccharides with *N*-Terminal Cellulose-Binding Domain of Cellulomonas Fimi Cenc. 2. NMR and Ultraviolet Absorption Spectroscopy". *Biochemistry*, **1996**. *35*, 13895-13906.

19. Quiocho, F.A., "Protein-Carbohydrate Interactions: Basic Molecular Features". *Pure Appl. Chem.*, **1989**. *61*, 1293-1306.

20. Ponyl, T., Szabo, L., Nagy, T., Orosz, L., Simpson, P.J., Williamson, M.P., and Gilbert, H.J., "Trp22, Trp24, and Tyr8 Play a Pivotal Role in the Binding of the Family 10 Cellulose-Binding Module from *Pseudomonas Xylanase a* to Insoluble Ligands". *Biochemistry*, **2000**. *39*, 985-991.

21. Wolfenden, R., "Analog Approaches to the Structure of the Transition State in Enzyme Reactions". *Acc. Chem. Res.*, **1972**. *5*, 10-18.

22. Marcaurelle, L.A. and Bertozzi, C.R., "New Directions in the Synthesis of Glycopeptide Mimetics". *Chem. Eur. J.*, **1999**. *5*, 1384-1390.

23. Levy, D.E., *The Chemistry of C-Glycosides*. 1995, Oxford: Pergamon.

24. Kishi, Y., "Preferred Solution Conformation of Marine Natural Product Palytoxin and of *C*-Glycosides and Their Parent Glycosides". *Pure Appl. Chem.*, **1993**. *65*, 771-778.

25. Bar, T. and Schmidt, R.R., "Synthesis of β-Lactosyl 1-Thioceramide". *Liebigs Ann. Chem.*, **1991**. *2*, 185-187.

26. Sparks, M.A., Williams, K.W., and Whitesides, G.M., "Neuraminidase-Resistant Hemagglutination Inhibitors - Acrylamide Copolymers Containing a *C*-Glycoside of *N*-Acetylneuraminic Acid". *J. Med. Chem.*, **1993**. *36*(6), 778-783.

27. Peluso, S. and Imperiali, B., "Asparagine Surrogates for the Assembly of *N*-Linked Glycopeptide Mimetics by Chemoselective Ligation". *Tetrahedron Lett.*, **2001**. *42*, 2085-2087.

28. Eason, P.D. and Imperiali, B., "A Potent Oligosaccharyl Transferase Inhibitor That Crosses the Intracellular Endoplasmic Reticulum Membrane". *Biochemistry*, **1999**. *38*, 5430-5437.

29. Imperiali, B. and Shannon, K.L., "Differences between Asn-Xaa-Thr-Containing Peptides: A Comparison of Solution Conformation and Substrate Behavior with Oligosaccharyltransferase". *Biochemistry*, **1991**. *30*(18), 4374-4380.

30. Schramm, V.L., "Enzymatic Transition States and Transition State Analog Design". *Ann. Rev. Biochem.*, **1998**. *67*, 693-720.

31. Imberty, A. and Perez, S., "Stereochemistry of the *N*-Glycosylation Sites in Glycoproteins". *Protein Eng.*, **1995**. *8*, 699-709.

32. Leteux, C., Childs, R.A., Chai, W., Stoll, M.S., Kogelberg, H., and Feizi, T., "Biotinyl-1-3-(2-Naphthyl)-Alanine Hydrazide Derivatives of *N*-Glycans: Versatile Solid-Phase Probes for Carbohydrate-Recognition Studies". *Glycobiology*, **1998**. *8*, 227-236.

33. Bendiak, B., "Preparation, Conformation, and Mild Hydrolysis of 1-Glycosyl-2-Acetylhydrazines of the Hexoses, Pentoses, 2-Acetamido-2-Deoxyhexoxes, and Fucose". *Carbohydrate Res.*, **1997**. *304*, 85-90.

34. Aubry, A., Bayeul, D., Mangeot, J.-P., Vidal, J., Sterin, S., Collet, A., Lecoq, A., and Marraud, M., "X-Ray Conformational Study of Hydrazino Peptide Analogs". *Biopolymers*, **1991**. *31*, 793-801.

35. Ernholt, B.V., Thomsen, I.B., Lohse, A., Plesner, I.W., Jensen, K.B., Hazell, R.G., Liang, X., Jakobsen, A., and Bols, M., "1-Azafagomine, Part 2: Enantiospecific Synthesis of 1-Azafagomine". *Chem. Eur. J.*, **2000**. *6*, 278-287.

36. Aleman, C. and Puiggali, J., "Preferences of the Oxalamide and Hydrazide Moieties in Vacuum and Aqueous Solution. A Comparison with the Amide Functionality". *J. Org. Chem.*, **1999**. *64*, 351-358.

37. Cervigni, S.E., Dumy, P., and Mutter, M., "Synthesis of Glycopeptides and Lipopeptides by Chemoselective Ligation". *Angew. Chem. Int. Ed. Engl.*, **1996**. *35*, 1230-1232.

38. Walker, S., Gange, D., Gupta, V., and Kahne, D., "Analysis of Hydroxylamine Glycosidic Linkages: Structural Consequences of the NO Bond in Calicheamicin". *J. Am. Chem. Soc.*, **1994**. *116*, 3197-3206.

39. Pathak, R., Hendrickson, T.L., and Imperiali, B., "Sulfydryl Modification of the Yeast Wbp1p Inhibits Oligosaccharyl Transferase Activity". *Biochemistry*, **1995**. *34*, 4179-4185.

40. Pathak, R., Parker, C.S., and Imperiali, B., "The Essential Yeast Nlt1 Gene Encodes the 64kDa Glycoprotein Subunit of the Oligosaccharyl Tranferase". *FEBS Lett.*, **1995**. *362*, 229-234.

41. Segel, I.H., *Enzyme Kinetics*. 1975, New York: John Wiley and Sons.

Chapter 4

Design of Bioavailable Inhibitors of OT

Introduction

Potent and specific enzyme inhibitors have been used as tools to determine the mechanisms of key biological transformations. Inhibitors have also provided invaluable information about the implications of important biological processes.[1] *N*-linked glycosylation is one of the most complex protein modifications in eukaryotic systems,[2] but currently the only bioavailable inhibitor of this process, tunicamycin, is not specific and its effect is not immediate.[3-6] It is desirable to obtain inhibitors that specifically target oligosaccharyl transferase (OT), the enzyme that catalyzes this process, within a cellular environment. The Imperiali group has synthesized potent *in vitro* inhibitors of OT.[7-10] The following chapter describes the efforts to obtain bioavailable inhibitors of OT based on the *in vitro* inhibitors described previously.

A large number of biologically active peptides have been discovered over the past four decades.[11-14] Many of these peptides, such as neurotransmitters, neuromodulators, hormones, and enzyme inhibitors, have been associated with a series of vital functions such as metabolism, immune defense, digestion, respiration, sensitivity to pain, reproduction behavior, and electrolyte levels. Therefore, there is an enormous interest in developing these compounds as drugs. However, the use of peptides as drugs has been limited by their low metabolic stability towards proteolysis by enzymes, and by their poor absorption due to high molecular weight and hydrophilicity.[15]

There are several factors that contribute to the bioavailability of a drug. In general, the target molecule should have a low molecular weight. The general consensus is that there is a molecular weight cutoff of 500-700 g/mol, as molecules larger than this cannot cross the cellular membrane passively. Also, the molecules should be lipophilic so that they can interact with the

membrane bilayer, and they should have a low hydrogen bonding potential. Finally, the targeted molecules should be stable to metabolic processes.

As mentioned earlier, peptides tend to be hydrophilic, and the backbone amides provide very good hydrogen bond donors and acceptors. In a study performed with Phe and Gly oligomers, it was shown that the membrane permeability does not correlate with the octanol/water partition coefficient, a common measure of lipid solubility.[16-19] The hydrogen bonding potential was a better predictor of membrane permeability.[20] In fact, the desolvation energy is the most significant factor for membrane transport.[21] Therefore, it is important to take into account the amide content as well as the hydrophobicity when designing peptide-based bioavailable inhibitors.

To design bioavailable inhibitors of OT, we would like to decrease the amide bond content of the peptide. However, the data presented in Chapter 2 revealed that the Thr and Xaa amides in the recognition sequence cannot be eliminated. Therefore, the amide bond of the Val-Thr dipeptide was targeted by introducing a dipeptide isostere. Dipeptide isosteres are defined by the isosteric replacement of the peptide backbone.[14, 22] They include mimetics such as ketomethylene derivatives,[23] (E)-olefin isosteres,[24] aminomethylene,[25] hydroxyethylene,[26] and thiomethylene derivatives.[27] Examples of some of these amide bond replacements are shown in Figure 4.1. The substitution of amide bonds by these isosteres should make peptides more stable to degradation by proteases and simultaneously make the target molecules more bioavailable.[28, 29]

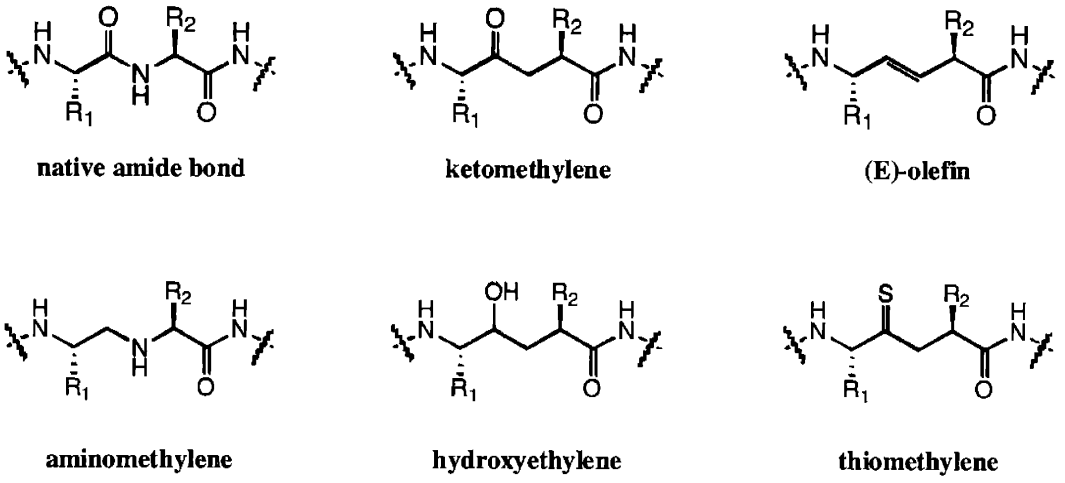

Figure 4.1. Schematic representation of dipeptide isostere mimetics

Protein Transduction Domains

Another method for passive transport is the use of protein translocation domains (PTDs). PTDs are portions of proteins that have been found to be responsible for the translocation of these natural proteins across cellular membranes, without the use of any receptor or transporter.[30, 31] The mechanism of internalization of these small domains, ranging from 9 to 30 residues in length, is not fully understood, though they seem to target the membrane bilayer directly through an energy independent pathway. PTDs have been linked to a wide variety of compounds, such as small molecules, peptides, proteins, oligonucleotides, plasmids, and nanometer-sized particles, and they have been successfully delivered into cells.[30, 32-40]

The data presented herein focuses on the use of three protein transduction domains. These three domains are characterized by a large number of positively charged residues. A description of the Tat HIV-1 domain, a poly-arginine (pArg) sequence, and a Penetratin-1 domain (see Figure 4.2) is presented below.

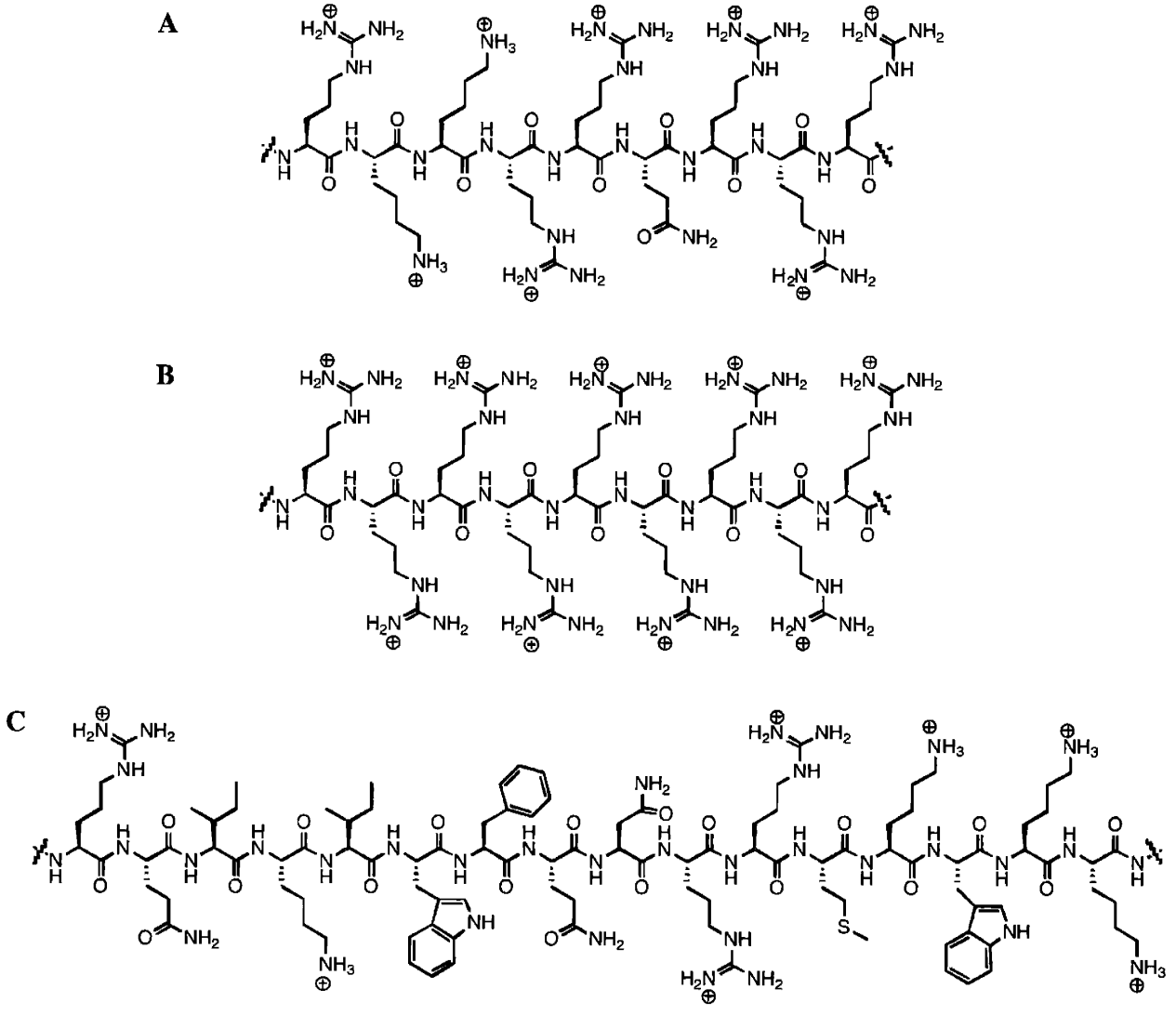

Figure 4.2. Schematic representation of the different protein transduction domains that will be discussed. **A**. TAT HIV-1 translocation domain. **B**. Poly-arginine, polycation derived from TAT. **C**. Penetratin-1, transduction domain of Antennapedia.

Tat-HIV

The translocation properties of Tat, a protein involved in the replication of HIV-1, have been attributed to a basic domain consisting of nine amino acids (Arg-Lys-Lys-Arg-Arg-Gln-Arg-Arg-Arg). This domain does not have a defined structure due to charge repulsion and it includes a nuclear localization sequence (NLS) RKKR at the *N*-terminus, which is not sufficient for internalization. Tat can be internalized by cells in culture after a short incubation (as short as 1 minute) even at 4°C. This indicates that it does not use an endocytic pathway for

internalization. The Tat peptide has been used as a carrier to deliver biologically active proteins and other molecules into mammalian cells.

Poly-arginine

Polycations have been used to enhance peptide delivery into cells. The most efficient polycation found was polyarginine. Buschle *et al*[41] describe the use of different molecular weight polycations to induce the internalization of peptides. From their studies, it is thought that uptake mediated by polylysine is due to cell permeabilization, while uptake mediated by polyarginines (pArg) might rely on an endocytic pathway. Contrary to these results, another study, in which arginine, lysine, ornithine, and histidine homo-oligopeptides were synthesized, demonstrated that only oligoarginine facilitates cellular uptake; homolysine peptides were only found bound to the cell surface.[42] Also, it has been determined that at least seven arginines are required to penetrate the plasma membrane, and a pArg consisting of nine arginine residues provides a peptide ~20-fold more efficient in cell internalization than the original Tat peptide.[43] We have followed this approach to synthesize our inhibitor with a polyarginine tag at either the *N*-terminus or the *C*-terminus. The importance of this carrier over the Tat peptide is that it does not have a NLS, and therefore it might help to localize the inhibitor in the cytosol, where it can be available for transfer to the ER, which is the site of OT activity.

Penetratin-1

It has been shown that the homeodomain of Antennapedia can be internalized by cells in culture.[39, 44] Moreover, Derossi *et al*[35, 45] found that the third helix of the three α-helices that comprise the homeodomain is necessary and sufficient for internalization. They have synthesized a 16-mer peptide corresponding to the sequence of the third helix and demonstrated that it can translocate through the cellular membrane into the cytoplasm and the nucleus. The

efficiency of translocation is similar to the entire homeodomain. Penetratin-1, as this peptide is called, is internalized at both 4°C and 37°C and can be retrieved without any detectable degradation. These data suggest that Penetratin-1 is not internalized by endocytosis.

In order to understand how this compound translocates through the cellular membrane, three variants of Penetratin-1 were synthesized. One variant had the same sequence, but all of the residues were in the (R) configuration. In the second variant, the order of amino acids was reversed, and in the third, the helicity was broken by introducing several prolines.[35] All of these peptides were translocated, therefore the mechanism does not involve a receptor, and it is not structure-specific. A mechanism was proposed by Derossi *et. al.* in which Penetratin-1 interacts with the negatively charged phospholipids on the surface of the cell. The membrane bilayer is destabilized, and an inverted micelle is formed that surrounds the peptide. Finally, the micelle goes through the membrane and delivers its contents into the cytoplasm. This mechanism allows the transport of highly hydrophilic molecules since they never leave an aqueous environment.

Penetratin-1 has been used to transport a wide variety of peptides to the inside of the cell, some of them longer than the Penetratin sequence. The homeodomain has been shown to transport fusion proteins under 100 amino acids in length.[35]

Results

Pseudopeptides containing a ketomethylene dipeptide isostere unit were synthesized and assayed *in vitro* against yeast OT, and *in vivo* with CHO3.6 cells in culture. Also, inhibitors attached to the Tat HIV protein transduction domain, a polyarginine, and a Penetratin-1 peptide were synthesized and assayed *in vitro* and *in vivo*. These domains were placed at either the *N*-terminus or *C*-terminus of the inhibitors, and the kinetic data were compared.

Synthesis of dipeptide isosteres

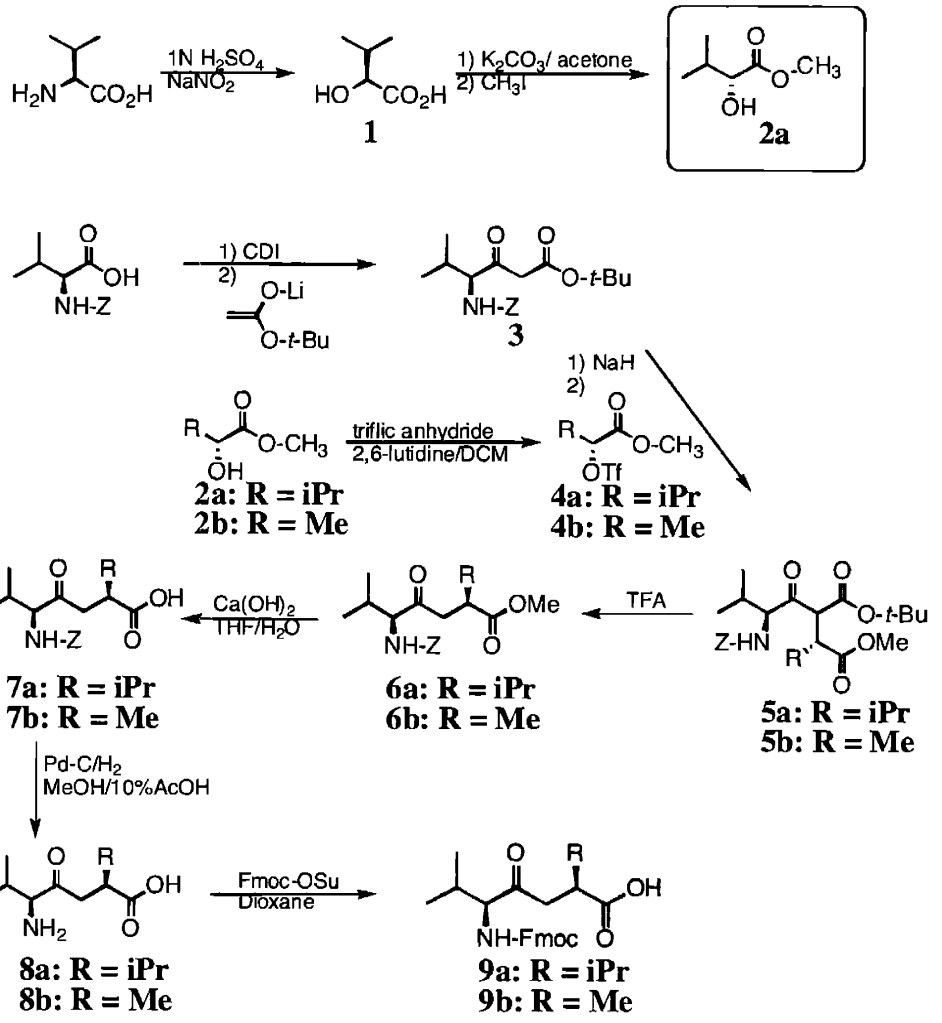

Scheme 4.1. Schematic representation of the synthesis of ketomethylene dipeptide isosteres

Ketomethylene dipeptide isosteres **9a** and **9b** were synthesized following the method of Hoffman and Tao.[46] A benzyloxycarbonyl-protected amino acid was activated with carbonyldiimidazole and added to a solution of lithium *tert*-butylacetate prepared from LDA and *tert*-butylacetate. The alkylation product, (S)-*t*-butyl-4-[(benzyloxycarbonyl)amino]-3-oxo-5-methylhexanoate (**3**), was obtained in a 90% yield. The hydroxy ester **2a** was obtained by diazotization of valine, followed by esterification. The product was obtained with a 56% yield;

2b, methyl-R-(+)-lactate, is commercially available. The hydroxy group of **2** was activated by conversion to the triflate. The 2-triflyloxy ester **4** was obtained in a 73% yield. Ketoester **3** was converted to the enolate with NaH, and reacted with 2 equivalents of **4** to obtain the tricarbonyl derivative **5**. Isostere **6** was obtained in a low yield after decarboxylation with TFA. The ester of isostere **6a** was hydrolyzed with a mixture of lithium iodide and sodium cyanide in refluxing pyridine for 5 days. Compound **7a** was obtained without any detectable epimerization, but the yield of this reaction was too low. The hydrolysis of the ester was repeated with LiOH, which produced two diastereomers (**7a**). The ester of isostere **6b** was hydrolyzed with $Ca(OH)_2$ in THF/H_2O without any detectable epimerization. The amino group of compound **7** was deprotected from the benzyloxycarbonyl group *via* hydrogenolysis, and dipeptide isostere **8** was protected with an Fmoc group to obtain compound **9**.

Synthesis of pseudopeptide inhibitors

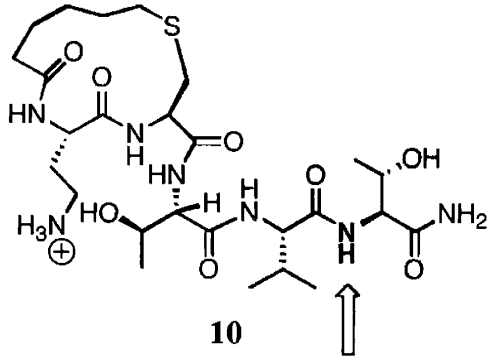

10

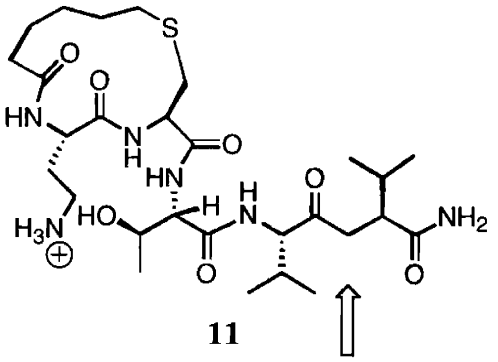

11

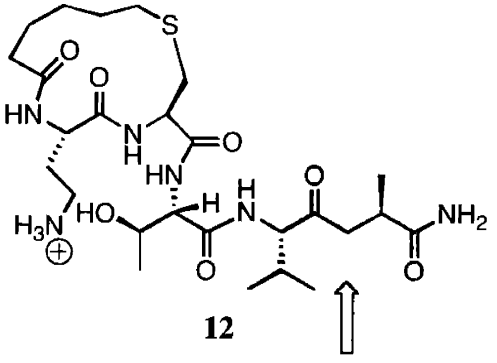

12

Dipeptide isosteres **9a** and **9b** were coupled using HOAt/HATU chemistry and DMAP to facilitate coupling of the building block to the resin. The rest of the amino acids were coupled using HOBt/HBTU chemistry, and the peptide was cyclized from the central amino acid of the recognition sequence (Cys) to the 6-bromo hexanoyl moiety at the *N*-terminus, as described in Chapter 2. Peptides **11** and **12** were assayed for activity against OT from the yeast *S. cerevisiae*, and compared to the parent peptide **10**. In peptide **11**, the Val-Thr dipeptide sequence from peptide **10** has been substituted by a Val-Val isostere analog bearing a ketomethylene unit in place of the dipeptide-connecting amide. For this peptide, the measured IC_{50} and K_i were 9 μM and 2.2 μM, respectively. An approximate 25-fold reduction in affinity for OT is observed for peptide **11**, when compared to peptide **10**. However, substitution of the Val-Thr dipeptide with a Val-Ala ketomethylene isostere in peptide **12** results in an inhibitor with an IC_{50} of 0.48 μM and K_i of 0.091 μM. These values are comparable to the parent peptide **10**, which has a K_i of 0.082 μM.

Peptide **13** was synthesized as a reference in order to directly compare the change in affinity provided by the elimination of this amide bond. In fact, when assayed against yeast OT, an IC_{50} of 0.5 μM and a K_i of 0.25 μM were measured. This peptide binds with approximately 2.5 times less affinity than peptide **12**. These data suggest that OT can tolerate the substitution of the Val-Thr dipeptide in inhibitor **10** for small, hydrophobic groups.

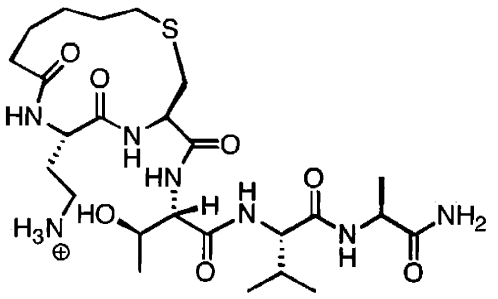

13

Synthesis and kinetic analysis of inhibitors with protein transduction domains

Protein transduction domain-linked inhibitors were synthesized as linear inhibitors with either an Ala or an α-aminobutanoic acid (Abu) as the central residue of the recognition sequence. We have synthesized inhibitors that include the Tat sequence at either the *N*-terminus or *C*-terminus of the inhibitor. *In vitro* experiments with yeast OT show that the Inhibitor-TAT peptide **14** conserves affinity for OT (K_i 86 nM). On the other hand, when the Tat sequence was placed at the *N*-terminus (peptide **15**), the inhibitor lost its high affinity for the enzyme (K_i 2.6 μM).

As we observed in the case of the Tat peptides, the inhibitor with the pArg tag at the *C*-terminus (peptide **16**) retained its affinity for OT (K_i 90 nM), but when the tag is at the *N*-terminus (peptide **17**) the inhibition constant shows an approximate 50-fold increase (K_i 4.3 μM).

For simplicity in cleavage and handling, the Penetratin peptide was used with a mutation of the methionine residue (see Figure 4.2) to a norleucine (Penetratin sequence, Arg-Gln-Ile-Lys-Ile-Trp-Phe-Gln-Asn-Arg-Arg-Nle-Lys-Trp-Lys-Lys). Also, in this case, Abu was used as the central amino acid of the recognition sequence and the amino terminus was capped with a benzoyl group. The purpose of these two changes was to try to achieve a more potent inhibitor.

The kinetic values obtained for peptide **18** were slightly lower than those obtained for peptides **14** and **16** (IC_{50} = 325 nM, K_i = 50 nM).

Table 4.1. Summary of PTDs-linked Inhibitors

SEQUENCE	IC_{50} (μM)	K_i (μM)
Ac-Phe-Dab-Ala-Thr-Val-Thr-Asp-Nph-Gly-TAT (**14**)	0.454	0.086 ± 0.004
TAT-Phe-Dab-Ala-Thr-Val-Thr-Asp-NH_2 (**15**)	13.1	3.6 ± 0.7
Ac-Phe-Dab-Ala-Thr-Val-Thr-Asp-Nph-Gly-Arg_9-NH_2 (**16**)	0.460	0.090 ± 0.005
Ac-Nph-Gly-Arg_9-Phe-Dab-Ala-Thr-Val-Thr-Asp-NH_2 (**17**)	21	4.3 ± 0.3
Bz-Dab-Abu-Thr-Val-Thr-Nph-Penetratin-NH_2 (**18**)	0.325	0.05 ± 0.01

It is important to note that the inhibitors retain their low nM potency even with sequences as long as 16 amino acids extending from the *C*-terminus of the inhibitor sequence. On the contrary, when these sequences are placed at the *N*-terminus, the affinity for OT is diminished and we obtain peptides that bind in the low μM range.

***In vivo* experiments – Metabolic Labeling**

CHOK1 cells were transformed to secrete a protein, M144, that has been mutated to contain only one glycosylation site. An antibody against this protein, 15C6, was raised in mice. The Bjorkman laboratory (California Institute of Technology) kindly provided us with this cell line and the antibody for the protein.[47]

In this experiment, cells were incubated with glycosylation inhibitors for 24 hours. After this period of time, the cells were grown in cysteine and methionine-free media in the presence of a labeling reagent, Tran^{35}S Label, which provides methionine and cysteine labeled with ^{35}S. Thus, the protein secreted into the media is labeled with ^{35}S. The secreted protein was immunoprecipitated and electrophoresed (SDS-PAGE, 10%). The gel was exposed to a

PhosphorImager screen for 16-24 h. A difference in molecular weight can be observed between the unglycosylated and glycosylated protein (Figure 4.3).

Tunicamycin (Tn) inhibits UDP-*N*-acetylglucosamine: dolichyl-phosphate *N*-acetylglucosamine-1-phosphate transferase, the enzyme that transfers *N*-acetylglucosamine-1-phosphate from UDP-GlcNAc to dolichol phosphate to generate *N*-acetylglucosamine-P-P-dolichol. This reaction is the first step in the assembly of the dolichol-linked oligosaccharides required for *N*-linked glycosylation. Tn is used in our experiments as a control to produce unglycosylated protein.

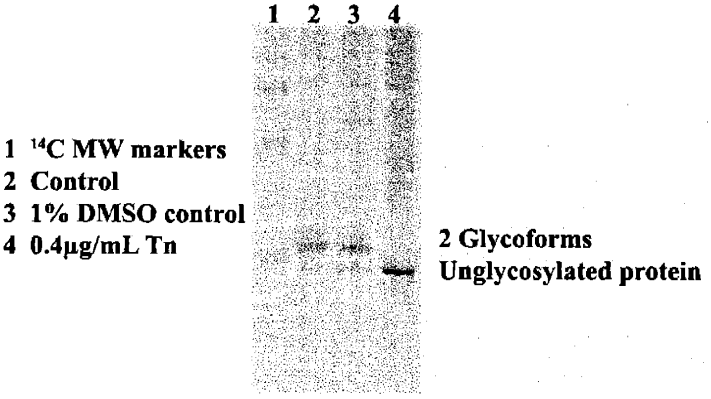

Figure 4.3. Metabolic labeling experiment using CHO3.6 cells. Lanes 2 and 3 are control experiments and show the two glycoforms of the N-linked protein M144. Lane 4 shows the unglycosylated protein; inhibition of glycosylation is induced by tunicamycin.

Inhibitors **11** and **12** contain dipeptide isosteres **9a** and **9b**. The dipeptide isosteres should make the inhibitors more hydrophobic, and therefore more prone to cross lipid bilayers. These peptides should be more resistant to peptidases, both due to the elimination of a peptidic bond, and because of their relatively small size. CHO3.6 cells were incubated with the inhibitors at concentrations up to 1 μM. No unglycosylated protein was detected.

Metabolic labeling experiments were performed to assess the ability of the inhibitors (Inh) with the Tat peptide and the pArg tags to inhibit OT *in vivo*. Figure 4.4 shows the results

for the Tat-containing peptides: TAT-Inh was used in concentrations ranging from 0.1-36 μM and Inh-TAT was used at 0.1-39 μM. The unglycosylated protein is not observed in any of the experiments. Perhaps a higher concentration of peptide is needed, or the peptide is being delivered to the nucleus of the cell where it cannot reach the ER. The experiment was repeated using concentrations ranging from 100-300μM. These concentrations were lethal for the cells.

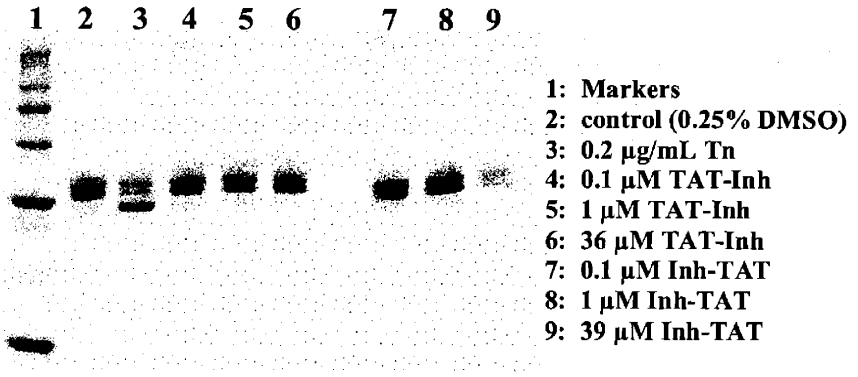

Figure 4.4. *In vivo* experiment using TAT-linked inhibitors.

Figure 4.5 shows the results of the experiment with the pArg-containing peptides. No inhibition is observed at 38μM pArg-Inh or at 49 μM Inh-pArg. As with the Tat peptides, the experiment was repeated with concentrations up to 300 μM, but this was lethal for the cells.

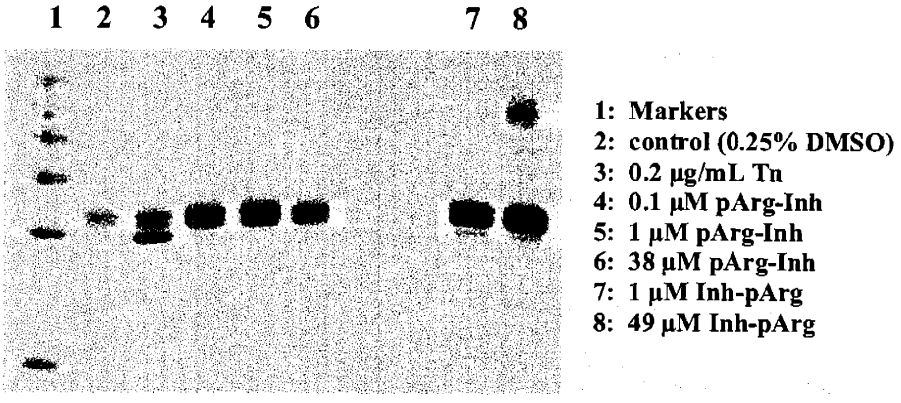

Figure 4.5. *In vivo* experiment with poly-arginine-linked inhibitors.

Metabolic labeling experiments were performed with InhPen. CHO3.6 cells were incubated overnight with 10 and 50 μM inhibitor. After a 12 h incubation period, the shape of the cells with the peptides at 50 μM was rounded instead of stretched, indicating that the cells were not healthy. Before starting the experiment with the ^{35}S-labeled amino acids, the inhibitor was added to 25 μM to wells that were plated with cells the day before. These cells were in contact with the inhibitor only for the 5 h period of the metabolic labeling experiment. Following the metabolic labeling experiment, both secreted and unsecreted proteins were collected together by lysing the cells to obtain the unsecreted protein. The gel in Figure 4.6 shows no inhibition of *N*-linked glycosylation with up to 50μM of InhPen (peptide **18**).

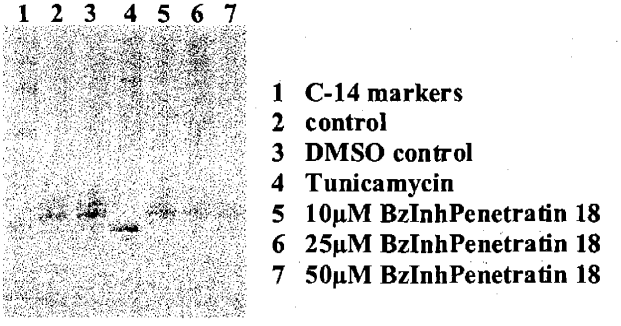

Figure 4.6. *In vivo* experiment with Penetratin-linked inhibitors.

Discussion

The synthesis of inhibitors containing dipeptide isosteres has been discussed. These peptides were tested as *in vitro* and *in vivo* inhibitors of OT. Inhibitor **9b** is a potent *in vitro* inhibitor of OT, while peptide **9a** is only a modest inhibitor with a binding constant in the low μM range. However, these compounds failed to show *in vivo* inhibition of OT when assayed against a modified CHO cell line in culture.

Protein transduction domains were used as carriers of the inhibitors to transport them across the cellular membrane into cells in culture. Inhibitors with PTD either at the *N*-terminus or *C*-terminus were synthesized. The PTD-linked inhibitors did not show any *in vivo* activity, despite being potent *in vitro* inhibitors of OT. These peptides showed cellular toxicity at high concentrations (100 – 300 μM).

Several questions arise from these results. What is the activity of these inhibitors against mammalian OT? The *in vitro* activity of the inhibitors has been determined using OT from the yeast *S. cerevisiae*. Are the peptides capable of crossing the cellular membrane? If so, are they being degraded by proteases in the cytosol? Can they cross the membrane of the ER? These questions will be addressed in the following chapter.

Acknowledgements

This work was supported by a grant from NIH (GM-39334) and by a Ford Foundation predoctoral fellowship to M. L. Ufret.

Experimental Section

*Synthesis of (R)-methyl 2-hydroxy-3-methylbutanoate (**2a**)*

A solution of valine in 1N H_2SO_4 was cooled to 0°C, then a solution of $NaNO_2$ in water was added dropwise to the amino acid solution. The reaction was stirred at 0°C for 3 hours and at room temperature overnight. The product was extracted with ethyl acetate, dried (Na_2SO_4) and concentrated. The 2-hydroxy acid **1** was dried by azeotropic distillation with benzene. Without further purification, the product was dissolved in acetone, and K_2CO_3 was added as a solid; this solution was stirred at room temperature for 3 hours. Iodomethane was added, and the

reaction was heated to reflux overnight. The milky solution was filtered, concentrated, and distilled by bulb to bulb distillation to give the 2-hydroxy ester **2a**.

^{1}H-NMR data ($CDCl_3$, 300 MHz): δ 0.86 (d, 3H, J = 6.9 Hz), 1.02 (d, 3H, J = 6.9 Hz), 2.08 (m, 1H), 3.79 (s, 3H), 4.05 (d, 1H, J = 3.22 Hz).

*Synthesis of (S)-tert-butyl 4-[(benzyloxycarbonyl)amino]-3-oxo-5-methylhexanoate (**3**)*

Cbz-L-Val-OH was washed with benzene and concentrated 3 times; the amino acid was dried under high vacuum overnight. To a stirred solution of Cbz-L-Val-OH in dry THF was added carbonyldiimidazole. The resulting solution was stirred at room temperature for 1 hour. Meanwhile, lithium diisopropylamide (LDA) was prepared from *n*-butyllithium and diisopropylamine at -78°C; *tert*-butylacetate was added to the LDA and stirred at -78°C for 20 minutes. The activated amino acid was added dropwise to the solution of lithium *tert*-butylacetate and the reaction was stirred at the same temperature for 1 hour. The reaction was quenched by the addition of 1N HCl and the product was extracted with ethyl acetate. The combined extracts were washed with brine, dried (Na_2SO_4), and concentrated. The product was obtained as a yellow oil, with a 90% yield after purification by flash column chromatography (hexane:ethyl acetate 4:1).

^{1}H-NMR data ($CDCl_3$, 300 MHz): δ 0.796 (d, 3H, J = 6.8 Hz), 1.03 (d, 3H, J = 6.8 Hz), 1.45 (s, 9H), 2.27 (m, 1H), 3.44 (s, 2H), 4.47 (dd, 1H, J = 3.9, 9 Hz), 5.11 (s, 2H), 5.37 (d, 1H, J = 8.9 Hz), 7.36 (m, 5H).

*Synthesis of (R)-methyl 2-triflyloxy-3-methylbutanoate (**4a**)*

The 2-hydroxy ester was dissolved in dry dichloromethane and cooled to 0°C. Triflic anhydride, followed by 2,6-lutidine, was added to this solution. The reaction was stirred at 0°C for 20 min, then concentrated by rotary evaporation, and the lutidine salts were precipitated with ice-cold pentane. The product was concentrated and used without further purification.

^{1}H-NMR data ($CDCl_3$, 300 MHz): δ 1.01 (d, 3H, J = 6.9 Hz), 1.1 (d, 3H, J = 6.9 Hz), 2.39 (m, 1H), 3.85 (s, 3H), 4.98 (d, 1H, J = 4 Hz)

*Synthesis of (R)-methyl 2-triflyloxy-propanoate (**4b**)*

The 2-hydroxy ester was dissolved in dry dichloromethane and cooled to 0°C. Triflic anhydride, followed by 2,6-lutidine, was added to this solution. The reaction was stirred at 0°C for 20 min, then concentrated by rotary evaporation, and the lutidine salts were precipitated with ice-cold pentane and filtered. The product was concentrated and used without further purification.

^{1}H-NMR data ($CDCl_3$, 300 MHz): δ 1.73 (d, 3H, J = 6.87 Hz), 3.87 (s, 3H), 5.25 (q, 1H, J = 6.87 Hz)

*Synthesis of (2R, 5S) Cbz-ValΨ[$COCH_2$]Val-OMe (**6a**)*

A solution of the 3-oxo ester **3** in dry THF was added dropwise to a suspension of NaH in THF at 0°C. This mixture was stirred at the same temperature for 10 min. A solution of the 2-triflyloxy ester **4a** in dichloromethane was added to the previous suspension. The reaction was stirred at room temperature for 24h and quenched with 1N HCl. The product **5a** was extracted with ethyl acetate, and then the combined extracts were washed with brine, dried (Na_2SO_4), passed through a short pad of silica gel, and concentrated to provide a yellow oil. This oil was dissolved in dichloromethane and treated with TFA at room temperature for 24 hours. The

reaction mixture was dissolved in DCM and washed with saturated $NaHCO_3$, brine, and dried (Na_2SO_4). The dipeptide isostere was purified by column chromatography (hexane:ethyl acetate 4:1 to 2:1) and obtained as a white solid.

^{1}H-NMR data ($CDCl_3$, 300 MHz): δ 0.774 (d, 3H, J = 6.8 Hz), 0.896 (d, 3H, J = 6.7 Hz), 0.912 (d, 3H, J = 6.7 Hz), 1.01 (d, 3H, J = 6.8 Hz), 1.98 (m, 1H), 2.23 (m, 1H), 2.73 (dq, 2H, J = 17.3 Hz), 2.79 (m, 1H), 3.64 (s, 3H), 4.38 (dd, 1H, J = 4, 8.6 Hz), 5.11 (s, 2H), 5.39 (d, 1H, J = 8.6 Hz), 7.35 (m, 5H). ^{13}C-NMR data: δ 16.5, 19.5, 19.7, 20, 29.8, 30.2, 38.7, 46.3, 51.6, 64.7, 66.9, 128, 128.1, 128.4, 136.3, 156.3, 174.6, 208.1.

*Synthesis of (2R, 5S) Cbz-ValΨ[COCH$_2$]Ala-OMe (**6b**)*

A solution of the 3-oxo ester **3** in dry THF was added dropwise to a suspension of NaH in THF at 0°C. This mixture was stirred at the same temperature for 10 min. A solution of the 2-triflyloxy ester **4b** in dichloromethane was added to the previous suspension. The reaction was stirred at room temperature for 3 h and quenched with 1N HCl. The product **5b** was extracted with ethyl acetate, and the combined extracts were washed with brine, dried (Na_2SO_4), passed through a short pad of silica gel and concentrated to provide a yellow oil. This oil was dissolved in dichloromethane and treated with TFA at room temperature for 3 hours. The reaction mixture was dissolved in DCM and washed with saturated $NaHCO_3$, brine, and dried (Na_2SO_4). The dipeptide isostere **6b** was purified by column chromatography (hexane:ethyl acetate 4:1 to 2:1) and obtained as a white solid.

^{1}H-NMR data ($CDCl_3$, 300 MHz): δ 0.79 (d, 3H), 1.05 (d, 3H), 1.25 (d, 3H), 1.7 (m, 1H), 2.3 (m, 1H), 2.55 (dq, 2H), 3.7 (s, 3H), 4.4 (dd, 1H), 5.1 (s, 2H), 5.35 (d, 1H), 7.4 (m, 5H).

*Synthesis of (2R, 5S) Cbz-ValΨ[$COCH_2$]Val-OH (**7a**)*

NaCN and LiI were added to a solution of dipeptide isostere **6a** in pyridine. The mixture was heated to reflux and stirred for 5 days. The reaction mixture was dissolved in ethyl acetate and washed with NH_4Cl, water, and brine, and then dried (Na_2SO_4) and concentrated. The product was purified by column chromatography (hexane:ethyl acetate 1:1) and obtained as a colorless oil.

^{1}H-NMR data ($CDCl_3$, 300 MHz): δ 0.75 (d, 3H, J = 6.8 Hz), 0.94 (d, 3H, J = 7.1 Hz), 0.96 (d, 3H, J = 7.2 Hz), 1.03 (d, 3H, J = 6.8 Hz), 2.05 (m, 1H), 2.28 (m, 1H), 2.83 (m, 1H), 2.49/3.05 (dq, 2H, J = 18.3 Hz), 4.39 (dd, 1H, J = 8.9 Hz), 5.09 (s, 2H), 5.35 (d, 1H, J = 8.9 Hz), 7.34 (m, 5H), 10 (b, 1H).

*Synthesis of (2R, 5S) Cbz-ValΨ[$COCH_2$]Ala-OH (**7b**)*

A solution of $Ca(OH)_2$ in water was added to a solution of dipeptide isostere in THF. This was added in small portions to avoid epimerization. The mixture was washed with $CHCl_3$. The aqueous layer was acidified to extract the acid with chloroform, and the organic layer was dried (Na_2SO_4) and concentrated. The product was purified by column chromatography (hexane:ethyl acetate 1:1) and obtained as a colorless oil.

^{1}H-NMR data ($CDCl_3$, 300 MHz): δ 0.79 (d, 3H), 1.05 (d, 3H), 1.25 (d, 3H), 1.7 (m, 1H), 2.3 (m, 1H), 2.55 (dq, 2H), 4.4 (dd, 1H), 5.1 (s, 2H), 5.4 (d, 1H), 7.4 (m, 5H), 9.5 (b, 1H).

*(2R, 5S) H_2N-ValΨ[$COCH_2$]Val-OH (**8a**) and (2R, 5S) H_2N-ValΨ[$COCH_2$]Ala-OH (**8b**)*

Deprotection of the amine was achieved by the addition of Pd/C to a solution of the isostere in MeOH/1%AcOH. The reaction was stirred under H_2 overnight. The catalyst was

filtered over celite and the filtrate was concentrated. The mixture was washed with toluene and concentrated under reduced pressure several times to eliminate the acetic acid. The crude product was stored without any further purification until the amine was protected again with Fmoc.

*Synthesis of (2R, 5S) FmocHN-ValΨ[COCH$_2$]Val-OH (**9a**)*

Dipeptide isostere **8a** was dissolved in dioxane and the pH of the solution was adjusted to 9-10 using aqueous Na_2CO_3. The amino acid solution was cooled in an ice bath and a solution of 1.2 equivalents Fmoc-OSu in dioxane was added dropwise over 15 min. After 10 minutes, the reaction was allowed to warm-up to room temperature and stirred for 1.5 h. The reaction mixture was concentrated and the product was dissolved in water. The unreacted Fmoc-OSu was extracted with ether, and the aqueous layer was acidified to pH 3 with 6N HCl. The product was extracted with DCM, dried over Na_2SO_4, filtered, and concentrated.

^{1}H-NMR data ($CDCl_3$, 300 MHz): δ 0.75 – 1.05 (m, 12H), 2.05 (m, 1H), 2.26 (m, 1H), 2.86 (m, 1H), 2.5/3.05 (dq, 2H, J = 18.3 Hz), 4.12 (dd, 1H), 4.22 (m, 1H), 4.38 (t, 2H), 5.49 (d, 1H, J = 8.69 Hz), 7.3 (t, 2H, J = 7.2 Hz), 7.39 (t, 2H, J = 7.4), 7.6 (d, 2H, J = 7.12), 7.76 (d, 2H, J = 7.4), 9.5 (b, 1H). MS: Calculated for $C_{26}H_{31}NO_5$, 437, observed 460 $(M+Na)^+$

*Synthesis of (2R, 5S) FmocHN-ValΨ[COCH$_2$]Ala-OH (**9b**)*

Synthesized as described for **9a**.

^{1}H-NMR data ($CDCl_3$, 300 MHz): δ 0.79 (d, 3H), 1.05 (d, 3H), 1.23 (d, 3H), 1.8 (m, 1H), 2.25 (m, 1H), 2.55 (dq, 2H), 4.22 (t, 1H), 4.4 (d, 2H), 4.55 (dd, 1H), 5.4 (d, 1H), 7.28 (t, 2H, J = 7.2

Hz), 7.36 (t, 2H, J = 7.4), 7.56 (d, 2H, J = 7.12), 7.75 (d, 2H, J = 7.4). MS: Calculated for $C_{24}H_{27}NO_5$, 409, observed 432 $(M+Na)^+$

*Synthesis of c[Hex-Dab-Cys]-Thr-Valψ[$COCH_2$]Val-NH_2 (**11**)*

Peptide **11** was synthesized on PAL-PEG-PS resin using standard, Fmoc-based SPPS. The dipeptide isostere **9a** was coupled to the resin using 2 equivalents of the isostere, HOBt and DIPCDI, and 4 equivalents DIPEA. Double coupling of the isostere was necessary, and HOAt, DIPCDI, and DMAP (2 equivalents) were used. Incorporation of the isostere onto the resin was determined to be 77%. The unreacted amines were capped, and coupling of the remaining amino acids proceeded without difficulty, using 4 equivalents of amino acids and HOBt/HBTU, and 8 equivalents of DIPEA. Fmoc-L-Cys(S-tBu)-OH was used as the central amino acid of the enzyme recognition sequence. The amino terminus was capped with 6-bromohexanoic acid, followed by deprotection of the Cys(S-*t*Bu) under N_2, with a large excess of tri-*n*-butylphosphine in degassed DMF (2 x 3h). The resin was rinsed with degassed DMF and cyclization from the thiolate of the Cys to the 6-bromohexanoyl was completed with shaking overnight under N_2 in the presence of a large excess of 1,1,3,3-tetramethylguanidine in degassed DMF . The resin was rinsed with DMF, DCM, and ether, and then dried and cleaved with TFA/H_2O/TIS (95:2.5:2.5). The purified peptide was dissolved in DMSO and quantified using QAA. The peptide was assayed *in vitro* against yeast OT, and *in vivo,* with CHO3.6 cells.

HPLC: t_R = 20.5 min (C_{18}, 0%–70% B over 25 min); ES-MS: Calculated for $C_{28}H_{50}N_6O_7S$ 614, observed 615 (MH^+)

*Synthesis of c[Hex-Dab-Cys]-Thr-Valψ[$COCH_2$]Ala-NH_2 (**12**)*

Coupling of the dipeptide isostere **9b** to the resin presented some difficulty. Coupling was achieved using HOAt/HATU and 2 equivalents of DMAP. The rest of the synthesis proceeded without difficulty, using HOBt/HBTU chemistry. Cyclization was performed as described for peptide **11**. The peptide was cleaved from the resin using TFA/TIS/H_2O (95:2.5:2.5). The purified peptide was dissolved in DMSO and quantified using QAA. The peptide was assayed *in vitro* against yeast OT, and *in vivo*, with CHO3.6 cells.

HPLC: t_R = 23 min (C_{18}, 0%–70% B over 25 min); ES-MS: Calculated for $C_{26}H_{46}N_6O_7S$ 586, observed 587 (MH^+)

*Synthesis of c[Hex-Dab-Cys]-Thr-Val-Ala-NH_2 (**13**)*

Peptide **13** was prepared using Fmoc-based standard SPPS, on PAL-PEG-PS resin. A 4-fold excess of amino acids and activating reagents (HOBt/HBTU) was used, with 8 equivalents of DIPEA. The peptide was cyclized as described above for peptide **11**, and cleaved from the resin using TFA/TIS/H_2O (95:2.5:2.5). The purified peptide was dissolved in DMSO, quantified using QAA, and assayed *in vitro* against yeast OT.

HPLC: t_R = 20.2 min (C_{18}, 0%–70% B over 25 min); ES-MS: Calculated for $C_{34}H_{49}N_7O_9$ 587, observed 588 (MH^+)

Synthesis of protein transduction domain-linked inhibitors

Protein transduction domain-linked inhibitors were synthesized on an automated solid phase peptide synthesizer, using HOBt/HBTU chemistry in PAL-PEG-PS resin. After completion of the synthesis, the peptides were cleaved from the resin using TFA/TIS/H_20/EDT (82:8:2:8) for 1.5h. The TFA was evaporated under a stream of N_2, and then the peptide was

precipitated with ice-cold ethyl ether. The white precipitate was resuspended in ether and washed 3 more times. The peptides were dissolved in water and a sample was run on a C_{18} analytical HPLC column using H_20/0.1% TFA (solvent A) and acetonitrile/0.1% TFA (solvent B). Samples were collected for MS, and the products were purified on a C_{18} preparative column, using a gradient of solvent A and B. The purified, lyophilized peptides were then dissolved in DMSO and quantified using the UV absorbance at 280 nm. Peptides were assayed against yeast OT as described in the previous chapters. The error in the binding constant was 5-20% of the measured value.

*Ac-Phe-Dab-Ala-Thr-Val-Thr-Asp-Nph-Gly- R-K-K-R-R-Q-R-R-R-NH_2 (**14**) - (Inhibitor-TAT)*

HPLC: t_R = 16.3 min (C_{18}, 7%–100% B over 28 min); ES-MS: Calculated for $C_{99}H_{170}N_{42}O_{26}$ 2363, observed 1182.88 $(M+2H)^{2+}$, 788.9 $(M+3H)^{3+}$, 591.9 $(M+4H)^{4+}$

*Ac-Nph-G-R-K-K-R-R-Q-R-R-R-Phe-Dab-Ala-Thr-Val-Thr-Asp-NH_2 (**15**) - (TAT-Inhibitor)*

HPLC: t_R = 14.4 min (C_{18}, 7%–100% B over 28 min); ES-MS: Calculated for $C_{99}H_{170}N_{42}O_{26}$ 2363, observed 1182.88 $(M+2H)^{2+}$, 788.9 $(M+3H)^{3+}$

*Ac-Phe-Dab-Ala-Thr-Val-Thr-Asp-Nph-Gly-Arg_9-NH_2 (**16**) - (Inh-TArg)*

HPLC: t_R = 16.3 min (C_{18}, 7%–100% B over 28 min); ES-MS: Calculated for $C_{101}H_{175}N_{47}O_{25}$ 2446, observed 727 $(M+4TFA)^{4+}$

*Ac-Nph-Gly-Arg_9-Phe-Dab-Ala-Thr-Val-Thr-Asp-NH_2 (**17**) - (TArg-Inh)*

HPLC: t_R = 17.6 min (C_{18}, 7%–100% B over 28 min); ES-MS: Calculated for $C_{102}H_{176}N_{46}O_{25}$ 2445, observed 1224.56 $(M+2H)^{2+}$, 817.05 $(M+3H)^{3+}$, 613.04 $(M+4H)^{4+}$

*Bz-Dab-Abu-T-V-T-Nph-R-Q-I-K-I-W-F-Q-N-R-R-Nle-K-W-K-K-NH_2 (**18**) - (Inh-Penetratin)*

HPLC: t_R = 24.95 min (C_{18}, 7%–70% B over 25 min); ES-MS: Calculated for $C_{142}H_{221}N_{43}O_{30}$ 3010, observed 1004.1 $(M+3H)^{3+}$, 753.3 $(M+4H)^{4+}$, 602.8 $(M+5H)^{5+}$, 502.5 $(M+6H)^{6+}$

Metabolic labeling of CHO3.6 cells

CHO3.6 cells were grown at 37°C and 5% CO_2, in α-MEM, 5% FBS, Penn/Strep, 100 μM MSX. Cells were plated at 3 x 10^5 cells/well in a 24-well plate and allowed to grow to confluency overnight. The cells were incubated with OT inhibitors or Tn overnight; a maximum final concentration of 1% DMSO (in which the inhibitors are dissolved) was used. After this period of time, the cells were grown in cysteine and methionine-free media (DMEM) in the presence of a labeling reagent, Tran^{35}S Label, which provides methionine and cysteine labeled with ^{35}S. Therefore, the M144 glycoprotein that is secreted into the media is labeled with ^{35}S. After a 5 h incubation period, the media was transferred to microcentrifuge tubes and centrifuged for 2 min to pellet any cell debris. The media was transferred to fresh eppendorf tubes and incubated at 4°C with the M144 antibody (15C6) in Tris-Cl (pH 7.5) to a final concentration of 100 mM. Protein G Sepharose beads were added and incubated for 1 h at 4°C. The beads were rinsed with PBS/0.5% Triton X-100 (3 x 500 μL) and boiled for 5 min with 15 μL reducing buffer (20% glycerol, 100 mM Tris pH 6.8, 200 mM DTT, 4% SDS, 0.2% bromophenol blue). The protein was electrophoresed (SDS-PAGE, 10%) and the gel was exposed to X-ray film or a PhosphorImager screen for 24 h.

In order to determine whether unglycosylated protein is retained inside the cell, the experiment was performed as usual to obtain the protein from the media. The cells were then permeabilized with 1%Triton X-100 in PBS for 20 min. The PBS was transferred to eppendorf tubes, which were centrifuged to precipitate the cell debris. The supernatant was transferred to fresh tubes, where it was incubated with the antibody, as described above.

References

1. Silverman, R.B., *Enzyme Inhibition and Inactivation*, in *The Organic Chemistry of Drug Design and Drug Action.* 1992, Academic Press, Inc.: San Diego. p. 146-219.

2. Varki, A., "Biological Roles of Oligosaccharides: All of the Theories Are Correct". *Glycobiology*, **1993**. *3*, 97-130.

3. Elbein, A.D., "The Tunicamycins: Useful Tools for Studies on Glycoproteins". *Trends Biochem. Sci.*, **1981**. *6*, 291-293.

4. Heifetz, A., Keenan, R.W., and Elbein, A.D., "Mechanism of Action of Tunicamycin on the UDP-GlcNAc:Dolichyl-Phosphate GlcNAc-1-Phosphate Transferase". *Biochemistry*, **1979**. *18*(11), 2186-2192.

5. Keller, R.K., Boon, D.Y., and Crum, F.C., "*N*-Acetylglucosamine-1-Phosphate Transferase from Hen Oviduct: Solubilization, Characterization, and Inhibition by Tunicamycin". *Biochemistry*, **1979**. *18*, 3946-3952.

6. Tamura, G., *Tunicamycin.* 1982, Tokyo: Japan Scientific Society Press.

7. Hendrickson, T.L., Spencer, J.R., Kato, M., and Imperiali, B., "Design and Evaluation of Potent Inhibitors of Asparagine-Linked Glycosylation". *J. Am. Chem. Soc.*, **1996**. *118*, 7636-7637.

8. Kellenberger, C., Hendrickson, T.L., and Imperiali, B., "Structural and Functional Analysis of Peptidyl Oligosaccharyl Transferase Inhibitors". *Biochemistry*, **1997**. *36*, 12554-12559.

9. Eason, P.D. and Imperiali, B., "A Potent Oligosaccharyl Transferase Inhibitor That Crosses the Intracellular Endoplasmic Reticulum Membrane". *Biochemistry*, **1999**. *38*, 5430-5437.

10. Ufret, M.d.L., Imperiali, B., "Probing the Extended Binding Determinants of Oligosaccharyl Transferase with Synthetic Inhibitors of Asparagine-Linked Glycosylation". *Bioorg. Med. Chem. Lett.*, **2000**. *10*, 281-284.

11. Krieger, D.T., "Brain Peptides: What, Where, and Why?" *Science*, **1983**. *222*, 975-985.

12. Schmidt, G., "Recent Developments in the Field of Biologically Active Peptides". *Top. Curr. Chem.*, **1986**. *136*, 109-159.

13. Schwarz, J.H., *Principles of Neural Science*, ed. E.R. Kandel, J.H. Schwarz, and T.M. Jessel. 1991: Elsevier. 213.

14. Giannis, A. and Kolter, T., "Peptidomimetics for Receptor Ligands - Discovery, Development, and Medical Perspectives". *Angew. Chem. Int. Ed. Engl.*, **1993**. *32*, 1244-1267.

15. Fawell, S., Seery, J., Daikh, Y., Moore, C., Chen, L.L., Pepinsky, B., and Barsoum, J., "Tat-Mediated Delivery of Heterologous Proteins into Cells". *Proc. Natl. Acad. Sci., USA*, **1994**. *91*, 664-668.

16. Conradi, R.A., Hilgers, A.R., Ho, N.F.H., and Burton, P.S., "The Influence of Peptide Structure on Transport Across Caco-2 Cells". *Pharm. Res.*, **1991**. *8*, 1453-1460.

17. Conradi, R.A., Hilgers, A.R., Ho, N.F.H., and Burton, P.S., "The Influence of Peptide Structure on Transport Across Caco-2 Cells. II. Peptide Bond Modification Which Results in Improved Permeability". *Pharm. Res.*, **1992**. *9*, 435-439.

18. Smith, R.N., Hansch, C., and Ames, M.M., "Selection of a Reference Partitioning System for Drug Design Work". *J. Pharm. Sci.*, **1975**. *64*, 599-606.

19. Austel, V. and Kutter, E., *Absorption, Distribution and Metabolism of Drugs*, in *Quantitative Structure - Activity Relationships of Drugs*, J.G. Topliss, Editor. 1983, Academic Press: New York. p. 437-496.

20. Kim, D.C., Burton, P.S., and Borchardt, "A Correlation between the Permeability Characteristics of a Series of Peptides Using an *In Vitro* Cell Culture Model (Caco-2) and Those Using an *In Situ* Perfused Rat Ileum Model of the Intestinal Mucosa". *Pharm. Res.*, **1993**. *10*, 1710-1714.

21. Ohki, S. and Spangler, R.A., *Passive and Facilitated Transport*, in *The Structure of Biological Membranes*, P. Yeagle, Editor. 1992, CRC Press: Boca Raton, FL. p. 655-720.

22. Spatola, A.F., *Chemistry and Biochemistry of Amino Acids, Peptides and Proteins*, ed. B. Weinstein. Vol. 7. 1983, New York: Marcel Dekker. 267-357.

23. Almquist, R.G., Chao, W.R., Ellis, M.E., and Johnson, H.L., "Synthesis and Biological Activity of a Ketomethylene Analogue of a Tripeptide Inhibitor of Angiotensin Converting Enzyme". *J. Med. Chem.*, **1980**. *23*, 1392-1398.

24. Hann, M.M., Sammes, P.G., Kennewell, P.D., and Taylor, J.B., "On the Double-Bond Isostere of the Peptide-Bond - Preparation of an Enkephalin Analog". *J. Chem. Soc., Perkin Trans. 1*, **1982**. *1*, 307-314.

25. Szelke, M., Leckie, B., Hallett, A., Jones, D.M., Sueiras, J., Atrash, B., and Lever, A.F., "Potent New Inhibitors of Renin". *Nature*, **1982**. *299*, 555-557.

26. Evans, B.E., Rittle, K.E., Homnick, C.F., Springer, J.P., Hirshfield, J., and Veber, D.F., "A Stereocontrolled Synthesis of Hydroxyethylene Dipeptide Isosteres Using Novel, Chiral Aminoalkyl Epoxides and Gamma-(Aminoalkyl) Gamma-Lactones". *J. Org. Chem.*, **1985**. *50*(23), 4615-4625.

27. Spatola, A.F., Agarwal, N.S., Bettag, A.L., Yankeelov, J.A., Bowers, C.Y., and Vale, W.W., "Synthesis and Biological Activities of Pseudopeptide Analogues of LH-RH: Agonists and Antagonists". *Biochem. Biophys. Res. Commun.*, **1980**. *97*, 1014-1023.

28. Pauletti, G.M., Gangwar, S., Siahaan, T.J., Aube, J., and Borchardt, R.T., "Improvement of Oral Peptide Bioavailability: Peptidomimetics and Prodrug Strategies". *Adv. Drug Delivery Rev.*, **1997**. *27*, 235-256.

29. Gillespie, P., Cicariello, J., and Olson, G.L., "Conformational Analysis of Dipeptide Mimetics". *Biopoly.*, **1997**. *43*, 191-217.

30. Schwarze, S.R. and Dowdy, S.F., "*In Vivo* Protein Transduction: Intracellular Delivery of Biologically Active Proteins, Compounds and DNA". *Trends Pharm. Sci.*, **2000**. *21*, 45-48.

31. Tung, C.-H. and Weissleder, R., "Arginine Containing Peptides as Delivery Vectors". *Adv. Drug Delivery Rev.*, **2003**. *55*, 281-294.

32. Schwartz, J.J. and Zhang, S., "Peptide-Mediated Cellular Delivery". *Curr. Opin. Mol. Ther.*, **2000**. *2*, 162-167.

33. Kueltzo, L.A. and Middaugh, C.R., "Potential Use of Non-Classical Pathways for the Transport of Macromolecular Drugs". *Expert Opin. Invest. Drugs*, **2000**. *9*, 2039-2050.

34. Fischer, P.M., Krausz, E., and Lane, D.P., "Cellular Delivery of Impermeable Effector Molecules in the Form of Conjugates with Peptides Capable of Mediating Membrane Translocation". *Bioconjug. Chem.*, **2001**. *12*, 825-841.

35. Derossi, D., Chassaing, G., and Prochiantz, A., "Trojan Peptides: The Penetratin System for Intracellular Delivery". *Trends Cell Biol.*, **1998**. *8*, 84-87.

36. Hawiger, J., "Non-Invasive Intracellular Delivery of Functional Peptides and Proteins". *Curr. Opin. Chem. Biol.*, **1999**. *3*, 89-94.

37. Schwarze, S.R., Hruska, K.A., and Dowdy, S.F., "Protein Transduction: Unrestricted Delivery into All Cells?" *Trends Cell Biol.*, **2000**. *10*, 290-295.

38. Prochiantz, A., "Messenger Proteins: Homeoproteins, Tat and Others". *Curr. Opin. Cell Biol.*, **2000**. *12*, 400-406.

39. Lindgren, M., Hallbrink, M., Prochiantz, A., and Langel, U., "Cell-Penetrating Peptides". *Trends Pharmacol. Sci.*, **2000**. *21*, 99-103.

40. Langel, U., *Cell-Penetrating Peptides: Processes and Applications*. 2002, Boca Raton, FL: CRC Press.

41. Buschle, M., Schmidt, W., Zauner, W., Mechtler, K., Trska, B., Kirlappos, H., and Birnstiel, M.L., "Transloading of Tumor Antigen-Derived Peptides into Antigen-Presenting Cells". *Proc. Natl. Acad. Sci. USA*, **1997**. *94*, 3256-3261.

42. Mitchell, D.J., Kim, D.T., Steinman, L., Fathman, C.G., and Rothbard, J.B., "Polyarginine Enters Cells More Efficiently Than Other Polycationic Homopolymers". *J. Pept. Res.*, **2000**. *56*, 318-325.

43. Wender, P.A., Mitchell, D.J., Pattabiraman, E.T., Pelkey, E.T., Steinman, L., and Rothbard, J.B., "The Design, Synthesis and Evaluation of Molecules That Enable or Enhance Cellular Uptake: Peptoids Molecular Transporters". *Proc. Natl. Acad. Sci. USA*, **2000**. *97*, 13003-13008.

44. Schwarze, S.R., Ho, A., Vocero-Akbani, A., and Dowdy, S.F., "*In Vivo* Protein Transduction: Delivery of a Biologically Active Protein into the Mouse". *Science*, **1999**. *285*, 1569-1572.

45. Derossi, D., Calvet, S., Trembleau, A., Brunissen, A., Chassaing, G., and Prochiantz, A., "Cell Internalization of the Third Helix of the Antennapedia Homeodomain Is Receptor-Independent". *J. Biol. Chem.*, **1996**. *271*, 18188-18193.

46. Hoffman, R.V. and Tao, J., "An Improved Enantiospecific Synthesis of Statine and Statine Analogs *Via* 4-(*N,N*-Dibenzylamine)-3-Keto Esters". *J. Org. Chem.*, **1997**. *62*, 2292-2297.

47. Chapman, T.L. and Bjorkman, P.J., "Characterization of a Murine Cytomegalovirus Class I Major Histocompatibility Complex (MHC) Homolog: Comparison to MHC Molecules and to the Human Cytomegalovirus MHC Homolog". *J. Virol.*, **1998**. *72*(1), 460-466.

Chapter 5

Intracellular Peptide Delivery

Introduction

Currently, the only bioavailable inhibitor of *N*-linked glycosylation is tunicamycin (Tn), a microbial product.[1-3] However, this complex natural product does not target the process of *N*-linked glycosylation directly. It targets the first step in the biosynthesis of the dolichol-linked sugar donor.[4-10] Since this is not a direct or an immediate effect on *N*-linked glycosylation, we are trying to develop bioavailable inhibitors that target this event directly.

Since the active site of OT is located on the lumenal side of the endoplasmic reticulum (ER), any inhibitor targeted at OT must be able to cross the cellular membrane, evade degradation in the cytosol, and cross the membrane of the ER, in order to inhibit OT *in vivo*. It was desirable to probe whether the peptides described in the previous chapter could cross the cell membrane more efficiently than the parent inhibitors. This chapter describes the strategies used to localize the inhibitors in the interior of the cell. Fluorescently labeled inhibitors were synthesized with a BODIPY fluorophore, in the case of small peptides, or fluorescein, in the case of peptides with internalization sequences. The use of a novel assay to test for *in vivo* inhibition of OT is also described.

Inhibitors were labeled with a BODIPY fluorophore (Figure 1A) to track the peptides inside the cell without the use of large internalization sequences or bulky fluorophores. This fluorophore has several advantages over others. A wide variety of derivatives with emission properties that span the visible spectrum are available. The various derivatives have high quantum yields, e_{max} values equal or higher than 60,000 $M^{-1}cm^{-1}$, and narrow spectral bandwidths (Figure 1B). BODIPY is non-polar and electrically neutral and it has been shown that BODIPY conjugates of small molecules are more cell permeable than conjugates of charged fluorophores.

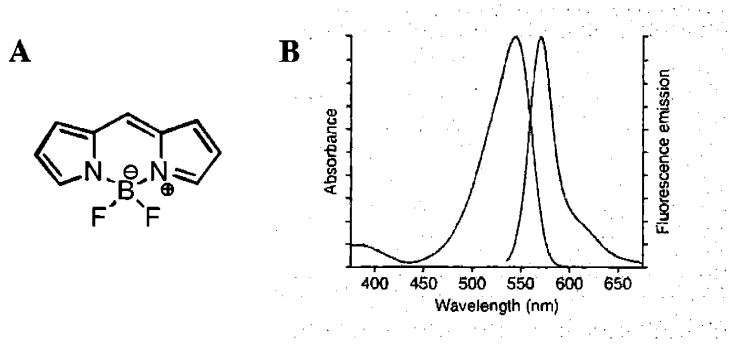

Figure 5.1.A. General structure of BODIPY; **B.** Example of an excitation/emission spectra of BODIPY.

Penetratin-linked inhibitors were labeled with fluorescein at the *N*-terminus. This fluorophore was selected because it is compatible with solid phase synthesis, and it can be coupled on the solid phase without affecting other reactive groups in the extended peptide sequence. Because it was shown that modifications at the *N*-terminus of the inhibitors compromise their affinity for OT, these inhibitors were used only to localize the peptides inside the cell. *In vivo* inhibition experiments were performed with non-labeled Penetratin-linked inhibitors.

To concentrate the inhibitors in the lumen of the ER, an ER retrieval sequence was incorporated. ER retrieval sequences form part of the quality control machinery in the secretory pathway (see Figure 5.2). Proteins destined for the plasma membrane, for secretion, and for secretory and endocytic organelles are synthesized by ribosomes attached to the membrane of the ER. These proteins are retained in the ER until they are completely assembled and correctly folded.[11, 12] Proteins that fail to fold correctly are subject to retrograde translocation to the cytosol and are degraded by the proteasome.[13-15]

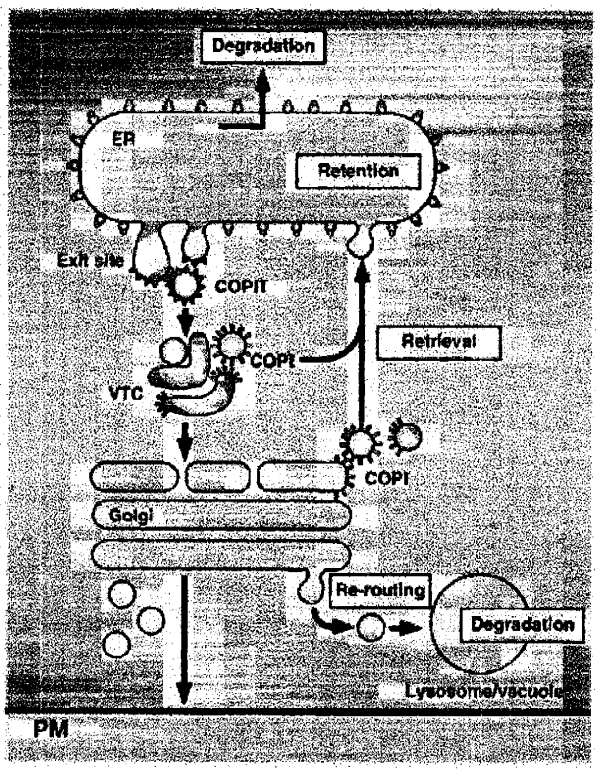

Figure 5.2. Schematic representation of the quality control machinery in the secretory pathway.[12]

Properly folded proteins enter the exit sites, where the COPII coat protein associates with the cytosolic surface of the membrane. The COPII coat mediates the budding off of vesicles and tubular elements that form the vesiculotubular clusters (VTC), or ER-Golgi intermediate compartment, which assist in transport to the Golgi apparatus.[16-18] Once the VTC is formed, the COPI coat replaces the COPII coat. The COPI coat mediates the formation of return vesicles from the VTC and the *cis*-Golgi, which deliver the contents back to the ER.[19, 20] Mature proteins are then delivered from the *trans*-Golgi network to the plasma membrane. Misfolded proteins are re-routed through endosomes to lysosomes for degradation.

The proteins responsible for ER retention of partially folded proteins are chaperones and folding enzymes, such as calnexin, calreticulin, and protein disulfide isomerase. These proteins are resident ER proteins and have a *C*-terminal ER retrieval sequence. Lumenal ER proteins have a KDEL retrieval sequence,[21, 22] while membrane proteins have a KKXX retrieval sequence,

where X is any amino acid.[20, 23, 24] These retrieval sequences ensure that ER quality control proteins are returned from the VTC and the Golgi complex if they escape. The retrieval sequence also assists proteins that escort other proteins from the ER to the Golgi. The KKXX motif is recognized directly by the COPI proteins,[20] while the KDEL sequence is recognized by a KDEL receptor, erd2, that is concentrated in the intermediate compartment and the Golgi apparatus.[25, 26]

Once inhibitors have been internalized by the cells and localized in the ER, an assay to detect *in vivo* inhibition of glycosylation is needed. For this purpose, the use of a secreted glycosylated protein, whose concentration can be detected, is desirable. A secreted version of placental alkaline phosphatase (PLAP) is obtained by a mutation in a hydrophobic domain at the *C*-terminus, which impairs the addition of the phosphatidylinositol glycan moiety that anchors it to the plasma membrane.[27] Truncation or deletion of this hydrophobic domain also prevents the addition of the GPI anchor, producing the secreted version of the protein.[28, 29] The secreted alkaline phosphatase (SeAP), as this mutated version of PLAP is called, has two glycosylation sites. This protein has proved to be useful as a reporter protein to monitor transfection efficiency and productivity of many systems.[30-33] Also, SeAP has been used for evaluation of glycosylation, since the difference in molecular weight between the glycosylated and unglycosylated protein can be detected by the difference in mobility in SDS-PAGE.[32]

The secretion of this glycoprotein into the media can be detected using a variety of techniques, since there are many substrates for the enzyme that produce an absorption of fluorescence signal when a phosphate is cleaved. The unglycosylated version of the protein has been shown to be catalytically active,[34] but most of the protein in this form is not secreted from

the cell.[35] Therefore, upon inhibition of glycosylation, a decrease in enzyme activity in the media should be observed.

A CHO cell line has been engineered to overexpress SeAP upon induction of a mouse mammary tumor virus (MMTV) promoter induced by the addition of the glucocorticoid hormone analog dexamethasone.[30] To produce high levels of the reporter protein, SeAP, the cell line was engineered to overexpress the glucocorticoid receptor necessary to induce the MMTV promoter with the hormone analog (see Figure 5.3). This cell line was kindly provided by the Kompala lab (University of Colorado, Boulder).[30]

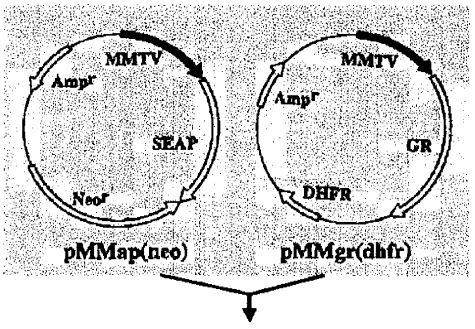

Figure 5.3. Plasmids used for SeAP-producing CHO cell line. MMapG cells were obtained by co-transfection of pMMap(neo) and pMMgr(dhfr) into CHO-DG44 cells.[30]

Since the production of SeAP can be induced, the cell line can be used to screen for inhibitors of OT by incubating the inhibitors with the cells prior to induction with dexamethasone. Then, secretion of SeAP can be measured with a substrate that fluoresces upon cleavage of the phosphate group. A decrease in fluorescence would indicate that the protein is not been secreted as a result of inhibition of glycosylation.

Results

Several peptides were synthesized with a KDEL ER retrieval sequence at the *C*-terminus. The *in vitro* activity of these inhibitors was compared to that of peptides without the KDEL

motif. The peptides were assayed against mammalian OT to determine if there is a significant difference in affinity for the enzyme from this source, since previous *in vitro* studies have been performed using yeast OT.

Other inhibitors were labeled with a BODIPY or fluorescein fluorophore to determine whether the peptides are capable of getting into cells, and to locate them in the interior of the cell. These inhibitors were tested for *in vivo* inhibition of OT using a SeAP assay.

PTD-linked inhibitors: Activity of KDEL containing peptides

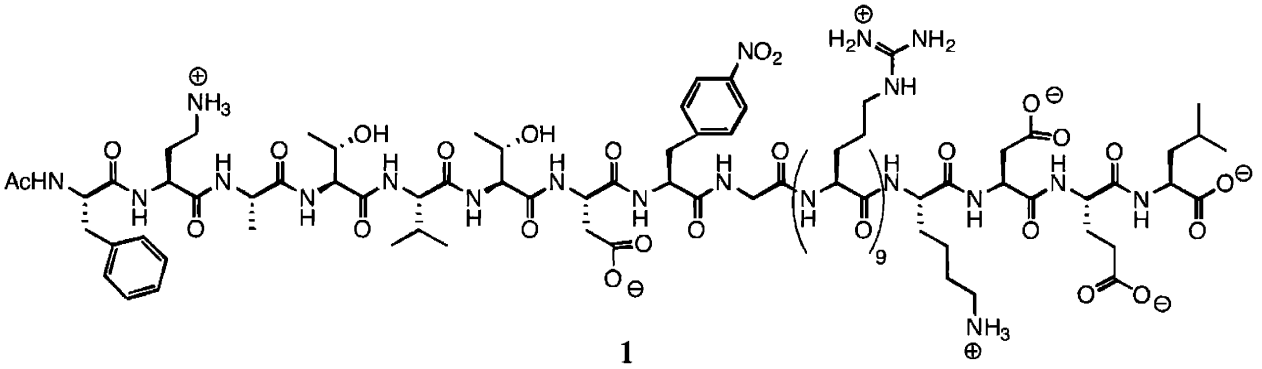

1

In the previous chapter the synthesis of PTD-linked inhibitors was presented. These inhibitors failed to show *in vivo* inhibition of OT when assayed with CHO3.6 cells. Inhibitors with a KDEL ER retrieval sequence were prepared in an effort to concentrate these inhibitors in the ER and increase the possibility of inhibiting OT *in vivo*. An inhibitor with a polyarginine tag at the *N*-terminus (peptide **16**, chapter 4) has an *in vitro* IC_{50} and K_i of 0.460 μM and 0.090 μM, respectively. Peptide **1**, with the same sequence as **16**, differing only by a free acid *C*-terminal KDEL sequence, has an IC_{50} and K_i of 0.240 μM and 0.050 μM, respectively.

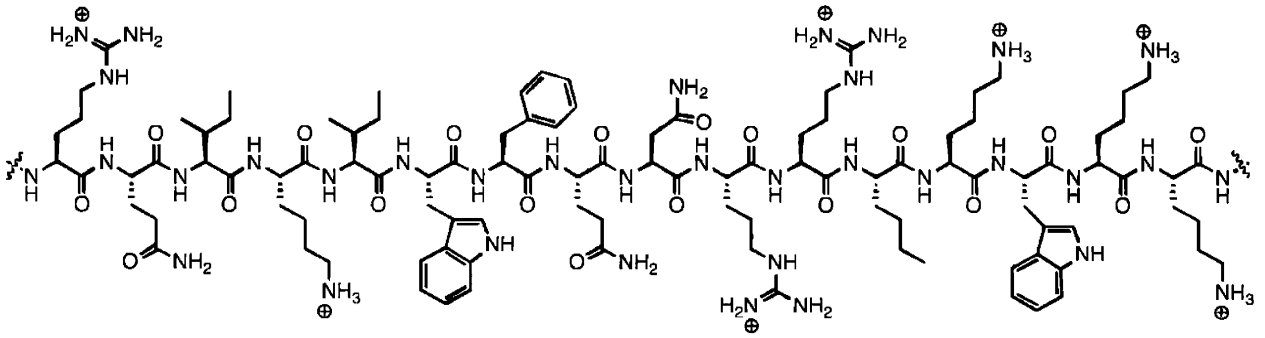

Penetratin

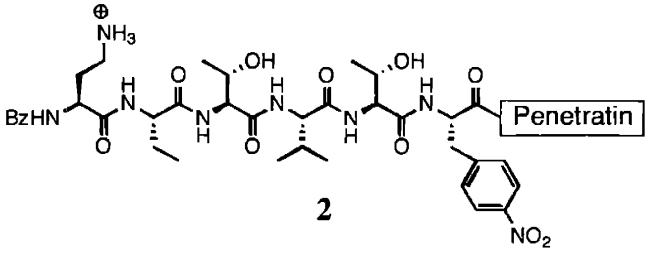

2

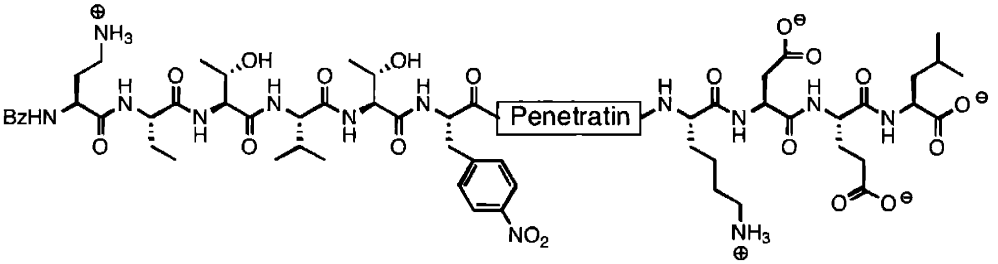

3

Figure 5.4. Structrures of Penetratin-linked inhibitors.

Peptide **2** (Figure 5.4), as mentioned in the previous chapter, has an IC_{50} and K_i of 0.325 μM and 0.050 μM, respectively. When a KDEL sequence was added to the *C*-terminus to obtain peptide **3,** an increased affinity for yeast OT was observed, with an IC_{50} and K_i of 0.110 μM and 0.024 μM, respectively. It is not clear why peptides **1** and **3** show higher affinity for OT when compared with the same peptides without the ER retrieval sequence. The KDEL sequence is far enough from the enzyme recognition sequence that it would not be expected to make such a difference. In addition, the enzyme preparation consists of solubilized microsomes, so that it is

reasonable to assume that the enzyme is equally accessible to peptides with or without the ER retrieval sequence.

Kinetic determinations using mammalian OT

Oligosaccharyl transferase purified from porcine liver was used to compare the affinity of some of the inhibitors for the fungal versus the mammalian enzymes. As seen in Table 5.1, all of the tested inhibitors are less potent against mammalian OT when compared with the enzyme purified from yeast. Inhibitors **3** and **4** are more than ten times worse for mammalian OT, while inhibitors **2** and **5** are only approximately six times and two times worse, respectively. Nevertheless, we can still obtain inhibitors that bind to mammalian OT in the low nanomolar range, as will be seen in the following sections.

Table 5.1. Comparison of kinetic data for yeast and mammalian OT

Peptide	Yeast OT		Mammalian OT	
	IC_{50} (μM)	K_i (μM)	IC_{50} (μM)	K_i (μM)
Inhibitor-Penetratin (**2**)	0.325	0.050	0.800	0.304
Inhibitor-Penetratin-KDEL (**3**)	0.110	0.024	1.13	0.365
Bz-Dab-Abu-Thr-Val-Thr-Nph (**4**)	0.052	0.010	0.290	0.122
Bz-Dab-Ser-Thr-Val-Thr-Nph (**5**)	0.358	0.072	0.440	0.137

Synthesis of fluorescently labeled inhibitors

Penetratin-linked inhibitors up to the Dab residue were synthesized on the solid phase using an automated solid phase peptide synthesizer. An Fmoc-protected 6-aminohexanoic acid (Fmoc-Ahx-OH) was manually coupled to the *N*-terminus of the inhibitor. After Fmoc deprotection, labeling with fluorescein was achieved by reacting the free amine with fluorescein isothiocyanate. It is important to note that a spacer is necessary for an efficient labeling reaction. The spacer can be either an Ahx moiety or several glycine residues. Cleavage from the resin

afforded peptides **6** and **7**. These peptides were used to determine the extent of internalization of the inhibitors in Rat-1 fibroblasts in culture.

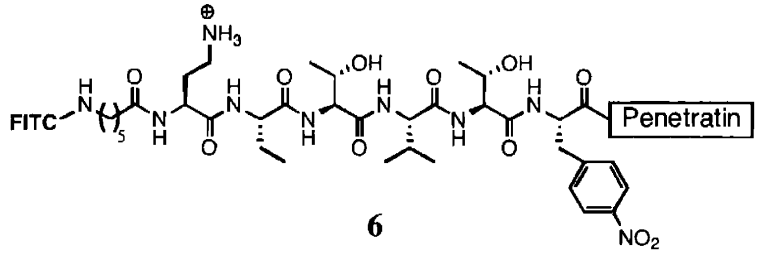

6

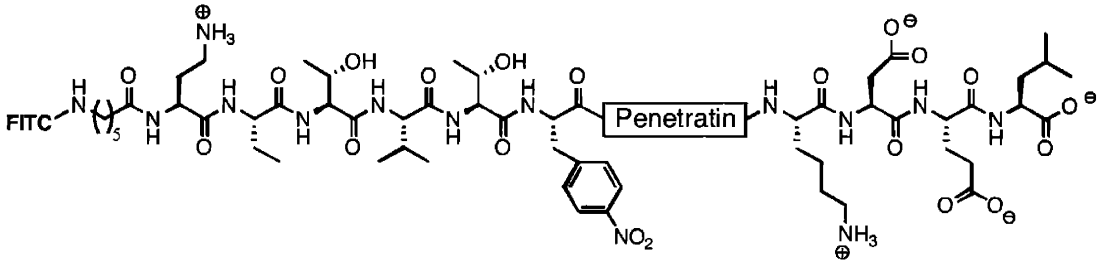

7

Alternatively, smaller peptides were labeled with a BODIPY fluorophore that emits at a longer wavelength. The chosen BODIPY derivative absorbs at 540 nm and emits at 570 nm, and is commercially available from Molecular Probes as the iodoacetamide derivative, which includes a sulfur reactive group. In contrast to the fluorophore labeling of peptides **6** and **7**, labeling with the BODIPY derivative is done in solution (see Figure 5.5) after the peptide has been cleaved from the resin and purified, since this fluorophore cannot survive the acidic peptide cleavage conditions.

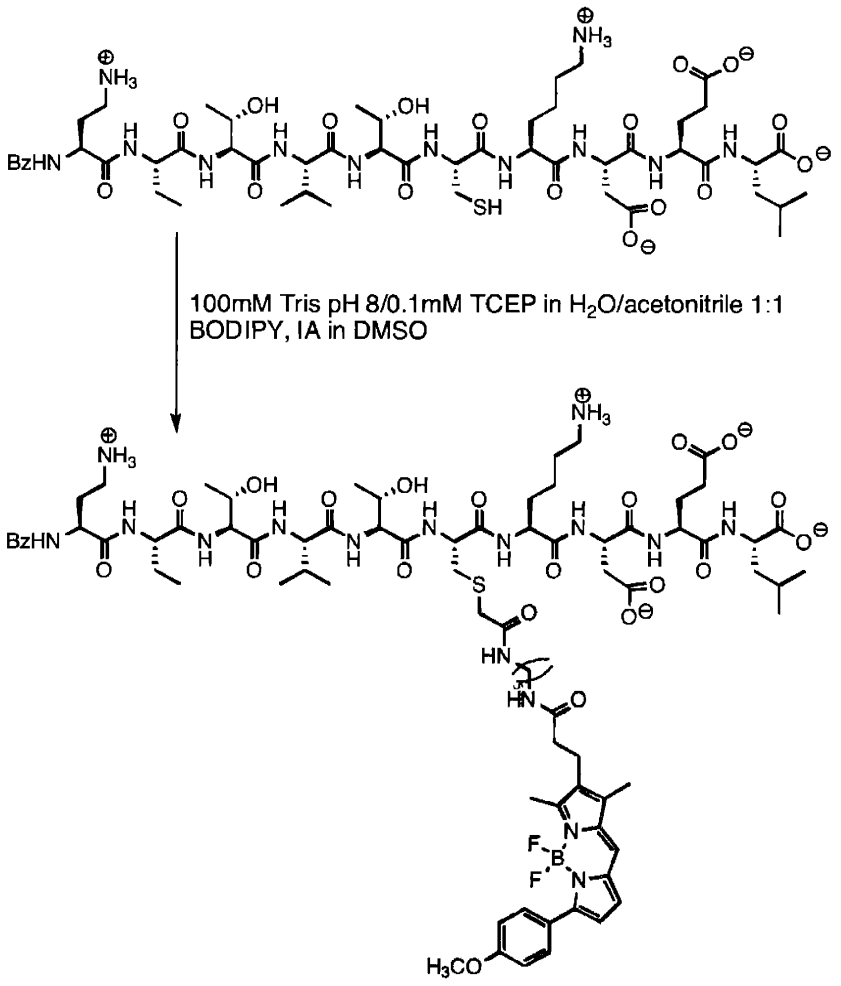

8

Figure 5.5. Schematic representation of the labeling of inhibitors with BODIPY iodoacetamide

As shown in Figure 5.5, the inhibitors were labeled in solution using a degassed Tris buffer at pH 8, in a 1:1 mixture of water/acetonitrile. Tris(2-carboxyethyl)phosphine (TCEP) was used as a reducing agent to avoid oxidation of the free cysteine. The BODIPY-IA was dissolved in a small amount of degassed DMSO, and the reaction was performed under N_2. The reaction was followed by reverse phase HPLC, using a C_{18} analytical column. This labeling reaction is very efficient, as can be observed from the HPLC traces. Peptide **8** was purified using preparative HPLC.

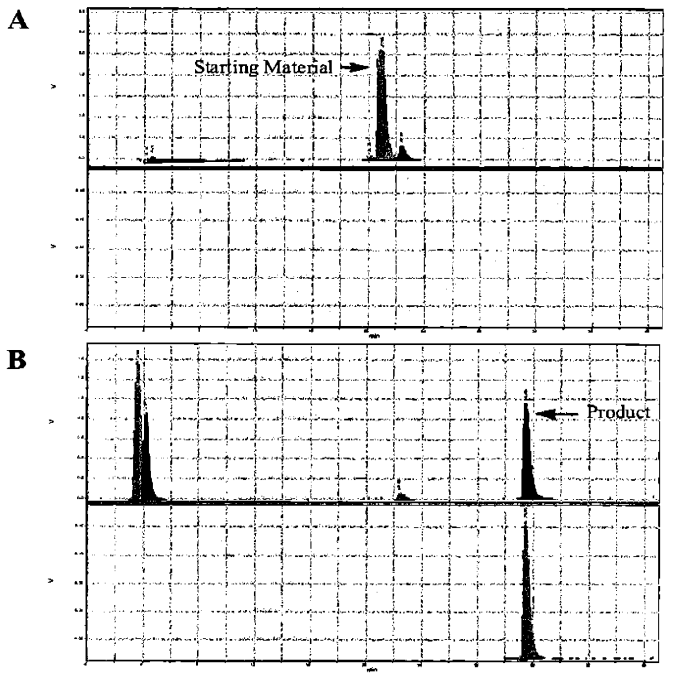

Figure 5.6. HPLC traces of a BODIPY-labeling reaction. A. Reaction at T_0, shows the starting material. B. Reaction after 2 h; only the product is present.

Peptides **9** and **10** in Figure 5.7 were labeled in solution, as described above. Peptide **9** has the same inhibitor sequence as peptide **8**, but lacks the KDEL sequence at the *C*-terminus. Peptide **10** was prepared with only the tripeptide recognition sequence and the ER retrieval sequence, in hopes that a smaller peptide would be more readily internalized by cells.

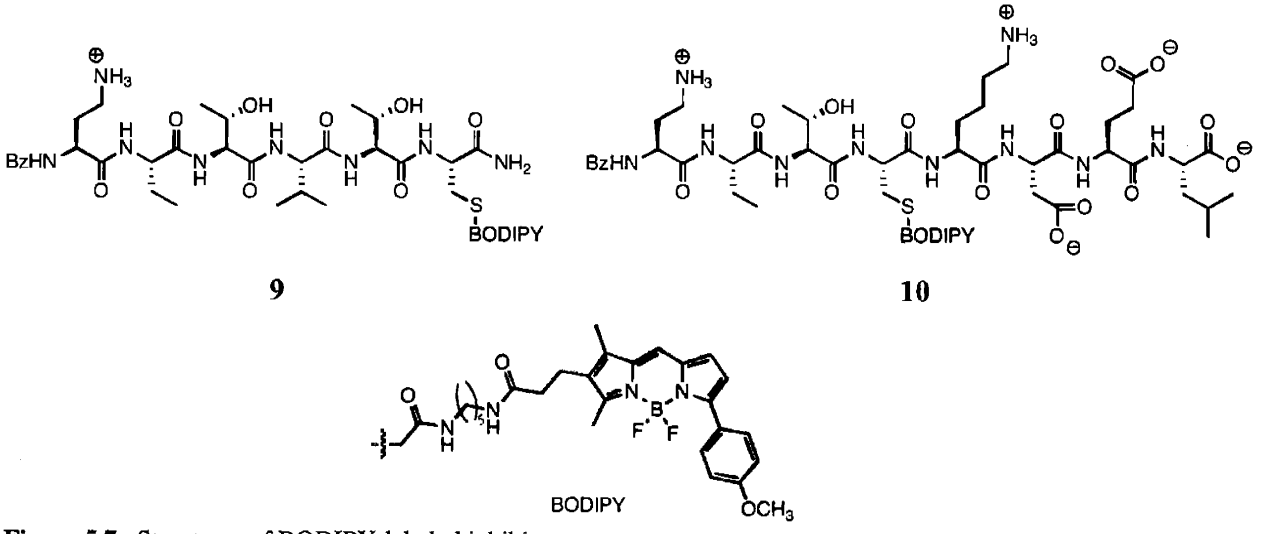

Figure 5.7. Structures of BODIPY-labeled inhibitors.

Peptides **8** and **9** were assayed *in vitro* against mammalian OT. Peptide **10** was not assayed *in vitro*, since it is known that inhibitors with charged amino acids one residue away from the recognition sequence are poorly accommodated by the enzyme. Peptide **8** has an IC_{50} and K_i of 0.150 μM and 0.053 μM, respectively. Peptide **9** has slightly higher IC_{50} and K_i values, 0.280 μM and 0.080 μM, respectively. These inhibitors contain the hydrophobic BODIPY fluorophore, and show a higher affinity for mammalian OT than does peptide **4**, which does not contain the fluorophore.

Localization of peptides inside cells

Rat-1 fibroblasts were seeded on chambered coverglasses at a cell density of 4.5 x 10^4 cells/well and grown overnight. Cells were incubated in FBS-free media for 2 hours, followed by incubation with the inhibitor for 1 hour. The cells were fixed, permeabilized, and stained with an ER marker. A Concanavalin A - FITC conjugate was used as the ER marker of cells incubated with BODIPY-labeled inhibitors. For cells incubated with FITC-labeled inhibitors, a Concanavalin A – tetramethylrhodamine conjugate was used as the ER marker.

Figure 5.8 Rat-1 fibroblasts incubated for 1h with the inhibitor BzDabAbuTVTC(BDP)KDEL (A), fixed and labeled with the ER marker FITC-Concanavalin A (B); merged images (C).

Figure 5.8.A shows the cells with the BODIPY-labeled inhibitor **8**; Figure 5.8.B shows the cells with the FITC-labeled ER marker, and Figure 5.8.C is a merged image of A and B.

From these pictures we can conclude that peptide **8** is colocalizing with the marker in the ER. Similar results were obtained for peptide **10**.

Rat-1 fibroblasts or CHO3.6 were seeded in chambered slides at 4.5 x 10^4 cells/well and grown overnight. The cells were labeled for 1 h with 10 μM of inhibitors **8**, **9** and **10**, as described above. In this case, after fixing, permeabilizing, and staining with the ER marker, the chamber was removed, and the slides were mounted to observe cells using a confocal microscope.

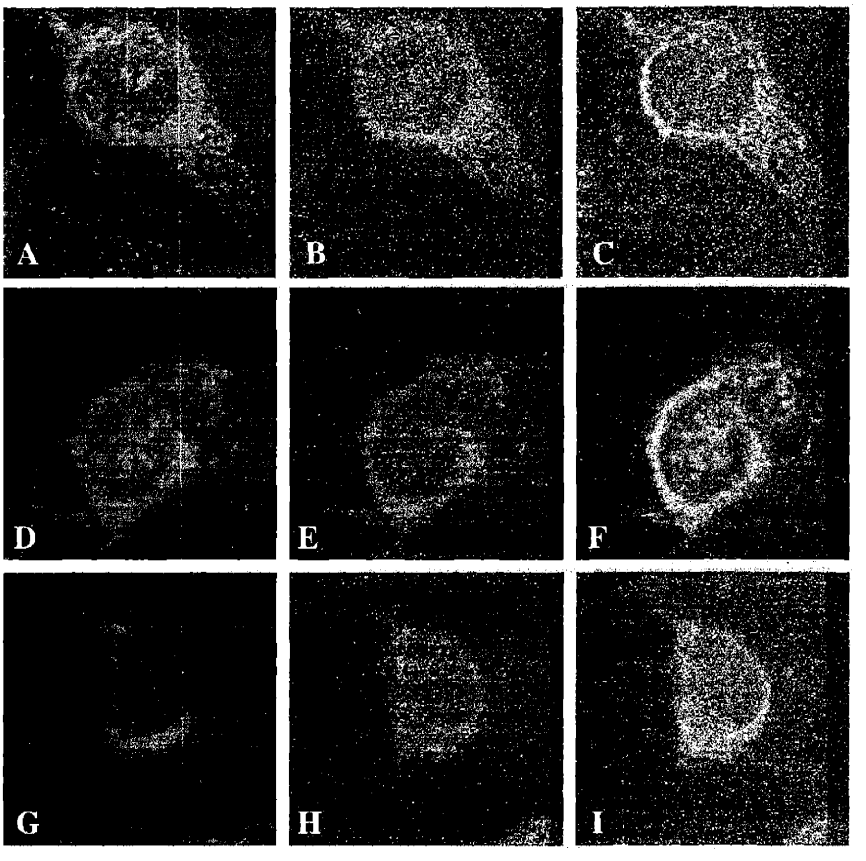

Figure 5.9. Confocal microscope images of Rat-1 fibroblasts (**A**-**F**) and CHO3.6 cells (**G**-**I**) incubated with BODIPY-labeled inhibitors **8**-**10**. The first column (images A, D and G) corresponds to the inhibitors **8**, **9** and **10**, respectively. The second column (images B, E and H) corresponds to the ER marker. The third column (images C, F and I) corresponds to pictures with both the inhibitor (**8**, **9** and **10**, respectively) and the ER marker.

Figure 5.9 shows that inhibitors **8**-**10** are internalized by cells in culture. Peptide **8** seems to colocalize with the ER marker. Peptide **9** is also found in the ER, although it seems to be

distributed in other parts of the cell as well. The concentration of this inhibitor inside the cell seems to be higher than the intracellular concentration of peptides **8** and **10**. This might be due to the fact that this inhibitor does not have the KDEL sequence, which has three charged amino acids and a free acid at the *C*-terminus. The inhibitors must cross the cellular membrane and the extra charges in peptides **8** and **10** may result in reduced internalization, even though the ER retrieval sequence should concentrate the peptides in the ER. Peptide **10** is also localized in the ER.

Figure 5.10 shows images of Rat-1 fibroblasts incubated for 1 h with FITC-labeled inhibitors **6** and **7**. Both inhibitors are capable of crossing the cellular membrane. Although both are found concentrated around the nucleus, it seems that the Inhibitor-Penetratin-KDEL peptide **7** (Figure 5.10.A) is localized in the ER (Figure 5.10.C), while the Inhibitor-Penetratin peptide **6** is found in vesicles located in the same area as the ER marker (Figure 5.10.F). Incubation with the inhibitor for longer periods (4 – 24 h) results in the appearance of more of these vesicle structures.

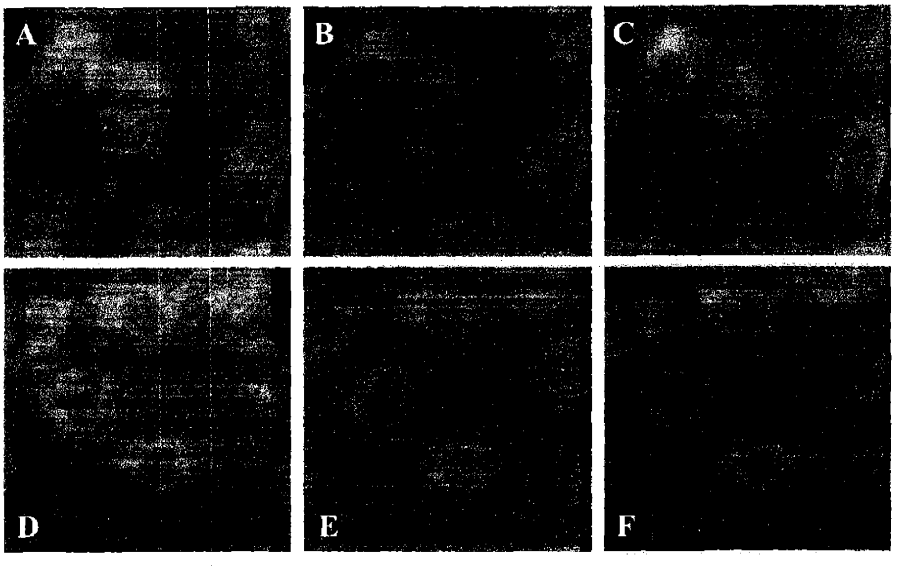

Figure 5.10. Fluorescence microscope images of Rat-1 fibroblasts incubated with FITC-labeled inhibitors **7** and **6**. The first column (images A, and D) corresponds to the inhibitors **7** and **6**, respectively. The second column (images

B and E) corresponds to the ER marker. The third column (images C and F) corresponds to merged images of the inhibitor (**7** and **6**, respectively) and the ER marker.

In vivo SeAP assays

The inhibitors with different internalization sequences presented in Chapter 4 were assayed with this system. However, a positive result was obtained only with inhibitors containing the Penetratin PTD. Therefore, peptides **12** and **13** were synthesized as control peptides to compare the effects of the inhibitors on SeAP activity in MmapG CHO cells with the effects of these non-inhibitors of OT. Peptides **12** and **13** consist of the Penetratin sequence, and peptide **13** has the *C*-terminus ER retrieval sequence. A positive response was also obtained with peptide **9** and peptide **11** was synthesized as a control. In peptide **11**, the central amino acid of the consensus sequence was substituted with a proline residue, since it is known that this residue is not accepted in glycosylation sites. The rest of the sequence is identical to peptide **9**.

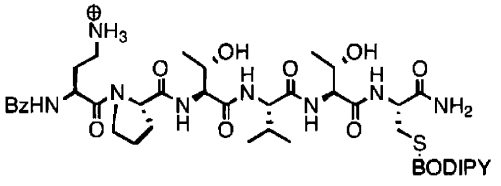

11

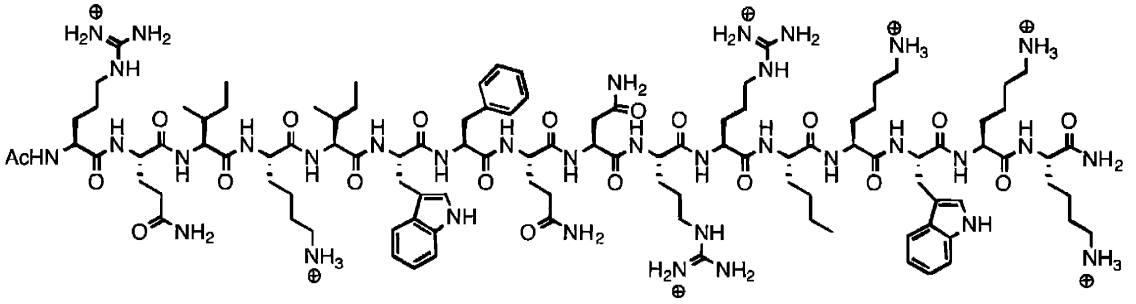

12

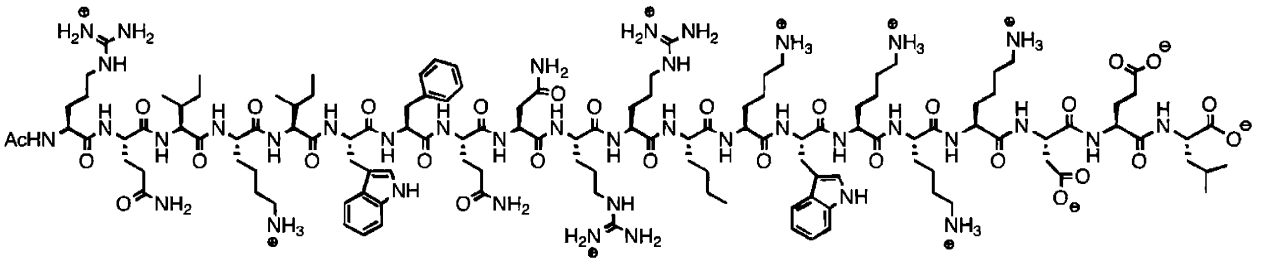

13

MMapG CHO cells were seeded into 96-well plates and allowed to grow to confluency. After aspirating the media from the wells, inhibitors diluted in fresh media were added at different concentrations. The cells were grown overnight in the presence of inhibitors. Then, the cells were induced to produce SeAP for 24 h by adding dexamethasone to a final concentration of 1 μM. After this incubation period, a 5 μL aliquot of media was extracted from each well and added to a solution of the 4-methylumbelliferyl phosphate (MUP) substrate in a black 96-well plate. The enzyme was incubated with the substrate at 27°C, and the fluorescence was measured using a plate reader (360 nm excitation filter, 430 nm emission filter). Tunicamycin was used as a control to see a decrease of the fluorescence signal due to inhibition of glycosylation.

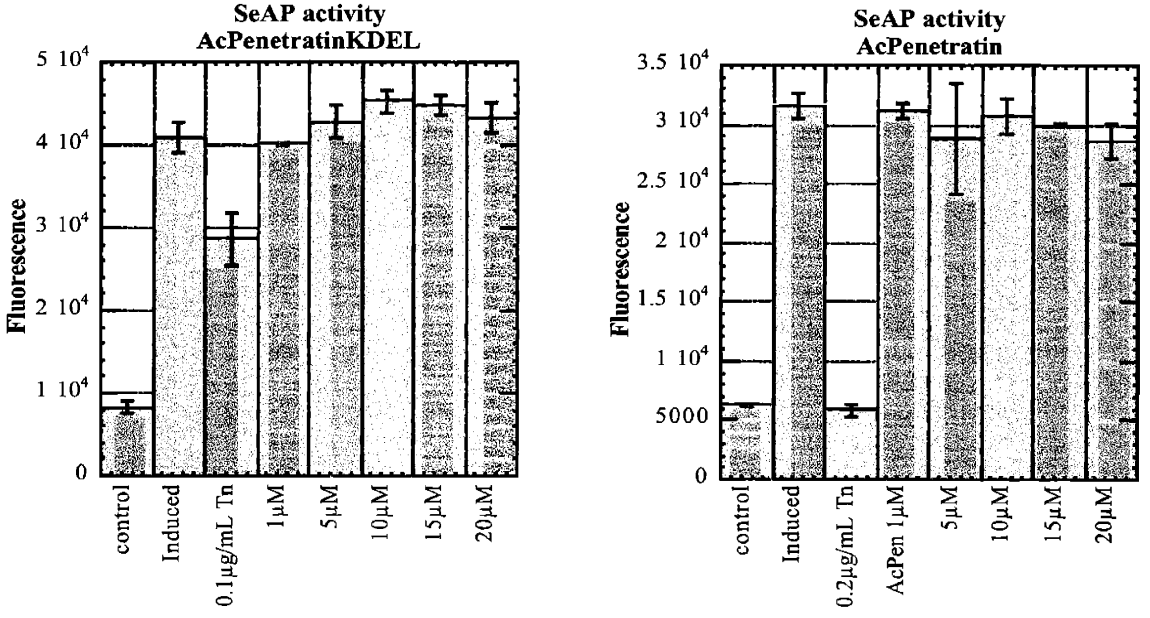

Figure 5.11. Control experiments with AcPenetratin and AcPenetratinKDEL

Figure 5.11 show control experiments performed with AcPenetratin (peptide **12**) and AcPenetratinKDEL (peptide **13**). Compared to the signal produced by the control induced cells, there was no significant change in fluorescence following incubation with peptides at concentrations up to 20 μM. Tunicamycin (Tn) inhibits glycosylation, and causes a decrease in the fluorescence signal. Figure 5.12 shows the results of experiments with peptides **2** and **3,** which are the same with the exception that peptide **3** contains a KDEL sequence at the *C*-terminus. In these cases, a decrease in the fluorescence signal in a concentration-dependent manner is observed with both inhibitors. In fact, the decrease in fluorescence is more accentuated with inhibitor **2** than with inhibitor **3**. An *in vivo* IC_{50} was calculated for both peptides: peptide **2** has an IC_{50} of 1 μM and peptide **3** has an IC_{50} of 5.8 μM. It should be noted that *in vitro*, inhibitor **2** binds to mammalian OT with a slightly higher affinity than peptide **3**. Also, recent evidence suggests that Penetratin peptides with a free acid at the *C*-terminus are internalized less efficiently than the same peptides with an amide capping at the *C*-terminus.[36]

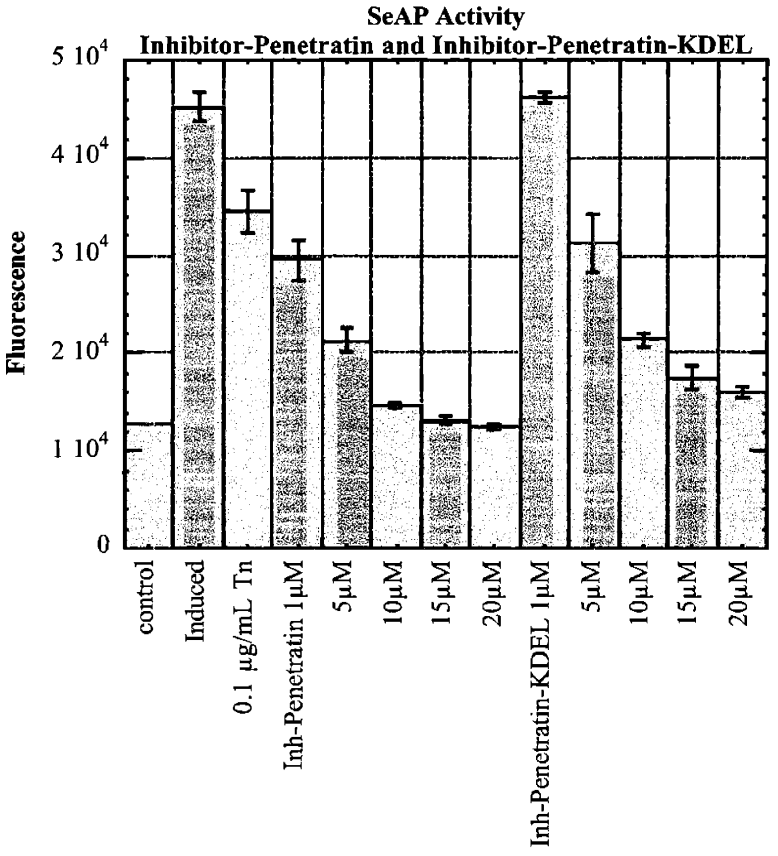

Figure 5.12. SeAP assay with inhibitors **2** and **3**.

Figure 5.13 shows the effect of peptide **9** on SeAP secretion from cells. A decrease in SeAP activity is observed with increasing concentrations of the inhibitor. The control peptide **11** does not have this effect on the cells, even at concentrations as high as those used with inhibitor **9**. These data suggest that the decrease in fluorescence is caused by inhibition of glycosylation. An *in vivo* IC_{50} of 11.4 μM was calculated.

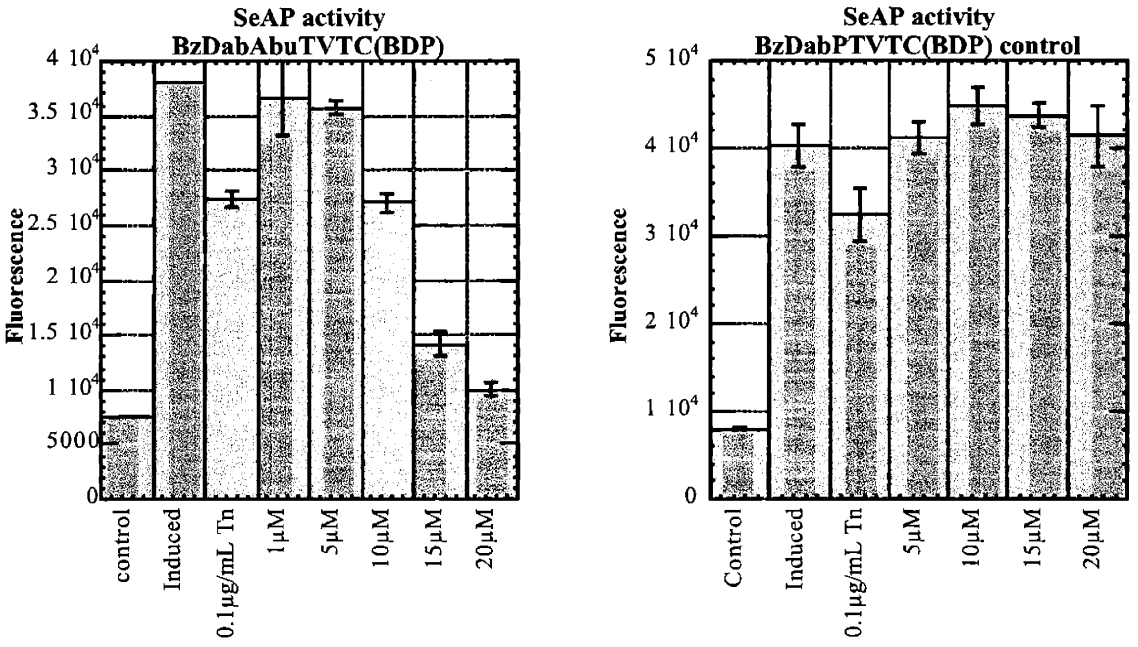

Figure 5.13. Control SeAP assay using MMapG CHO cells with peptide **11** and experiment with peptide **9**.

This experiment was also done with peptides **8** and **10**. Peptide **10** did not show any decrease in SeAP activity with concentrations up to 40 μM. Although initially peptide **8** caused a concentration dependent decrease in SeAP activity, these results were not reproducible. An HPLC trace confirmed that the peptide was not degraded, so these initial results were discarded.

Discussion and future directions

Penetratin-linked inhibitors have been labeled with a FITC fluorophore at the *N*-terminus. These peptides, one of which contains an ER retrieval sequence at the *C*-terminus, were able to cross the cellular membrane and seem to concentrate around the nucleus in the same area where the endoplasmic reticulum is located. After prolonged periods of incubation (4-24 h), the fluorescence is found around the nucleus, but in what seem to be vesicular structures. It is not clear if the peptides are being degraded by the cells. The non-fluorescently labeled peptide analogs were assayed *in vivo*, with a MMapG CHO cell line that overexpresses the glycoprotein

secreted alkaline phosphatase. The unglycosylated version of this protein is not secreted by the cells, and this allows an indirect measurement of *in vivo* inhibition of glycosylation. A concentration dependent decrease in SeAP activity was found with both Penetratin-linked inhibitors, suggesting that *N*-linked glycosylation was being inhibited.

BODIPY-labeled inhibitors **8**-**10** are internalized by cells in culture. In fact, the fluorescence of the inhibitors colocalizes with an ER marker. Although peptide **9** seems to be distributed across the cell, its intracellular concentration is higher than that of peptides **8** and **10**. A concentration-dependent decrease in SeAP activity was found when MMapG CHO cells were grown in the presence of inhibitor **9**. This suggests that peptide **9** is inhibiting *N*-linked glycosylation *in vivo*.

As mentioned earlier, this SeAP assay provides an indirect measurement of *in vivo* inhibition of glycosylation. A direct observation of this effect is needed to corroborate these data. SeAP has been previously used as a reporter protein to determine the glycosylation state of proteins by extracting the protein and observing the difference in mobility between the glycosylated and unglycosylated protein on SDS-PAGE.[32] This experiment can be used to observe the unglycosylated SeAP produced by MMapG CHO cells treated with the inhibitors, confirming that the response we see with the SeAP assay is, in fact, due to *in vivo* inhibition of glycosylation.

Conclusions

Inhibitors that provide information about the extended binding determinants of OT, the requirement for certain amide bonds, and the requirement for a positive charge on the Asn position have been obtained. Also, inhibitors that provide information about the conformational

requirements for peptide recognition have been obtained. The first product inhibitors of OT have been synthesized by substituting the natural glycosyl amide linkage with more flexible linkages obtained through the use of asparagine surrogates.

In summary, the synthesis and kinetic activity of the best known OT inhibitor have been presented. The structure of this inhibitor has been modified to improve bioavailability. Inhibitors were made more hydrophobic by the elimination of amide bonds, or by the addition of hydrophobic moieties at the side chain of the Dab or at the *C*-terminus. These modifications failed to enhance cellular uptake.

The addition of a penetratin protein sequence did result in inhibitor uptake, as demonstrated by fluorescence localization. An indirect assay indicates that the inhibitor functions *in vivo*. The same results were obtained when the inhibitor without the penetratin sequence was labeled with a BODIPY fluorophore.

Acknowledgements

This work was supported by a grant from NIH (GM-39334) and by an NIH Cancer Training Grant fellowship to M. L. Ufret. Confocal microscope pictures were acquired at the W. M. Keck Foundation Biological Imaging Facility at the Whitehead Institute.

Experimental Section

Synthesis of PTD-linked inhibitors

PTD-linked inhibitors were synthesized on PAL-PEG-PS resin, on an automatic solid phase peptide synthesizer using 4 equivalents of amino acids and HOBt/HBTU. After completion of the synthesis, the peptides were cleaved from the resin using TFA/TIS/H_20/EDT

(82:8:2:8) for 1.5h. The TFA was evaporated under a stream of N_2, and then the peptide was precipitated with ice-cold ethyl ether. The white precipitate was resuspended in ether and washed 3 additional times. The peptides were dissolved in water and a sample was injected on a reverse-phase (C_{18}) analytical HPLC column using H_20/0.1% TFA (solvent A) and acetonitrile/0.1% TFA (solvent B). Samples were collected for ES-MS, and each product was purified on a C_{18} preparative column, using a gradient of solvent A and B. The purified, lyophilized peptides were then dissolved in DMSO and quantified using the UV absorbance at 280 nm, as described by Kellenberger *et al.*[37] Peptides were assayed against yeast OT as described in the previous chapters. The error in the binding constant was 5-20% of the measured value.

Ac-Phe-Dab-Ala-Thr-Val-Thr-Asp-Nph-Gly-Arg$_9$-Lys-Asp-Glu-Leu-OH (1)

HPLC: t_R = 17.14 min (C_{18}, 7%–100% B over 28 min); ES-MS: Calculated for $C_{122}H_{209}N_{51}O_{34}$ 2934, observed 979.2 $(M+3H)^{3+}$, 587.9 $(M+4H)^{4+}$, 734.66 $(M+5H)^{5+}$

Bz-Dab-Abu-Thr-Val-Thr-Nph-R-Q-I-K-I-W-F-Q-N-R-R-Nle-K-W-K-K-NH$_2$ (2)

HPLC: t_R = 24.95 min (C_{18}, 7%–70% B over 25 min); ES-MS: Calculated for $C_{142}H_{221}N_{43}O_{30}$ 3010, observed 1004.1 $(M+3H)^{3+}$, 753.3 $(M+4H)^{4+}$, 602.8 $(M+5H)^{5+}$, 502.5 $(M+6H)^{6+}$

Bz-Dab-Abu-Thr-Val-Thr-NphR-Q-I-K-I-W-F-Q-N-R-R-Nle-K-W-K-K-D-E-L-OH (3)

HPLC: t_R = 25.65 min (C_{18}, 7%–70% B over 25 min); ES-MS: Calculated for $C_{157}H_{243}N_{45}O_{38}$ 3368, observed 1123.4 $(M+3H)^{3+}$, 843.1 $(M+4H)^{4+}$, 674.5 $(M+5H)^{5+}$, 562.2 $(M+6H)^{6+}$

*Ac-R-Q-I-K-I-W-F-Q-N-R-R-Nle-K-W-K-K-NH_2 (**12**)*

HPLC: t_R = 25.54 min (C_{18}, 7%–70% B over 25 min); ES-MS: Calculated for $C_{107}H_{173}N_{35}O_{20}$ 2269, observed 757.4 $(M+3H)^{3+}$, 568.3 $(M+4H)^{4+}$, 454.8 $(M+5H)^{5+}$

*Ac-R-Q-I-K-I-W-F-Q-N-R-R-Nle-K-W-K-K-D-E-L-OH (**13**)*

HPLC: t_R = 24.95 min (C_{18}, 7%–70% B over 25 min); ES-MS: Calculated for $C_{128}H_{207}N_{39}O_{29}$ 2756, observed 919.71 $(M+3H)^{3+}$, 690.1 $(M+4H)^{4+}$, 552.25 $(M+5H)^{5+}$

Synthesis of FITC-labeled inhibitors

Penetratin-linked inhibitors were assembled on PAL-PEG-PS resin, on an automated solid phase peptide synthesizer up to the Dab residue, using HOBt/HBTU chemistry. An Fmoc-protected 6-aminohexanoic acid (Fmoc-Ahx-OH) was coupled manually at the *N*-terminus of the inhibitor, using 3 equivalents of the Fmoc-Ahx-OH and PyBOP/HOBt, and 6 equivalents of DIPEA. After removal of the Fmoc group, 2 equivalents of fluorescein isothiocyanate and 4 equivalents of DIPEA were added in DMF. The reactions were stirred in the dark for 12h. The resin was rinsed with DMF, DCM, and ether, and then dried under high vacuum. The peptides were cleaved from the resin, precipitated, and purified, as described previously.

*FITC-Ahx-Dab-Abu-Thr-Val-Thr-Nph-R-Q-I-K-I-W-F-Q-N-R-R-Nle-K-W-K-K-NH_2 (**6**)*

HPLC: t_R = 25.2 min (C_{18}, 5%–70% B over 25 min); ES-MS: Calculated for $C_{162}H_{239}N_{45}O_{35}S$ 3408, observed 1137.0 $(M+3H)^{3+}$, 853.2 $(M+4H)^{4+}$, 682.8 $(M+5H)^{5+}$

*FITC-Ahx-Dab-Abu-Thr-Val-Thr-Nph-R-Q-I-K-I-W-F-Q-N-R-R-Nle-K-W-K-K-D-E-L-OH (**7**)*

HPLC: t_R = 25.40 min (C_{18}, 5%–70% B over 25 min); ES-MS: Calculated for $C_{177}H_{261}N_{47}O_{43}S$ 3010, observed 1256.8 $(M+3H)^{3+}$, 942.7 $(M+4H)^{4+}$, 754.2 $(M+5H)^{5+}$

Synthesis of BODIPY-labeled inhibitors

Peptides were synthesized on PAL-PEG-PS resin using a glass reaction vessel fitted with a sintered glass frit. Discharge of solvent and excess reagents was accomplished by the use of vacuum. The resin was swelled in DMF for 10 min. Fmoc deprotection was effected with 20% piperidine in DMF (3 x 3 min). Coupling of the amino acids was performed in DMF using 4 equivalents of amino acids, 4 equivalents of HOBt/HBTU, and 8 equivalents of DIPEA. The success of each coupling reaction was determined using a TNBS test, as described in page 89. A capping step (Ac_2O/DIPEA 2:3 in DMF/DCM 4:1) was performed after each successful coupling to ensure that any remaining undetected, unreacted peptide is capped to avoid deletion peptides. The *N*-terminus was capped using 10 equivalents of benzoic anhydride and 10 equivalents of DIPEA in DMF. The resin was rinsed with DMF, DCM and ethyl ether and dried under vacuum. Peptides were cleaved from the resin using TFA/TIS/H_2O/EDT (93:2:2:3), concentrated, precipitated with ice-cold ether, rinsed twice with ether, analyzed and purified by HPLC, and characterized by ES-MS.

To label the peptides with the BODIPY iodoacetamide, reactions were carried out in a 2 ml reaction vial with a stir bar, under N_2. The peptide was dissolved in degassed buffer (100mM Tris pH 8, 0.1mM TCEP, in 1:1 H_20/acetonitrile). The BODIPY iodoacetamide (2 equivalents) was dissolved in a minimum amount of degassed DMSO and added dropwise to the peptide solution. The progress of the reaction was followed by reverse phase HPLC. The reaction was completed after 2 h, and the product was purified by HPLC on a C_{18} preparative column.

Bz-Dab-Abu-Thr-Val-Thr-Cys(BODIPY)-Lys-Asp-Glu-Leu-OH (8)

HPLC: t_R = 18.05 min (C_{18}, 25%–68% B over 25 min); ES-MS: Calculated for $C_{80}H_{117}BF_2N_{16}O_{21}S$ 1719.75, observed 860.3 $(M+2H)^{2+}$

Bz-Dab-Abu-Thr-Val-Thr-Cys(BODIPY)-OH (9)

HPLC: t_R = 33.12 min (C_{18}, 20%–70% B over 30 min); ES-MS: Calculated for $C_{59}H_{83}BF_2N_{12}O_{12}S$ 1232.6, observed 1233.5 $(M+H)^+$

Bz-Dab-Abu-Thr-Cys(BODIPY)-Lys-Asp-Glu-Leu-OH (10)

HPLC: t_R = 31.45 min (C_{18}, 15%–85% B over 40 min); ES-MS: Calculated for $C_{71}H_{101}BF_2N_{14}O_{18}S$ 1519.5, observed 760.7 $(M+2H)^{2+}$

Bz-Dab-Pro-Thr-Val-Thr-Cys(BODIPY)-NH_2 (11)

HPLC: t_R = 27.5 min (C_{18}, 7%–100% B over 30 min); ES-MS: Calculated for $C_{60}H_{83}BF_2N_{12}O_{12}S$ 1245.25, observed 1246.5 $(M+H)^+$

Determination of IC_{50} and K_i values using mammalian OT

The radiolabeled carbohydrate substrate Dol-P-P-GlcNAc-[^{3}H]-GlcNAc was dissolved in DMSO for the control measurements or DMSO containing the inhibitor for the inhibition studies. Assay buffer (50 mM Hepes pH 7.5, 140 mM sucrose, 1.2% Triton X-100, 0.5 mg/ml PC, 10 mM $MnCl_2$) and crude OT-containing microsomes from porcine liver were mixed to obtain a homogeneous solution. An aliquot of this solution was added to the carbohydrate substrate.

After incubation for 30 minutes, the assay was initiated by addition of the Bz-NLT-NHMe peptide substrate (500 μM). Reaction aliquots (4 x 40 μL) were removed at two minute intervals and quenched into 3:2:1 chloroform:methanol:4 mM $MgCl_2$. The tritiated glycopeptide in the upper aqueous layer was separated from the unreacted glycolipid through a series of extractions. The combined aqueous layers were quantified for tritium content. The disintegrations per minute (dpm) were plotted as a function of time for the control and 3-5 different inhibitor concentrations. The percentage inhibition was determined from this plot in order to estimate the IC_{50}. Three concentrations were then selected to give between 30% and 70% inhibition. All experiments were performed in duplicate. In each case, the approximate K_i was determined using the following equation:[38]

$$K_i = \frac{[I] \times (1-i)}{i + \left(\frac{[S]}{K_M} \times i \right)}$$

Cellular localization of fluorescently labeled inhibitors

Rat-1 fibroblasts were cultured at 37°C and 5% CO_2, in high glucose DMEM with 10% FBS and Penn/Strep. Cells were seeded at 4.5 x 10^4 cells/well in Lab-Tek 4-well chamber slides or 4-well chambered coverglasses and grown overnight. The cells were incubated for 2 h in FBS-free media, and then for 1 h with the inhibitor dissolved in FBS-free media. After rinsing with PBS containing Ca^{2+} and Mg^{2+} (3 x 500 μL x 5 min), the cells were fixed and permeabilized with 4% paraformaldehyde and 0.1% Triton X-100 in PBS for 15 min. The cells were rinsed with PBS (3 x 500 μL) and the excess fixative was scavenged with 100 mM glycine (2 x 10 min x 500 μL), and then blocked with 5% FBS in PBS (20 min) to avoid non-specific binding. The

ER was labeled by incubating with a FITC or tetramethylrhodamine conjugate of Concavalin A (15 min). The cells were rinsed with PBS (3 x 500 μL x 15 min) and images of cells in coverglasses were taken in an inverted fluorescence microscope (Olympus IX50). The chamber of the chamber slides was removed and slides were mounted using PPD (1 mg/ml *p*-phenylene diamine in 75% glycerol in PBS).

SeAP assay

MMapG CHO cells were cultured under humidified conditions at 37°C and 5% CO_2, in α-MEM media, with no ribonucleosides or deoxyribonucleosides, but with L-glutamine, 0.4 mg/ml Geneticin, 10% FBS, and Penn/Strep. Cells were seeded on a 96-well plate and grown to confluency. Inhibitors, dissolved in DMSO, were diluted in media, keeping the DMSO concentration at 1%. The media in the wells was substituted with this inhibitor-containing media, and the cells were grown overnight in the presence of inhibitors. Then, the media in the wells was substituted with fresh media containing only 1% FBS, the inhibitors, and 1 μM dexamethasone, which induces the production of SeAP. The cells were induced for 24 h, and 5 μL of the supernatant media were transferred to a black 96-well plate that contained 195 μL of 1 mM MUP (MUP solution in 2 M diethanolamine in water). The enzyme was incubated with the substrate for 1.5 h at 27°C. SeAP activity was determined by measuring the fluorescence on an Perkin-Elmer HTS 7000 plate reader (360 nm excitation filter, 430 nm emission filter).

References

1. Elbein, A.D., "The Tunicamycins: Useful Tools for Studies on Glycoproteins". *Trends Biochem. Sci.*, 1981. *6*, 291-293.

2. Heifetz, A., Keenan, R.W., and Elbein, A.D., "Mechanism of Action of Tunicamycin on the UDP-GlcNAc:Dolichyl-Phosphate GlcNAc-1-Phosphate Transferase". *Biochemistry*, 1979. *18*(11), 2186-2192.

3. Keller, R.K., Boon, D.Y., and Crum, F.C., "*N*-Acetylglucosamine-1-Phosphate Transferase from Hen Oviduct: Solubilization, Characterization, and Inhibition by Tunicamycin". *Biochemistry*, 1979. *18*, 3946-3952.

4. Heifetz, A. and Elbein, A.D., "Solubilization and Properties of Mannose and *N*-Acetylglucosamine Transferases Involved in Formation of Polyprenyl-Sugar Intermediates". *J. Biol. Chem.*, 1977. *252*, 3057-3063.

5. Struck, D.L. and Lennarz, W.J., "Evidence for the Participation of Saccharide-Lipids in the Synthesis of the Oligosaccharide Chain of Ovalbumin". *J. Biol. Chem.*, 1977. *252*, 1007-1013.

6. Lehle, L. and Tanner, W., "The Specific Site of Tunicamycin Inhibition in the Formation of Dolichol-Bound *N*-Acetylglucosamine Derivatives". *FEBS Lett.*, 1976. *71*, 167-170.

7. Tkacz, J.S. and Lampen, J.O., "Tunicamycin Inhibition of Polyisoprenyl *N*-Acetylglucosaminyl Pyrophosphate Formation in Calf-Liver Microsomes". *Biochem. Biophys. Res. Commun.*, 1975. *65*(1), 248-257.

8. Kuo, S.C. and Lampen, J.O., "Tunicamycin: Inhibitor of Yeast Glycoprotein Synthesis". *Biochem. Biophys. Res. Commun.*, 1974. *58*, 287-295.

9. Waechter, C.J. and Hartford, J.B., "Evidence for Enzymatic Transfer of *N*-Acetylglucosamine from UDP-*N*-Acetylglucosamine into Dolichol Derivatives and Glycoproteins by Calf Brain Membranes". *Arch. Biochem. Biophys.*, 1977. *181*(1), 185-198.

10. Heifetz, A. and Elbein, A.D., "Biosynthesis of Man-Beta-GlcNAc-GlcNAc-Pyrophosphoryl-Polyprenol by a Solubilized Enzyme from Aorta". *Biochem. Biophys. Res. Commun.*, 1977. *75*(1), 20-28.

11. Hammond, C. and Helenius, A., "Quality Control in the Secretory Pathway". *Curr. Opin. Cell Biol.*, 1995. *7*, 523-529.

12. Ellgaard, L., Molinari, M., and Helenius, A., "Setting the Standards: Quality Control in the Secretory Pathway". *Science*, 1999. *286*, 1882-1888.

13. Bonifacino, J.S. and Klausner, R.D., *Degradation of Proteins Retained in the Endoplasmic Reticulum*, in *Cellular Proteolytic Systems*, A. Ciechanover and A.L. Schwartz, Editors. 1994, Wiley-Liss: New York. p. 137-160.

14. Bonifacino, J.S. and Weissman, A.M., "Ubiquitin and the Control of Protein Fate in the Secretory and Endocytic Pathways". *Annu. Rev. Cell Dev. Biol.*, 1998. *14*, 19-57.

15. Brodsky, J.L. and McCracken, A.A., "ER Protein Quality Control and Proteasome-Mediated Protein Degradation". *Semin. Cell Dev. Biol.*, 1999. *10*, 507-513.

16. Rothman, J.E. and Wieland, F.T., "Protein Sorting by Transport Vesicles". *Science*, 1996. *272*, 227-234.

17. Schekman, R. and Orci, L., "Coat Proteins and Vesicle Budding". *Science*, 1996. *271*, 1526-1533.

18. Bonfanti, L., Mironov, A.A., Martinez-Menarguez, J.A., Martella, O., Fusella, A., Baldassarre, M., Buccione, R., Geuze, H.J., and Luini, A., "Procollagen Traverses the Golgi Stack without Leaving the Lumen of Cisternae: Evidence for Cisternal Maturation". *Cell*, 1998. *95*, 993-1003.

19. Allan, B.B. and Balch, W.E., "Protein Sorting by Directed Maturation of Golgi Compartments". *Science*, 1999. *285*, 63-66.

20. Letourneur, F., Gaynor, E.C., Hennecke, S., Demolliere, C., Duden, R., Emr, S.D., Riezman, H., and Cosson, P., "Coatomer Is Essential for Retrieval of Dilysine-Tagged Proteins to the Endoplasmic Reticulum". *Cell*, 1994. *79*, 1199-1207.

21. Pelham, H.R.B., "Control of Protein Exit from the Endoplasmic Reticulum". *Annu. Rev. Cell Biol.*, 1989. *5*, 1-23.

22. Munro, S. and Pelham, H.R., "A *C*-Terminal Signal Prevents Secretion of Lumenal ER Proteins". *Cell*, 1987. *48*, 899-907.

23. Nilsson, T. and Warren, G., "Retention and Retrieval in the Endoplasmic-Reticulum and the Golgi-Apparatus". *Curr. Opin. Cell Biol.*, 1994. *6*, 517-521.

24. Nilsson, T., Jackson, M., and Peterson, P.A., "Short Cytoplasmic Sequences Serve as Retention Signals for Transmembrane Proteins in the Endoplasmic Reticulum". *Cell*, 1989. *58*, 707-718.

25. Lewis, M.J. and Pelham, H.R., "Ligand-Induced Redistribution of a Human KDEL Receptor from the Golgi Complex to the Endoplasmic Reticulum". *Cell*, 1992. *68*, 353-364.

26. Griffiths, G., Ericsson, M., Krijnselocker, J., Nilsson, T., Goud, B., Soling, H.D., Tang, B.L., Wong, S.H., and Hong, W.J., "Localization of the Lys, Asp, Glu, Leu Tetrapeptide Receptor to the Golgi-Complex and the Intermediate Compartment in Mammalian-Cells". *J. Cell Biol.*, 1994. *127*, 1557-1574.

27. Lowe, M.E., "Site-Specific Mutations in the COOH-Terminus of Placental Alkaline Phosphatase: A Single Amino Acid Change Converts a Phosphatidylinositol-Glycan-Anchored Protein to a Secreted Protein". *J. Cell Biol.*, 1992. *116*, 799-807.

28. Berger, J., Howard, A.D., Brink, L., Gerber, L., Hauber, J., Cullen, B.R., and Udenfriend, S., "COOH-Terminal Requirements for the Correct Processing of a Phosphatidylinositol-Glycan Anchored Membrane Protein". *J. Biol. Chem.*, 1988. *263*, 10016-10021.

29. Caras, I.W., Weddell, G.N., and Williams, S.R., "Analysis of the Signal for Attachment of a Glycophospholipid Membrane Anchor". *J. Cell Biol.*, 1989. *108*, 1387-1396.

30. James, R.I., Elton, J.P., Todd, P., and Kompala, D.S., "Engineering CHO Cells to Overexpress a Secreted Reporter Protein Upon Induction from Mouse Mammary Tumor Virus Promoter". *Biotechnol. Bioeng.*, 2000. *67*, 134-140.

31. Durocher, Y., Perret, S., and Kamen, A., "High-Level and High-Throughput Recombinant Protein Production by Transient Transfection of Suspension-Growing Human 293-EBNA1 Cells". *Nucleic Acids Res.*, 2002. *30*, 1-9.

32. Davis, T.R., Trotter, K.M., Granados, R.R., and Wood, H.A., "Baculovirus Expression of Alkaline-Phosphatase as a Reporter Gene for Evaluation of Production, Glycosylation, and Secretion". *Biotechnology*, 1992. *10*, 1148-1150.

33. Berger, J., Hauber, J., Hauber, R., Geiger, R., and Cullen, B.R., "Secreted Placental Alkaline Phosphatase: A Powerful New Quantitative Indicator of Gene Expression in Eukaryotic Cells". *Gene*, 1988. *66*, 1-10.

34. Onishi, H.R., Tkacz, J.S., and Lampen, J.O., "Glycoprotein Nature of Yeast Alkaline Phosphatase - Formation of Active Enzyme in the Presence of Tunicamycin". *J. Biol. Chem.*, 1979. *254*, 11943-11952.

35. Davis, T.R., Shuler, M.L., Granados, R.R., and Wood, H.A., "Comparison of Oligosaccharide Processing among Various Insect Cell Lines Expressing a Secreted Glycoprotein". *In Vitro Cell. Dev. Biol.*, 1993. *29A*, 842-846.

36. Fischer, R., Waizenegger, T., Kohler, K., and Brock, R., "A Quantitative Validation of Fluorophore-Labelled Cell-Permeable Peptide Conjugates: Fluorophore and Cargo Dependence of Import". *Biochim. Biophys. Acta*, 2002. *1564*, 365-374.

37. Kellenberger, C., Hendrickson, T.L., and Imperiali, B., "Structural and Functional Analysis of Peptidyl Oligosaccharyl Transferase Inhibitors". *Biochemistry*, 1997. *36*, 12554-12559.

38. Segel, I.H., *Enzyme Kinetics*. 1975, New York: John Wiley and Sons.

Curriculum Vitae

María de L. Ufret-Vincenty

Personal Data

Date of Birth: April 3, 1974
Place of Birth: Humacao, Puerto Rico

Education

Graduate

1999 – 2000 **Massachusetts Institute of Technology** **Cambridge, MA**
2001 – 2003 Doctoral Program in Organic Chemistry
1996 – 1999 **California Institute of Technology** **Pasadena, CA**
Doctoral Program in Chemistry

Undergraduate

1996 **University of Puerto Rico** **Humacao, P.R.**
B.S. in Chemistry received on June, 1996

Honors and Awards

2001 – 2003 - NIH Cancer Training Grant: M.I.T.
2002 - MIT Wyeth-Ayerst Scholar Award
1997 - 2000 - Ford Foundation Predoctoral Fellowship
1994 - 1996 - NIH - Minority Access for Research Careers (MARC):U.P.R.
1996 - Summa cum Laude
1995 - Best Chemistry Student of Puerto Rico Award - Chemistry Board of Puerto Rico
1995, 1996 - Most Outstanding Natural Sciences Student Award
1993 - 1994 - NSF - Research Careers for Minority Scholars:U.P.R.

Societies

1993 - 1996 - American Chemical Society - Student affiliate

Publications

- Peluso, S., Ufret, Maria L., O'Reilly, M. K., and Imperiali, B. Neoglycopeptides as Inhibitors of Oligosaccharyl Transferase: Insight into Negotiating Product Inhibition. *Chemistry and Biology,* **2002**, 9, 1323-1328.
- Ufret, Maria L. and Imperiali, B. Probing the Extended Binding Determinants of Oligosaccharyl Transferase with Synthetic Inhibitors of Asparagine-Linked Glycosylation. *Bioorg. Med. Chem. Lett.* **2000**, 10, 281-284.
- Ortiz-Marciales, M., Tirado, L.M., Colon, R., Ufret, M. L., Figueroa, R., Lebron, M., De Jesus, M., Martinez, J., Malave, T. *N-t*-Butyldimethylsilyl Imines as Intermediates for the Synthesis of Amines and Ketones. *Synthetic Communications* **1998**, 28, 4067-4075.
- Ortiz-marciales, M., Pinero, L., Ufret, L., Algarin, W., Morales, J. New Method for the Synthesis of Nitriles via the *O-t*-Butyldimethylsilyl Aldoximes. *Synthetic Communications* **1998**, 28, 2807-2811.